Czech Technical University in Prague

Faculty of Electrical Engineering

Doctoral Thesis

August 2018

Antonín Pošusta

Czech Technical University in Prague

Faculty of Electrical Engineering
Department of Cybernetics

Surface EMG Signal Decomposition into Individual Action Potentials and its Use for Control

Doctoral Thesis

Antonín Pošusta

Prague, August 2018

Ph.D. Programme: Electrical Engineering and Information Technology
Branch of study: Biocybernetics and Artificial Intelligence

Supervisor: ***Jakub Otáhal***
Supervisor-Specialist: Adam Sporka

Abstract

Use of surface electromygraphic activity for machine control is being investigated over last three decades. Assistive technologies based on surface EMG activity in form of active prosthesis are becoming more common and also new commercial solutions for entertainment purposes or as a new peripheries for personal computer (Myo) emerges in recent time. Yet most of these technologies are based on recognition of different discrete grasps.

Thesis is concerned with utilization of continuous muscle activity level estimates for use in human-computer interaction as an assistive technology. Study presents designed user interface for typing text and general control of a computer. User interface is controlled by developed fast and stable amplitude muscle activity estimation method. Thesis also presents qualitative findings from participatory sessions, possible approaches to decomposition task and discusses usability of EMG decomposition based approach with use as an assistive technology.

Human-computer interaction method using continuous muscle activity level estimates was designed with regard to universally intuitive usage and simple calibration and was successfully verified by continual evaluation with participants.

Keywords:

Surface electromyogram, EMG, assistive technologies, input methods, input technologies, decomposition, human-computer interaction

Abstrakt

Využití elektromyografické aktivity pro ovládání zařízení bylo zkoumáno během posledních 3 dekád. Asistivní technologie založené na EMG aktivitě ve formě aktivních protéz se stávají běžnými a zároveň se začínají objevovat řešení určené pro zábavu nebo ovládání osobních počítačů (Myo). Avšak většina těchto technologií je založena na rozpoznávání rozdílných diskrétních stavů – gest.

Závěrečná práce se zabývá využitím kontinuálního odhadu úrovně svalové aktivity pro užití v rozhraní člověk-počítač jakožto asistivní technologií. Práce představuje navržené uživatelské rozhraní pro zadávání textu a obecné ovládání počítače. Uživatelské rozhraní je ovládáno pomocí vyvinuté rychlé a stabilní metody odhadující svalovou aktivitu z povrchového EMG. Práce představuje kvalitativní poznatky z uživatelských testů, nastiňuje možnosti pro užití dekompozice EMG a diskutuje užitečnost přístupu založeného na dekompozici s užítím pro asistivní technologie.

Metoda pro interakci člověk-počítač užívá kontinuální odhady svalové aktivity, které byly navrženy s ohledem na intuitivní použití, snadnou kalibraci a byly úspěšně ověřeny během průběžných testů s participanty.

Klíčová slova:

Povrchový elektromyogram, EMG, asistivní technologie, metody vstupu, zadávání textu, dekompozice, rozhraní člověk-počítač

Acknowledgements

I would like to express my thanks to my supervisor doc. MUDr. Jakub Otáhal, PhD. for advices given throughout the studies and to my supervisor-specialist doc. Ing. Adam Sporka, PhD. for valuable inputs on qualitative experiments methodologies and cooperation on TextAble project.

My gratitude belongs to my parents, friends and colleagues for moral support.

Many thanks also belongs to all participants of the studies for their patience and help with evaluation of the methods.

Funding Information

The research has been partly supported by (1) grant LH12070 awarded by the Ministry of Education, Youth and Sports of the Czech Republic, funding PROGRAM LH KONTAKT II, (2) grant SGS10/290/OHK3/3T/13 awarded by the CTU Prague, (3) grant P304/12/G069 awarded by the Czech Science Foundation, and (4) project AV0Z50110509 of the Academy of Sciences of the Czech Republic

Contents

1 Introduction

Thesis is concerned with electromyographic (EMG) muscle activity estimation and its mapping to controls of human-computer interface and use in applications for assistive technology. EMG signal is used widely in medicine (analysis of muscle disorders, pre-birth contractions detection, sports) and also is being examined as possible input for control and human-computer interaction over last three decades.

In control applications and commercially available assistive technologies only few parameters of electromyographic signals were used in most cases. The simple thresholding principle with on/off regulation is used in most of prosthetic commercial products up to date. More advanced approaches are using statistics and feature parameters as integral sum, RMS value, variance, frequency spectrogram or wavelet coefficients combined with a classifier. These parameters are easy to obtain, but EMG signal contains much more information, thus, such a control system, able to decompose it, may gather more precise muscle behavior characteristics and also more degrees of freedom. Correctly decomposed signal would mean more precise response of such system.

Most of the works concerning surface EMG for control or human-computer interaction utilize recognition of various grasps and muscle movements represented as discrete states. This thesis examine the hypothesis if continuous muscle activation estimate and real-time signal decomposition is applicable for human-computer interaction applications usable in assistive technologies, which were also part of the development.

Aims:

- Summarize state of art. Research methods utilizing surface EMG signals as control input for use in human-machine interfaces and available methods for surface EMG decomposition.
- Design algorithm for real-time continuous muscle activity estimation – with possible use of realtime surface EMG decomposition.
- Maintain proper response and minimum delay of the algorithm, minimize the need to train (easy calibration).
- Design user interface method, which would be suitable for interaction using continuous muscle activity estimates.
- Evaluate usability of proposed method.

Contribution of the Thesis:

- A new method for controlling user interface using continuous muscle activity estimates with use as an assistive technology with easy calibration and intuitive control was described.
- Practical use of online decomposition was outlined, discussed and compared to amplitude based muscle estimates.
- New method based on contexts working with minimal number of inputs and capability of formatting text and control of computer was developed and described.
- Method was evaluated and presented also in dynamic experiments in developed VR environment training application.

Outputs of this work were a major part of project TextAble. Main aim of the project was development of text input method, which utilize alternative peripheries as assistive technology for disabled people, thus studies with participants were targeted mostly on text input applications. Surface EMG muscle activity estimation was major part of developed human-computer interface input.

The text describes solution and progress in work on proposed system. In the second chapter is described physiological nature of problem and model. The chapter also contains research on methods utilized for processing of the surface EMG, feature-extraction, recognition and signal decomposition. The third chapter aims on related works utilizing surface EMG for control purposes. Fourth chapter describes used and developed methods for human-machine interaction and applications. The chapter reveals details about design of whole system, developed hardware part, possible electrode setups and the real-time algorithm for classifying muscle activity of surface EMG. Fifth chapter captures evaluation of developed system and developed applications. Following discussion and conclusion of the thesis.

2 State of the art

2.1 Electrophysiology of muscles

This chapter contains all needed prerequisites for further reading – characteristics of signal, its origin and short introduction to anatomy consequences.

2.1.1 Signal generation and origin

Skeletal muscles are built from clusters of muscle fibers, which are composed of actin and myosin. These fibers may vary in size over different types of muscles and also between different individuals (depending on age, sex, weight, etc.).

Skeletal muscles are innervated by axons of motoneurons from the spinal cord (scheme in figure 1) – area of innervation is approximately in the middle of the muscle body. Each muscle is composed of a large number of muscle fibers. Compound of muscle fibers and neuromuscular connection with common nerve is called motor unit. Motor units are randomly distributed over whole muscle (in average – between muscles are (existing) differences in MU distribution. Motor unit transmits the activation signal (discharge firings) from motor neuron to the contractile proteins. The electrical discharge (nerve impulse initiates depolarization of muscle cells) then cause twitch – contraction of innervated muscle fibers, which will generate force. Muscle fibers and other nearby tissues conduct electrical discharge. Amplitude of signals – motor unit action potentials (MUAPs) depends on size of the motor unit. Power of contraction depends on firing frequency of these units (and number of involved units). Signals spreads from CNS through spinal cord via motoneurons (in form of action potentials) to motor units, where are being converted on mechanic contraction. These action potentials (from alpha-motoneurons) then propagating through muscle tissue and are measurable on skin surface as electrical signal. Typical template of surface measured action potential is plotted in figure 3. Activating new motor units is called recruitment in literature.

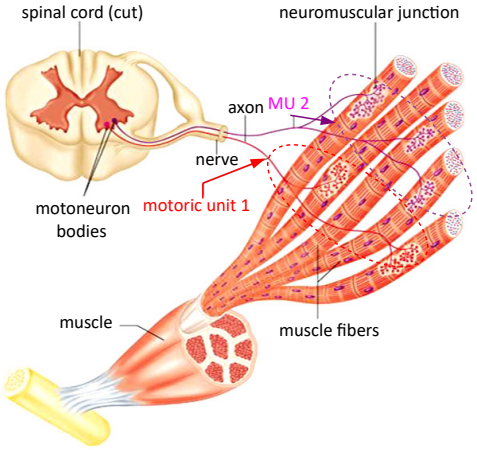

Figure 1: Muscle fibers and motor units

Signals may be acquired from body surface or by invasive method. It is possible to gather much clearer signal with better characteristics using invasive method, but this method also brings few complications – needle electrode should be fixed (in order to obtain same signal – minor movement changes the shape of signal), method is uncomfortable (there are also implated solution for patients if needed), experiments cannot be repeated in short period (due to tissue damage, which also changes the shape of AP) and finally there is always a risk of

infection (especially if used in long-term experiment). Nevertheless, it is indispensable method for investigation of muscle disorders and research of motor unit behaviour. This work is concerned with use of surface signal measurement. Usage of the surface EMG measurement method is superior to invasive, thus it minimizes the probability of infection and is more comfortable, but also has its disadvantages, which are described in text hereafter.

2.1.2 Signal propagation model

Accurate mathematical model of motor unit action potential was defined by McGill et. al. [86], who defines MUAP as the sum of intracellular action potentials, which are estimated by formulas:

$$v(t) = a\,g(t) + b\,g(t) * \left(e^{\frac{-t}{t_A}}\,u(t) \right) \qquad g(t) = \begin{cases} \dfrac{k^{n+1}}{\Gamma(n+1)}\,t^n e^{-kT}\,u(t) & \langle t \in 0, t_s \rangle \\ 0 & elsewhere \end{cases}$$

where $g(t)$ is monophasic waveform modeled using gamma density function, a specifies size of the potential, b afterpotential, t_A is time constant and $u(t) = I(t \geq 0)$ is unit step function (equals one, if condition in brackets is true).

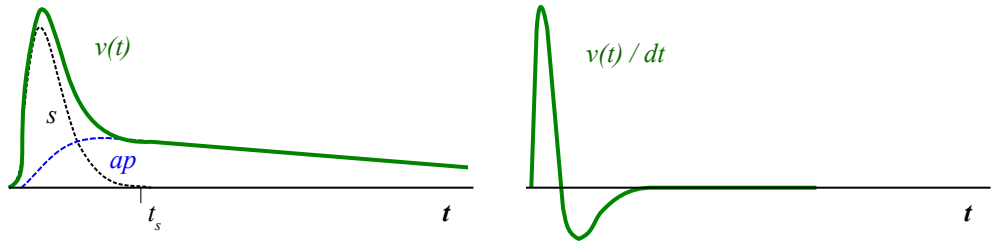

Figure 2: Intracellular action potential (v) modeled as sum of spike (s) and afterpotential (ap) on the left, derivated IAP on the right

Sum of derivated intracellular action potentials $dv(t)/dt$ convolved with spatial weighting functions gives us the motor unit action potential train in time measured on muscle fiber. Weighting function depends on properties of volume conductor, fiber path, conduction velocity, fiber ends and end-plates (neuro-muscular junction).

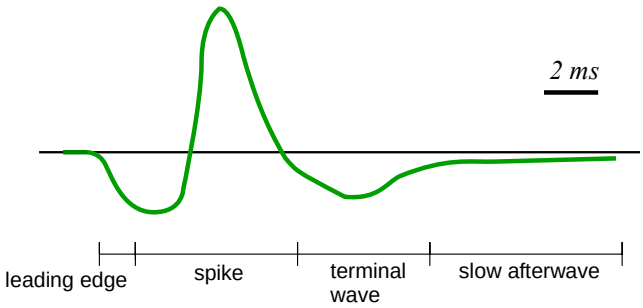

Figure 3: Typical measured motor unit action potential shape

Since the motor unit innervates more muscle fibers, the measured MUAP on surface is sum of these single muscle fiber spikes filtered by transition through subcutaneous fat, skin and skin-to-electrode transfer path.

Human body tissue is an electrical volume conductor, which electrical conductivity varies with tissue type. Diagram in figure 4 presents model of spatial signal propagation in conductive environment. On the input side we may observe signals originating from motor units ($s_i(t)$). Signals then diffuse throughout the tissue (H_{ik} represents transfer system of the tissue) and are deformed. Each electrode then records summation of all these signals filtered through skin acting as a low pass filter summed up with additive noise. On the right side of the model is an electrode array, where the mixture is obtained. But due to different transfer paths signals the same MU looks on each electrode a bit differently. Fact that skin (and other biological tissues) acts as a natural (spatial and temporal) low-pass filter is a disadvantage compared to invasive methods, where one obtains much sharper and clearer MU spikes. Surface spikes are blurred and this effect makes the decomposition task harder. Second, obtained signal is a summation from greater number of motor units and therefore contains more superimposed signals. Finally, signal is burdened by higher levels of noise (in comparison to invasive method, in figure as $n_i(t)$ for each electrode) - which are of biological character (sweat, movement, problem with proper contact, oiliness) or electrical character (50Hz, amplified interference, …) Subcutaneous fat can be also unfavorable, since the motor units are then further from sensor and therefore more deformed signal is obtained due to longer transfer path.

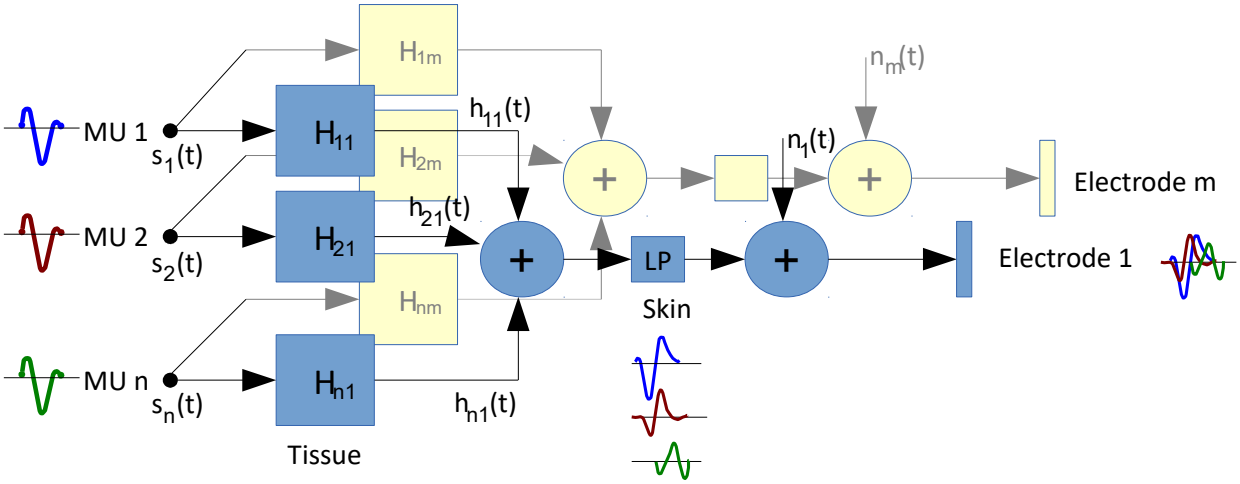

Figure 4: Signal propagation model

If the electrodes are placed too far away from each other, then signals from same motor units coming with higher transition delay (depending on their true spatial location) and signals are also being more deformed by another tissue path (H_{ik}). Nearer motor units are rendered sharper and stronger than further ones.

Input signals from neurons to MU are modeled as dirac pulses, their output measured on

electrodes side is accordingly impulse response. Most of detected MUAPs from body surface are monophasic, biphasic and triphasic, very rare (minor) quadriphasic. [1]

Signal gathered by the k-th electrode in such sensor array system may be described by formula:

$$y_k(t)=\sum_{i=1}^{n} h_{ik}(t)+ n_k(t) \quad (1)$$

for simplicity in this formula *h(t)* is skin low-pass filtered repetitive AP shape. This is also a model used by most of (various) approaches to decomposition task (chapter 2.4). Formula (1) is a model for stationary signal – constant fraction of maximum voluntary contraction.

More sophisticated model (for motor unit action potentials mixture), which considers variability of signals and their presence (in non-stationary case) represents formula:

$$y_k(t)=\sum_{i=1}^{n}\sum_{f=1}^{F} h_{ikf}(t-\tau_{f,t})+n_k(t) \quad (2)$$

In this case *h(t)* represents a single MUAP firing (more precisely system impulse response in this model), τ_f describes time location of this MUAP firing, *i* indexes MUAP template, *f* indexes individual MUAP firing. This model can be also applied on dynamic EMG signals.

Furthermore, each of detected AP may be described (estimated) by formula:

$$h(t)=\sum_{i=1}^{3} a_i \cdot g(t+\tau_i,\sigma_i)=\sum_{i=1}^{3} a_i e^{-\frac{(t-\tau_i)^2}{\sigma_i^2}} \quad (3)$$

where *g(t, s)* is Gaussian distribution (p.d.f.) curve, $a\in(-A,A)$. *A* is maximal amplitude σ_i^2 is variance and τ_i . Therefore, each AP may be characterized by 9 parameters. [16]

Formula 3 is simplification, which is sufficient for purposes of pattern recognition modeling.

The consequence of skin LP filter effect is that surface MUAPs lasts longer than those gathered using invasive method. Invasive method offers signal acquisition up to 10kHz, which is sufficient for easier decomposition and needle electrode configurations also acquires very strong signals from nearby MU. But due to skin LP filter effect (typically up to 1,7-2,5kHz in depency on circumstances) it is clear that anything obtained above 2,5kHz is noise. In most circumstances it is success to obtain signals up to 1kHz. Most energy of surface EMG signal lies between 6 and 500 Hz with most significant part distributed between 20 and 150Hz.

2.1.3 Characteristics, motor units behavior

Various types of motor units across various muscles behave with bit different recruit stragy, but in average all of them have similar properties. The number of recruited units is raising with voluntary contraction. Motor units in muscle differs in size – smaller one are being recruited earlier, larger then during higher contractions and strengths. Simultaneously – those MUs, that were recruited earlier, raising their firing frequency. Above approximately 80 percent of maximal voluntary contraction (MVC) are usually not recruited new motor units, but strength increases only due to rise of firing frequency. For soft fine motor muscles is this threshold lower – approximately 55 percent [3]. Peak discharge rates during slow force changes during isometric contractions reaches 30 to 50 action potentials per second, but during fast force changes discharge rates can reach up to 120 action potentials per second [88].

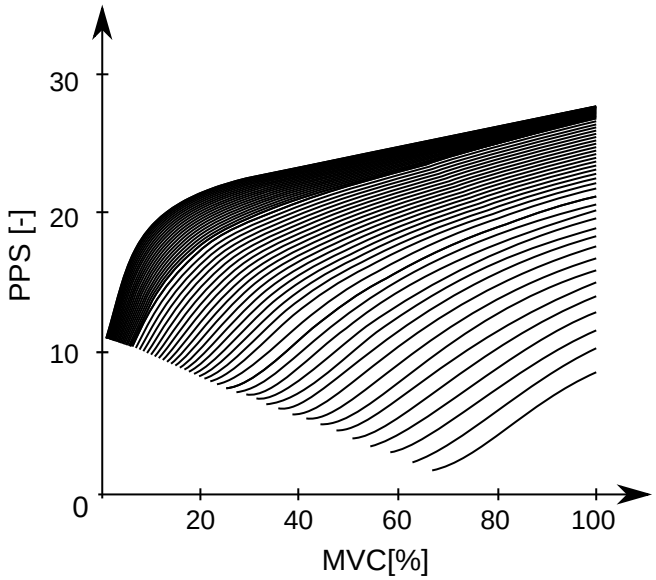

Figure 5: Motor unit recruitment of first dorsal interosseous muscle during slow constant increasing muscle activation, modified [3]

Motor units are being recruited from smallest to largest (Henneman's size principle [44]). Small motor units are also called low threshold (bigger MUs – high threshold). In smaller muscles are MUs dispersed randomly, in larger (more powerful) muscles are bigger motor units placed nearer skin surface. Signal from them is stronger, they are recruited afterwards → this can be utilized for better template search in decomposition. Henneman also describes that small (low-threshold) MU fires lower MUAPs than large (high-threshold) MUs.

Contraction strength of smaller muscles (like first dorsal interosseous or finger control muscles) is regulated rather with frequency of firings (recruitment of MUs is secondary effect), whereas bigger muscles (deltoid, biceps) are rather controlled by recruiting of new motor units (frequency raising is low). Purpose of smaller muscles is performing soft fine

motor tasks, so smoother control is required. Smaller muscles also contains less motor units than larger ones (up to 10x), therefore larger muscles may be controlled smoothly by recruitment mechanism.

Mostly classified characteristic is inter-pulse interval (and calculated firing rate) – e.g. time between 2 firings of same unit. From this characteristic was observed [2, 3, 8, 9], that firings on constant MVC level are not absolutely periodic – their periodicity may be expressed in average over several firings (typically six) – firing rate. Also it is important to stress that each motor unit may fire after a short delay after last discharge (simplification for decomposition). As action potential lasts together with inactive state for approximately 10 ms, maximum frequencies are limited approximately to 100 firings/s, typically lowest threshold units fires at maximal frequency of 50 firings/second. MUs decruitment occurs typically on lower MVC levels than their recruitment (strength decreases at first with firing frequency). It was also observed that recruitment procedure differs for faster contraction rates (MVC/s) [3] – strength of faster contraction is firstly generated by higher frequency of firings.

Recruitment, decruitment and frequency regulation characteristics differs for each individual human in dependency on the way of daily utilization of muscles. Significant differences are between average person and sportsman. For instance weightlifter's MUs are having smaller firing rates for same MVC level, which is relative index of maximum individual's power. Few weeks training of rapid contractions can increase average discharge rate from 60 to 100 action potentials per second [88].

This behavior was well described by De Luca [2] and newly more specified in [3, 49].

Individual motor units have tendency to synchronize during fatigue. Firstly become fatigued high threshold motor units. This effect is observable as spectral changes in frequency spectrum calculated from EMG signal during isometric contraction.

Differences of MU recruitment and coding are considered to be reason for different EMG amplitude to force relations. EMG signal amplitude grows with muscle activity. In some muscles, such as those controlling the fingers, the relationship between force and EMG amplitude growth was found to be linear other relate rather with parabolic shape [89]. Electromechanical delay between muscle activation and force production ranges from 30 to 100 ms, there is intersubject variability [90].

2.1.4 Anatomy consequences, EMG properties

For correctness and completeness of work it is appropriate to take into an account anatomy consequences. Parts of this work were used for creation of suitable human – computer interface for project TextAble – main point of interest were muscles, which perform fine motor voluntary movements (hand and facial). Remaining limb muscles may still contain surface EMG pulses earlier used to control fingers. This of course depends on the place of amputation. Facial muscles are in most severe disabled persons the last remaining option. Target of the project was to create text input method for disabled persons.

Muscles responsible for finger flexion and extension movement are located on forearm part near elbow (see figure 6). In this location is a large number of muscles placed close to each other. This means high probability of superimposed signals, but also a lot of potentially extractable information. Due to muscle cross-talk is possible from few places on skin gather information for movement of more fingers.

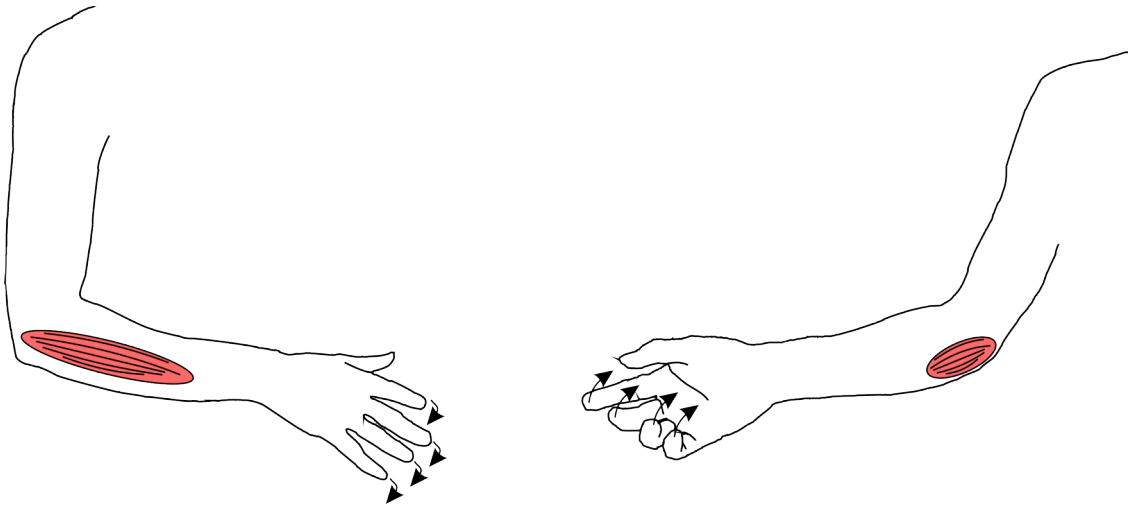

Figure 6: Finger control muscles responsible for finger flexion and extension

The idea was a creation of recognition system for distinction between extended and relaxed fingers and creation of continuous fast real-time muscle contraction estimator. Furthermore it was then possible to create a chord-based text input method from muscle electrical activity. This might be a new chance for disabled people with finger or hand amputated since method works also for other muscle groups (facial for instance).

Muscles mostly measured during development phase of this work were extensor carpi ulnaris, extensor digitorum, extensor carpi radialis longus, palmaris longus, flexor carpi radialis (figure 7) and masseter (face muscle). For decomposition testing were examined also biceps brachii and first dorsal interosseous.

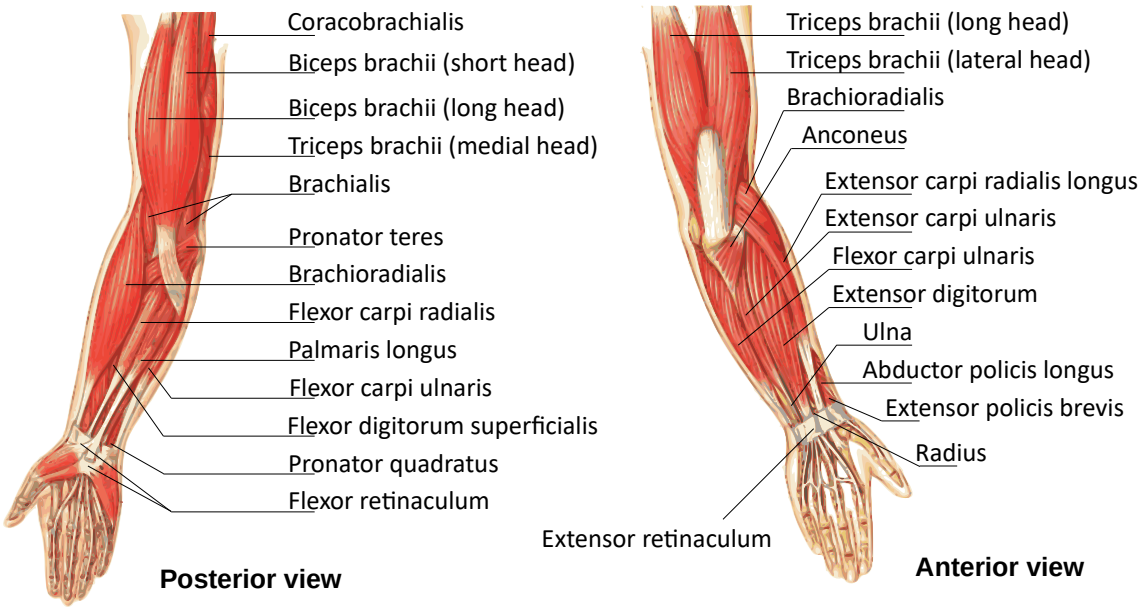

Figure 7: Arm muscles[modified, 45]

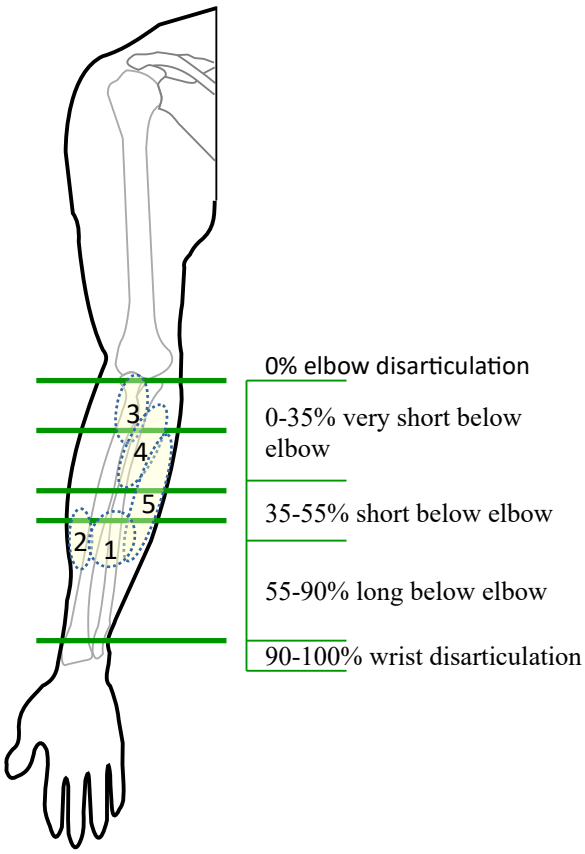

Figure 8: Finger control muscle electric activity regions related to level of amputation. 1 - thumb control activity, 2 - pointing finger, 3 - middle finger, 4 - ring finger, 5 small finger

Level of amputation affects the amount of extractable information based on EMG signals. Figure 8 exposes regions of EMG activity during extension movements of fingers. Drawing suggests that all 5 finger extension movements can be possibly recovered, if there is remaining at least 60 percent of limb (long below elbow). This possibility also depends on level of muscle damage.

Interesting fact is also possibility of EMG signal generation in paralyzed people. [42]

2.2 Measurement methods

2.2.1 Electrodes

The acquired EMG signal is affected by electrode size, shape, inter-electrode distance and most importantly by skin-electrode impedance. Impedance of electrodes depends on their surface size and build. Typically are used wet (gel electrodes fig. 9 on the left), but dry ones can be also applied. Dry electrode has much higher impedance. With higher impedance we obtain higher levels of noise measured on electrode therefore it gives lower signal to noise ratio (SNR). The impedance of each electrode should be equal to prevent parasitic coupling with the power line. Parasitic capacitance may form voltage divider, which may generate much larger voltages than is the signal and measurement equipment should be designed to reject this effect as possible to prevent amplifier input saturation.

Treatment of skin will also lower skin-electrode impedance. Impedance of the skin can be lowered by [46]:

- scratching
- rubbing with ethyl alcohol, abrasive paste, stripping with adhesive tape
- washing with soap

Electrode also acts as a spatial low pass filter. With decrease of electrode area the filtering effect also decreases (for area of size around units of millimeters almost negligible), which is for instance main advantage of the dry electrode in figure 9. For instance 5mm diameter electrode has cutoff frequency 360Hz, electrode with 20mm dimater has 100Hz cutoff [47].

Dimitrova [48] shown that filtering effect depends stronger on longitudal electrode dimension affects than transversal direction in axis of MU position. Longitudal dimension influences main phases of MUAP shape, with greater electrode surface area the measured amplitude of MUAP is lower. Furthermore misalignment of bipolar electrode with respect to muscle fiber direction will also reduce signal amplitude [51]

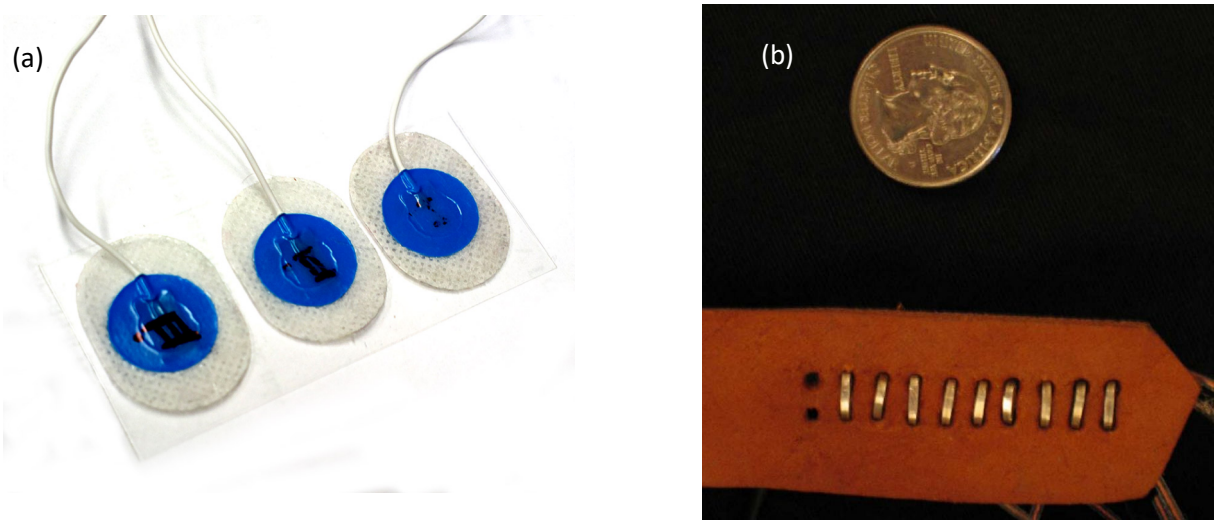

Figure 9: Typical electrodes used for feature-extraction of movement (a) surface ECG electrodes(b) wristband with stainless pins [19]

Regarding the signal propagation model, MUAP from further MU has lower frequency spectrum and also lower amplitude. Relation between electrode distance from motor unit and properties of detected MUAP using surface EMG with different interelectrode distances (fig. 10) was well described by Fuglevand et al. [50].

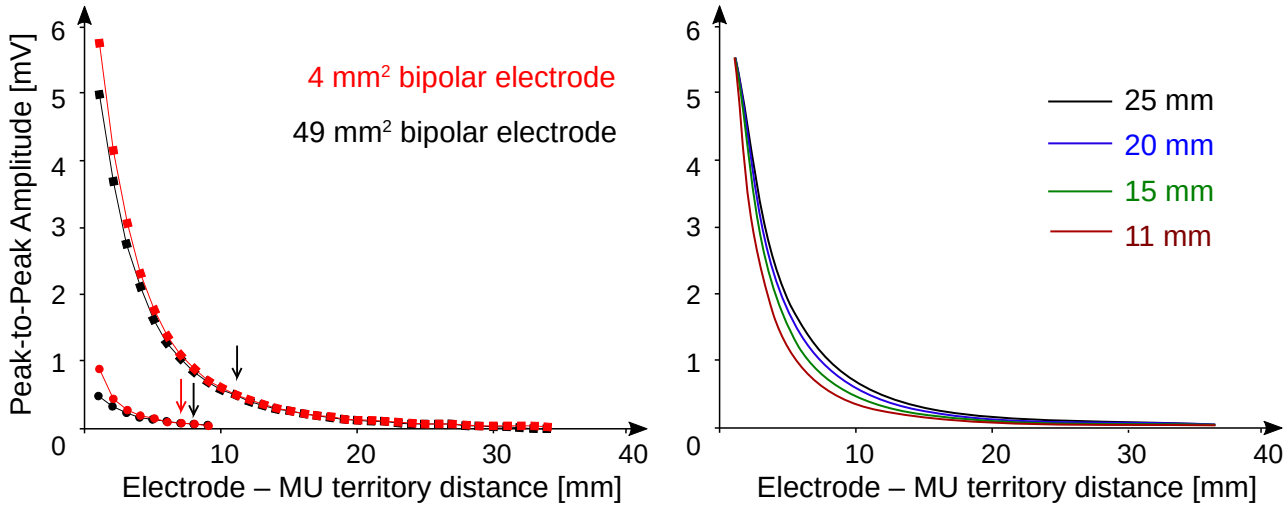

Figure 10: Left: change of MUAP peak-to-peak amplitude in dependency on MU territory distance for large MU (square) innvervating 2500 fibers and small MU (circle) innervating 50 fibers measure by bipolar electrodes with interelectrode distance 20mm, Right: MUAP peak-to-peak amplitude dependency on various interelectrode distances for large MU (innervating 2500 fibers) detected with 4mm² electrode, modified [50]

2.2.1.2 Electrodes used for decomposition

Typical electrodes used for signal decomposition to single MUAPs in classical physiological sense are in fig. 11.

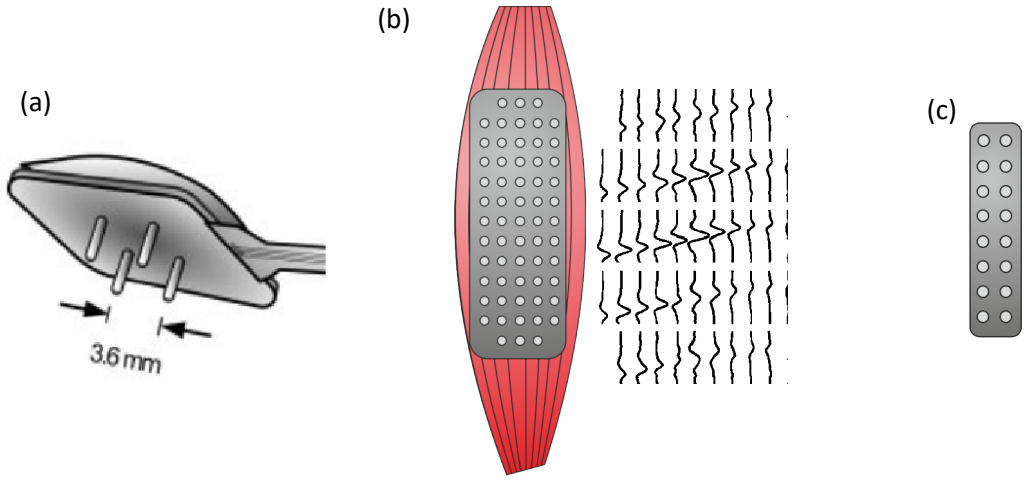

Figure 11: typical electrodes used for decomposition (a) DeLuca's [8] (b) HDEMG array used with CKC algorithm decomposition [13] and single detected MUAP (c) other various types [24]

The first from left side was used for precise decomposition PD3 algorithm proposed by DeLuca at. al. [8]. Example (b) is electrode array used by Holobar and Zazula for HD EMG CKC decomposition method [13] (described in section 2.4). Electrode is placed above a single muscle. Moreover, with this array is also possible proper spatial localization of MUAP sources. All channels of these electrodes are usually differentially amplified (configuration is for each different). These are mostly used for experimental purposes and MUAP behavior analysis. High-channel count electrodes may not be suitable for easy-to-use assistive technology based on movement or muscle activity recognition due to possibility of different impedances in each channel, complicated processing and expensive hardware.

In figure 9 are electrode types used mostly for movement recognition using feature extraction. Electrode wristband 9(b) can be also utilized for decomposition into MUAPs, whereas (a) ECG-like electrode type is less suitable for this task. These electrodes are mostly used for amplitude processing approach based on statistics from time and frequency features extraction (described in section 2). ECG-like electrodes can be for this task used as in configuration like (b) – differentially with more channels in specific localization above muscle. Advantage of ECG electrodes (especially gel ones) is their better signal conductivity and lower resistance on skin-electrode contact, but gathers stronger integral signals over many MUs, which are harder to decompose.

2.2.2 Amplifiers and sampling

Typical biosignal monitoring system consists of signal conditioning filters, amplifiers, analog-to-digital converters and interface to PC.

Most important parameters for amplifiers are

- high input impedance (electrode-skin impedance to amplifier impedance ratio should be low)
- high common mode rejection ratio
- high power supply rejection ratio
- flat voltage gain within EMG bandwidth
- good linearity
- low voltage and current noise
- if we consider also portable application, the important parameter would be also power consumption in case of wearable human-machine interface.

Conventional systems for medical and physiological purposes mostly utilize electrodes similar to ECG electrodes (gel, Ag/AgCl) or sticky surface. These systems are operating at frequencies up to 500-1000Hz. Signals are quantized at 16bit resolution in most conventional systems. Inputs of surface EMG amplifiers are mostly designed for skin impedance from 2 to 50kOhm.

Systems for decomposition utilize various types of custom built electrodes mentioned above. Operates at frequency range from hundreds Hz up to 10KHz, therefore the sampling frequencies are usually above 5 kHz.

EMG systems utilizing high number of electrodes sampled at high frequencies are in literature reported as high density EMG systems (HDEMG). These systems were unforgettable point of interest in research area during last decade. HDEMG mostly utilizing high number of surface electrodes formed in 2 dimensional electrode arrays. Typical design has preamplifier for each electrode, multiplexer and amplifier with analog to digital converter. Preamplification is important step, since connecting electrodes directly to multiplexer would introduce high levels of switching artifacts. Some solutions also introduce sample/hold element, which is important for proper, easier and more accurate MU action potential localization. Systems without sample-hold are sampling each channel in different time point.

2.2.2.1 Amplifier input configurations

Shape and amplitude of measured MUAP also depends on amplifier input (electrode) configuration. Mostly utilized configurations are monopolar and differential (bipolar). In recent high number input channel approaches (HDEMG) are utilized configurations similar to filtering in image processing methods. Signals obtained from these configurations can be also calculated from monopolar measured data. Monopolar electrode configuration is more sensitive to noise. All channels has common reference (connected to positive or negative input of amplifier array).

Chosen configuration may affect also measured spectrum of single MUAP. [53] This may not be visible in measured power spectrum, since it is summation from all MUs. Differential electrode configuration acts as a periodic bandstop spatial filter (comb filter) for a single MUAP. This effect depends on tissue conduction velocity and inter-electrode distance. Figure 12 shows the difference between unipolar and bipolar configuration with different inter-electrode distance and constant conduction velocity for example of $5\,m\cdot s^{-1}$

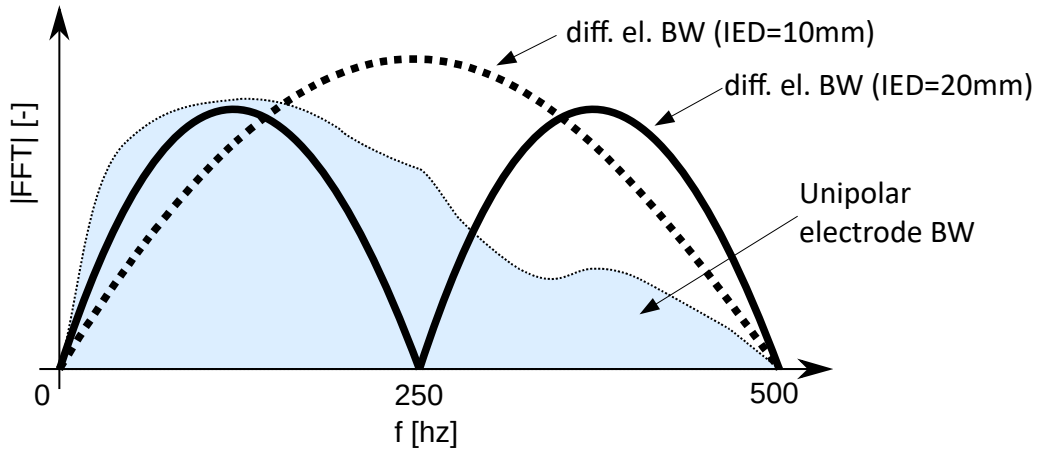

Figure 12: MUAP power spectrum measured with different inter -electrode distances (IED)

Other used differential connection is double-differential electrode, which can be achieved using two-amplifiers with common negative input or by calculation from 3 unipolar channels using filter mask

$$M_{NDD}=\begin{bmatrix}1\\-2\\1\end{bmatrix}$$

Similar result can be achieved using branched electrode configuration on one amplifier (fig. 13). [54]

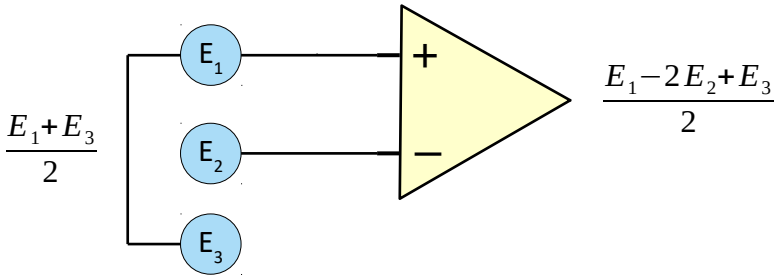

Figure 13: Branched electrode

Advanced differential configurations computing one channel from multiple measured channels using filter mask. For instance 2D laplace filter called normal double-differenting filter (NDD) is used for 5 pin electrode or popular inverse binominal filter (IB^2) [Disselhorst-Klug] is used for 9 pin electrode. Such measurement configuration sharpens and focuses MUAP shapes and also suppresses the muscle crosstalk effects. [55]

$$M_{NDD}=\begin{bmatrix}0 & 1 & 0\\ 1 & -4 & 1\\ 0 & 1 & 0\end{bmatrix} \qquad M_{IB^2}=\begin{bmatrix}1 & 2 & 1\\ 2 & -12 & 2\\ 1 & 2 & 1\end{bmatrix}$$

2.2.2.2 Application-specific integrated circuits

During last decade also emerged very integrated solutions combining preamplification, multiplexer and digitization in one chip. These are reported as application-specific integrated circuits. Commercially available examples are Intan RHD2000 or cheaper TI ADS129x. These chips doesn't provide such a high specifications as precise laboratory-grade equipment, but enable engineers to design much smaller or wearable devices.

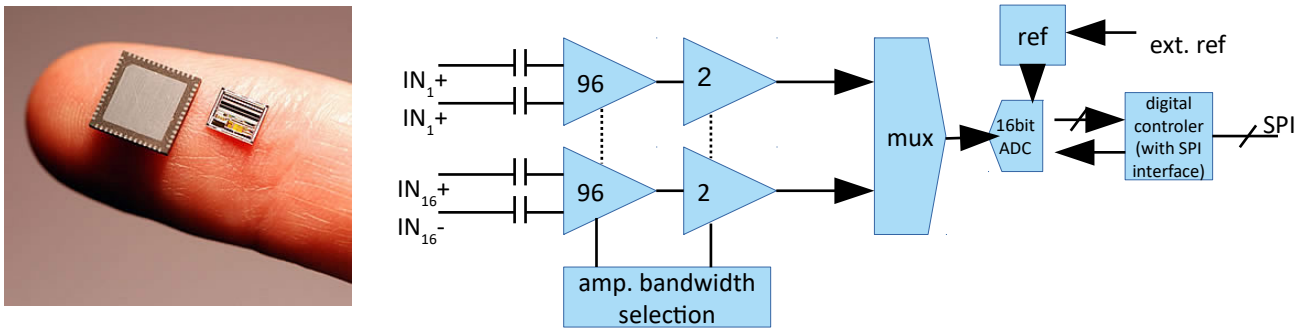

Figure 14: Application-specific integrated circuit solution (INTAN)

Intan RHD2000 offers up to 64 channels with common reference or 16 differential (see fig. 14 on the right) digitized up to 30kHz at 16 bits. But cost of their chips is still quite high

(above thousand dollars – depends on channel count and build). On the other side are solutions from Texas Instruments – last revision of ADS129x family. ADS1299 offers 8 channels with sampling up to 16kHz at 24bit and amplification up to 24x. But real signal resolution degrade in dependency on sampling frequency. ADS1299 was used in later phase of the work.

2.2.3 Noise sources

There is a plenty of noise sources in surface EMG signal – movement artifacts, electromagnetic interference, muscle cross-talk and others.

2.2.3.1 Movement artifacts

Movement artifacts are usually in range from 1 to 10 Hz and are observable due to:

- movement of the cable connecting the electrode
- motion of the surface electrode on the skin creates motion artifacts
- during movement (muscle contractions) muscles change its length and electrodes move on the surface with respect to each other

This kind of noise has similar amplitude as EMG itself. Another type of artifact, noticeable in signal decomposition, is movement between innervation zone and electrode.

2.2.3.2 Electromagnetic interference

Since human body acts as an antenna, it can accumulate power line interference and other electromagnetic signals. Most noticeable is 50Hz (Europe) and its four first harmonics. Measured interference is not accurate 50Hz in all cases and can fluctuate around this frequency, which means the same for the higher harmonics. Power lime interference can change with contact impedance fluctuations (for instance movement / sweat).

Another interference type is usually remarked as electrode inherent noise. Inherent noise origins from all types of electronic equipment nearby and ranges from zero to several thousand hertz.

2.2.3.3 Muscle crosstalk

In areas with high concentrations of muscle groups occurs muscle cross-talk effect – potentials of MUs of one muscle conducts through tissue to measurement electrode above another muscle. (Tissue has a volume conductor properties.) Signal origins from activation of another muscle. This effect is for investigation of specific muscles unwanted, but for control

can be advantageous, when is properly utilized. If we are able to decompose signal properly, we can distinguish between actions even with measurement from another muscle than the one performing movement. Crosstalk was investigated by DeLuca and Merletti by electrical stimulation.

Crosstalk bandwidth can be larger than the bandwidth of measured muscle signals, therefore its reduction can't be achieved by use of simple high pass filter. Signal shape of crosstalk signal in further electrode may also differ from the signal on the electrode of the measured muscle. Foreign muscle signal cannot be effectively filtered by temporal filters. Crosstalk effect can be partly compensated by blind source separation techniques (chapter 2.3.5)

Spatial filtering (differential electrode configurations) is most effective method to lower the crosstalk effect, therefore it can be reduced by choosing proper electrode size and inter-electrode distances carefully. ([54, 56] 1-2 cm). Crosstalk will increase with subcutaneous fat thickness.

2.2.3.4 Other sources

Other sources of noise are ECG or of biological character. ECG can be recognized as periodically repetitive pattern (QRST complex) and may emerge in some electrode setups, especially with common reference and electrodes placed over large body surface (similar setup to ECG measurement). The ECG is visually identifiable below 25 percent MVC of muscle activation. [56] High pass filtering over 100Hz will remove effectively possible ECG interference.

2.3 Signal processing

This chapter covers signal processing methods and approaches mostly used for surface EMG signal processing (that can be used in human machine interaction). Most current studies estimate the movements from muscle activity from surface EMG with the use of feature extraction, however machine learning with feature extraction allows to eliminate redundant information, noise and also provides algorithms that can be learned to provide physically accurate force estimation.

Typical signal processing techniques includes conditioning (noise filtering, separation), feature set selection and computation, removal of redundant information (feature dimension reduction) and recognition. Output of such system may be recognized gesture (most recent studies) or level of force. Typical signal processing pipeline is depicted in figure 15 below.

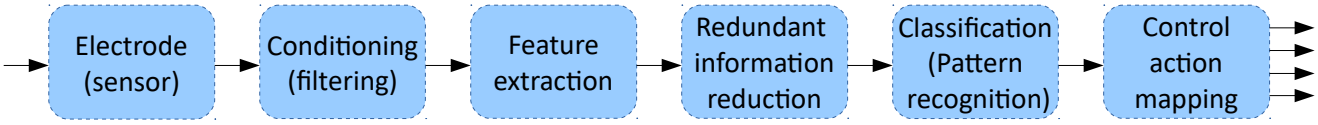

Figure 15: Signal processing pipeline

Actually probably most successfully used methods for recognition of surface EMG for control usage are neuro-fuzzy based systems [36, 37, 38, 39]. Follows review of used methods for conditioning, feature extraction, dimensionality reduction and recognition approaches used for surface EMG processing.

2.3.1 Conditioning / Noise filtering

The first step in every biosignal processing setup is signal conditioning and noise filtering. Classic filters (of arbitrary order) are mostly used to get acceptable quality of input signal.

In literature prevails usage of high-pass filtering from 5 to 30 Hz. For classic EMG processing approaches is recommended to use high-pass from 10-20 Hz (due to movement artifacts). Low pass filtering is in most cases set to 500Hz, this value varies between 250 – 1000Hz.

Some works propose [18, 40, 57, 80] differential filters to be used for filtering and amplification of motor unit action potentials (described in chapter 4). Other studies propose to use techniques as wavelets [21, 22, 83], empirical mode decomposition [27, 84, 93] or artificial neural networks.

Surface EMG usually contains all types of noise described in previous chapter. Noise sources are mathematically represented as:

- white Gaussian noise

- slowly changing base frequency with its higher harmonics (power line interference)
- baseline wandering (movement artifacts, sweat,…).

Denoising of the signal in online recognition system was accomplished also using artificial neural network, which needs learning, wavelets or suitable combination of various filters. Ensemble empirical mode decomposition method [93] is superior to others and capable to remove all of these noises, but is not suitable for fast online recognition. Empirical mode decomposition method itself was very recently [84] also modified for online purposes using time windows, but still has too large delay for fast online applications.

Filtering of rectified surface EMG in signal processing signal is being used to estimate the level of muscle activity. This is done in combination with moving average filter, integral envelope or their modifications. But for control purposes in real-life applications are outputs of these filters used mostly as only single bit on-off information, for instance in commercial prosthetic systems.

Potvin and Brown [85] proposed that high pass filtering above 140Hz in combination with amplitude estimation reduces error of muscle force estimation. In study were tested various cutoffs up to 440Hz. Using such a high value for high pass does also remove around 90% of signal power, but is also optimal for signal decomposition, since blurred peaks from further motor units are filtered out.

Liu et al. [77] proposed Wiener filtering of surface EMG for neurologically injured patients, which has their recordings often corrupted by involuntary interference – spikes similar to MUAPs. This imposes potential difficulties for myoelectric human machine interface. Using Wiener filter were authors able to filter out involuntary background activity of different levels. Wiener filters were also used [78] for filtering out the other present sources of noise.

Wiener filter is widely used in image processing and also for audio waveform processing. For Wiener filter holds if there is convolution kernel set correctly, then blurred (filtered) superimposed signals may be focused. Problem is that the noise can be also amplified after applying this filter. Wiener filter for signal focusing is mostly used for applications where is noise-to-signal ratio 5-10 times higher than in typical EMG measurement setup.

2.3.2 Features used in conventional EMG methods

There is a large spectrum of methods for extracting features for later classification with usability for control purposes. Features are being extracted from time domain, time-frequency domain, using various transformations (as STFT, wavelets, cepstral analysis,...), various approaches are adopted from artificial intelligence area – iterative optimization algorithms, artificial neural networks, fuzzy logic, etc. or their combination. Before developing the

pronounced system was useful to come through methods used in various attempts of similar works. The following subchapters describing usage of these methods. Following text is focused on methods utilizing feature-extraction and their processing for control purposes.

2.3.2.1 Time domain features (methods and statistics)

As time domain features are often utilized simple statistics over raw EMG signal as RMS, mean average, variance, skewness, higher order moments. RMS and mean average was used as first control features in ON-OFF control system of active prosthesis and in commercial products is used up to this date. With more strength, more motor units are recruited and peak-to-peak amplitude of signal grows, same holds for its variance and mean frequency. ON-OFF control is achieved by comparing measured value with chosen threshold.

For obtaining more degrees of freedom from EMG signals were in various attempts calculated combinations (feature sets) of these simple statistics as RMS, variance, mean average value, skewness, zero-crossings, AR (autoregressive) coefficients, integrated EMG value, and many more... In combination with classifier based method for instance perceptron, linear discriminant analysis or neural network was possible to extract distinguishable information for control.

In this case may be also used higher order statistics [127] as only a features of detected signal. For lower number of inputs is advantage of using this method in their low computational complexity.

Table I contains a summary of features extracted in time domain found in literature (conducted from studies, references in section 3.1) and their physiological meaning.

Table I Summary of features extracted from time domain

Root mean square (RMS)	$RMS=\frac{\sqrt{(\sum_{i=1}^{N} x_i^2)}}{N}$	Muscle contraction indication before starting of the fatigue during constant force
Mean absolute value (MAV)	$MAV=\frac{1}{N}\cdot\sum_{i=1}^{N}\lvert x_i\rvert$	Muscle contraction points, can reflect muscle intensity (approximately)
Modified mean absolute value (MMAV)	$MMAV=\frac{1}{N}\cdot\sum_{i=1}^{N} w_i\lvert x_i\rvert, w_i\begin{cases}1 & if\ 0.25N<i<0.75N\\ 0 & otherwise\end{cases}$	
Modified mean absolute value 2 (MMAV2)	$MMAV2=\frac{1}{N}\cdot\sum_{i=1}^{N} w_i\lvert x_i\rvert, w_i\begin{cases}1 & if\ 0.25N<i<0.75N\\ 4 & if\ 0.25N\le i\\ \frac{4(i-N)}{i} & if\ 0.75N\le i\end{cases}$	
Standard deviation	$STD=\sqrt{\frac{1}{N-1}\cdot\sum_{i=1}^{N}\lvert x_i^2\rvert}$	
Zero crossing (ZC)	$ZC=\sum_{i=1}^{N} sign(x_i-x_{i+1}), sign(x)\begin{cases}1\ if\ x>0\\ 0\ if\ x\le 0\end{cases}$	Shows signal sign variation, measures frequency shift
Slope sign change (SSC)	$SSC=\sum_{i=1}^{N} sign[(x_i-x_{i-1})\times(x_i-x_{i+1})],$ $sign(x)\begin{cases}1 & if\ x\ge threshold\\ 0 & otherwise\end{cases}$	
Variance (VAR)	$VAR=\frac{1}{N-1}\cdot\sum_{i=1}^{N}\lvert x_i^2\rvert$	measure of the EMG variability, indicator of the signal power, helps in identifying movement onset and contraction
Wavelength (WL)	$WL=\frac{1}{N}\cdot\sum_{i=1}^{N-1}\lvert x_{i+1}-x_i\rvert$	Measure of complexity Can reflect freq. information, amplitude and duration of signal
Wilson amplitude	$WA=\sum_{i=1}^{N} f(x_i-x_{i+1}), f(x)\begin{cases}1\ if\ x>th\\ 0\ if\ x<th\end{cases}$	Related to movement of muscles, reflects the degree of muscle contraction indirectly [102]
Mean absolute value of the slope	$MAVS=MAV(i+1)-MAV(i)$	
Integrated EMG	$IEMG=\sum_{i=1}^{N}\lvert x_i\rvert$	Relation to action potential of the motor unit
Absolute maximum and absolute minimum (in window)	$AbsMax=max\lvert x_i\rvert$	[60]

Sample median value	$MED = \begin{cases} x_{(N+1)/2} & if\ N\ is\ odd \\ \frac{x_{N/2} + x_{N/2+1}}{2} & if\ N\ is\ even \end{cases}, x_1 < x_{N/2} < x_N$	[60]
V-Order detector	$VO = \frac{1}{N} \sqrt[v]{\sum_{i=1}^{N} \lvert x_i \rvert^v}$	Estimates size of the muscle force for v=1 is MAV, for v=2 we get RMS
Log detector	$LogD = e^{\frac{1}{N} \cdot \sum_{i=1}^{N} \log \lvert x_i \rvert}$	
Energy (also simple square integral, SSI)	$E = \frac{1}{N} \cdot \sum_{i=1}^{N} x_i^2$	Signal power
AR coefficients	$\hat{x}_n = -\sum_{i=1}^{N} a_i x_{n-i} + w_n$	Mostly are used AR4 to AR6
Skewness	$SKW = \frac{\frac{1}{N} \sum_{i=1}^{N} (x_i - \bar{x})^3}{\left(\frac{1}{N} \sum_{i=1}^{N} (x_i - \bar{x})^2 \right)^{\frac{3}{2}}}$	

MAV feature is reported by various studies [23, 102] to be most accurate for force estimation. Best representative features for grasps classification from EMG signal is then combination of AR coefficients with MAV feature. Very promising results were also achieved by incorporating of RMS value, wavelength (WL) and Wilson amplitude [134].

Standard deviation, Zerocrossing (ZC), Variance (VAR) and other listed statistics are mostly used as a supporting features in feature sets.

2.3.2.2 Frequency domain features and transformations

Table II contains sumary of frequency features conducted from from studies remarked in section 3.1. In table II P_i remarks power amplitude on corresponding frequency f_i

Table II Summary of frequency features

Mean frequency	$MF = f_c = \sum_{i=1}^{N} f_i P_i \div \sum_{i=1}^{N} P_i$	Average frequency also called as center frequency and spectral center of gravity.
Median frequency	$\sum_{i=1}^{MDF} P_i = \sum_{i=MDF}^{N} P_i = \frac{1}{2} \sum_{i=1}^{N} P_i$	Median of power spectrum
Peak frequency	$PF = max\, P_i, i = 1, \ldots, N$	Returns frequency where maximal power occurs.
Mean power	$MP = \sum_{i=1}^{N} P_i \div N$	Average power of power spectrum.
Total power	$TP = \sum_{i=1}^{N} P_i = SM_0$	Integrated power spectrum.
1st spectral moment	$SM_1 = \sum_{i=1}^{N} P_i f_i$	First three spectral moments are most important for alternative statistical analysis of EMG
2nd spectral moment	$SM_2 = \sum_{i=1}^{N} P_i f_i^2$	
3rd spectral moment	$SM_3 = \sum_{i=1}^{N} P_i f_i^3$	
Variance of central frequency	$VCF = \frac{1}{SM_0} \sum_{i=1}^{N} P_i (f_i - f_c)^2 = \frac{SM_2}{SM_0} - \left(\frac{SM_1}{SM_0} \right)^2$	
Frequency ratio	$FR = \sum_{i=LLC}^{ULC} P_i \div \sum_{i=LHC}^{UHC} P_i$	Distinguish between contraction and relaxation of muscle using ratio between low (LLC to UHC) and high (LHC to UHC) frequency components.
Power spectrum ratio	$PSR = \frac{P_0}{P} = \sum_{i=f_0-n}^{f_0+n} P_i \div \sum_{i=-\infty}^{\infty} P_i$	If set to range from 10 to 500Hz, which is main energy of EMG signal, can be used as detector of its presence.

This category also contains a large number of transformations. Most of them are used for extraction of describing parameters for further recognition from simple Fourier spectrogram, wavelet transformations.

Some approaches utilized extraction of mean and median frequency, frequency variance

(and similar simple statistics in frequency domain). Regarding the muscle fatigue – mean frequency can be used as detector of fatigue (mean frequency decreases).

As EMG signals are non-stationary (during movement), frequency spectrum of the signal should be used for time windowed signal (also with overlapping), i. e. spectrogram (short time Fourier transform). It is possible to read out much more information about signal from spectrogram, furthermore in one channel and one sample we obtain many observations, which are should be analyzed using some feature-reduction method as is independent component analysis or principal component analysis to find proper decisive features (coefficients) and also get optimized feature space for later recognition steps. Obviously it is needed to choose a proper smoothing window function, due to possibility of occurrences of sharp discontinuities between vectors of frequencies in time. For this purpose should be chosen a window function (Hamming, sinusoidal, etc.).

STFT and other frequency methods are often marked as inappropriate, but are valuable step for more sophisticated methods like independent component analysis or principal component analysis (PCA), which are able to select for instance in case of PCA most variant feature and get viable information for later processing. Frequency features may be utilized for detection of muscle fatigue, which may also be valuable information in a muscle controlled system.

Due to fixed window size the STFT cannot increase frequency and time resolution simultaneously. Using only frequency features didn't had accurate results in movement classifying approaches [62]. In contrast the wavelet transform has great frequency resolution for lower frequency signal components and better time resolution for high frequency components. Wavelet packet transform is proposed to get higher frequency resolution in high-frequency band [133]. In literature by many researchers [27, 28, 29, 30, 31, 32] was shown that wavelet transform methods performs better than STFT on EMG signals. This is due to its characteristics – mixture of MUAPs. Moreover STFT method (and also some of the others) needs proper selection of window length. Successful extraction of suitable coefficients in case of utilization of WT method needs proper selection of base wavelet functions, which is depending also on electrode setup, measurement and individual muscles. For use as a feature-extractor were tested various types of mother wavelets [29, 30]. As instance for biceps muscle were most suitable Daubechies (of 4^{th} and 7^{th} order), Coiflets (of 3^{rd} order) and Symlets (of 4^{th} order), Morlet [101] wavelet and Biorthogonal family, which all have wavelet functions very similar to MUAP shape. It was possible to gather maximally distinguishable parameters for later classification using these wavelet functions. Haar wavelet transformations were used for task of grasp types resolution in similar manner [33]. Signal was analyzed for features using HWT and then classified using SVM (support vector machine). In this case was classified integral signal over whole muscle using standard surface ECG-like electrodes (fig. 9(a), section 2.2.1.2). Using this method for six different grasp types authors achieved average correct recognition rate 86 %.

Similarly for EMG was used short time cepstral analysis (spectral coefficients features), which is mostly used in signal processing of speech waveforms (extraction of unique speech tract describing parameters). As was described on example of use short time Fourier transformation, all these methods may be used online, when appropriate windowing function is chosen. In various works were used window lengths mostly in range 50 ms – 200 ms to meet condition of recommended system delay smaller than is generally accepted 300ms [61].

2.3.2.4 Other features

To complete the list of features used in surface EMG recognition methods the cepstral parameters and entropy has to be mentioned.

Power cepstrum is defined as:

$C(t)=|F^{-1}\{\log(|F(x(t))|^2)\}|^2$, where F denotes the Fourier transform

Independent variable in cepstrum is called quefrency. Definition above suggests that quefrency would lie in time domain, but markedly modified. Property of cepstrum is that convolution operation (in time domain) becomes sum operation (in cepstrum time domain) – effect of logarithm.

Kang et al. [146] found cepstral parameters to be 5% better than AR coefficients in combination with Bayesian-based classifier. Recently [110] the cepstrum analysis methods were applied also as a technique for decomposition of surface EMG to single MUAPs (details in subchapter 2.4.3).

Entropy measures

Entropy measures such as approximate entropy and sample entropy were proposed as approaches to quantify complexity in nonlinear dynamical systems and also were widely applied in analyses of nonstationary biosignals including EMG. Surface EMG signals exhibits nonlinear properties, which conventional time or frequency domain parameters fail to capture. Surface EMG complexity reflects its generative processes as MU firing behavior and recruitment during contractions. Entropy of surface EMG also changes with increasing muscle fatigue and serves as better indicator of fatigue than are the traditional frequency methods. [115]

Sample entropy of scalar time series $\{x_{1,}\dots,x_N\}$ of length N is defined:

1. Embed time series in delayed m-dimensional space:

$X_m(i)=[x(i),x(i+1),\dots,x(i+m-1)]i=1,\dots,N-m$

2. Calculate the frequency of occurrence:

$B_i^m(r)=\frac{N(i)}{N-m-1}$ *N(i)* is number of all other vectors satisfying the condition that their distances from $X_m(i)$ are smaller than the tolerance r

3. Average frequency of occurrence:

$$B^m(r)=\frac{1}{N-m}\sum_{i=1}^{N-m} B_i^m(r)$$

4. Sample entropy:

$$SE(m,r,N)=-\ln\left(B^{m+1}(r)/B^m(r)\right)$$

The dimension m has to be determined, tolerance r can be selected from $\langle 0.15, 0.25\rangle$ of standard deviation of the input series.

Using combination of sample entropy, nonextensive entropy and fractal analysis as features combined with minimum distance classifier were Zhang et al. [79] able to achieve 94 % classification accuracy, but computational cost for processing these features was multiple times higher than the usual features as MAV, RMS, ZC, WL (500 times) or frequency methods (10 times).

2.3.2.3 Signal decomposition based methods

Here word decomposition doesn't denote decomposition to single MUAPs. Main effort in surface EMG signal processing is often to find some repeating component, emerging when corresponding movement is performed. Good preprocessing tool for this task is empirical mode decompostion (EMD[1]) [27] In EMD stage is signal decomposed into maximal and minimal envelopes by finding local minima and maxima. Second step is calculation of their mean (which is the component of signal) and procedure is repeated for this mean. For surface EMG recognition was empirical mode decomposition used to find oscillatory trends and then RMS and AR features were classified to obtain discrete commands for control of robot. [120]

Principal component analysis directly applied on surface EMG patterns will decompose signal to significant trends. Bosco [35] used PCA method for direct decomposition of signals on raw EMG. Principle is similar as one used for STFT and other transformation methods – signal was analyzed with use of window function for differently fast performed movements. Method decomposed signal on two most significant variance components that were correlated with speed of movements. This was done with integral signal from ECG-like surface electrodes on distant muscles. But more usually is this method used to reduce dimensionality of feature space.

1 *Empirical mode decomposition, which is a first step of HHT (Hilbert-Huang transform). HHT is the result of empirical mode decomposition and is a great tool for analyzing of nonlinear and nonstationary data.*

2.3.2.4 Feature sets

Preferred combinations of surface EMG features are called feature sets in literature. These are frequently used as input for the classifier. For instance Hudgins' time domain feature set consists of five features: MAV, MAVS, WL, ZC and SSC, which is often used for evaluating EMG recognition components [62]. Another example is feature set consisting from EMG histogram and 4th-order AR coefficients. Time-domain features together with AR coefficients could have great performance in EMG pattern recognition [115]. Finally, feature set can consist from reduced coefficients of wavelet packed transform or various combinations of features listed in table I.

2.3.4 Feature space reduction methods

PCA method in EMG signal processing is mostly utilized for purpose as is its general typical usage – feature-space reduction (after use of some feature extraction method in time or time-frequency domain), since it has ability to identify the most varying components. By eigen decomposition or more general singular value decomposition of covariance matrix we obtain eigen values and eigen vectors, which can be used to project vectors of features to low dimensional space, since eigen values gives us information on importance of each feature projected by corresponding eigen vector. Similarly the independent component analysis (ICA) method can be used to reduce dimensionality.

Other used feature reduction methods applied on surface EMG were canonical correlation analysis (CCA) and Fisher's linear discriminant analisys (LDA) [37, 62, 79]. Of course for LDA we need labels to separate objects into classes and then it can be used to reduce dimension to C-1, where C is number of classes. LDA can be utilized also as a classifier.

Feature space can be also reduced by extraction of wavelet coefficients, reduction of frequency spectrum or discrete cosine transform. All of these methods were applied in processing of surface EMG signals.

Next possible usage of PCA is for finding correlations and synergies between multiple muscles using multi-electrode arrays above multiple muscles (not an array placed over one muscle) during performing various movements and in fact much better for this kind of tasks performs ICA.

2.3.5 Sources identification

Blind source separation techniques were used by many researchers for EMG signal analysis, since they are useful for lowering the muscle cross-talk effect [68, 103, 108] and also can be used for better identification of significant features. One of these separation techniques is principal component analysis, but since the technique assumes that the original signals are uncorrelated at time lag 0, resulting principle components are always orthogonal and data are

projected in their maximum variance directions, which is not best approach to separate non-Gaussian signals. [99, 107, 126] This is not case of independent component analysis (ICA), where computed independent components does not have to be orthogonal.

ICA has similar usages as PCA. It can be used to reduce dimension or for feature extraction. ICA generates components independent as possible through minimizing second order and higher order dependencies in measured data, whereas PCA uncorrelates data and uses up to second order moments. ICA utilizes central limit theorem presumption that the distribution of a sum of 2 random variables is closer to Gaussian distribution than original distributions of random variables. Therefore ICA cannot be used for Gaussian signals. In case of Gaussian signals is better to use PCA.

Non-Gaussanity estimation can be achieved by calculation of kurtosis: $k(x)=E(x^4)-3(E(y^2))^2$, which is zero for Gaussian distribution, but is sensitive to measured outliers. Second option is to use negentropy;

$J(x)=H(x_{gauss})-H(x)$

Negentropy is used in fast and popular ICA implementation – FastICA, which works on principle of maximization of negentropy. Another example is Infomax ICA, which is based on principle of mutual information minimization:

$I(X;Y)=H(X)-H(X|Y)$, where *H(X)* is entropy and *H(X|Y)* is conditional entropy:

$H(X|Y)=H(X,Y)-H(Y)$, where *H(X, Y)* is joint entropy.

Independent component analysis is being used as a tool for separating independent whole-muscle components (integral signal of more MU from different muscles). This tool can be also used for denoising signals (artifacts), because noise (from artifacts) can be separated from mixture as independent component. Mixing process is expressed as:

$x[k]=A\cdot s[k]$ (where *A* is a mixing matrix, *s* original signal and *x* obtained measurement)

Method is used to calculate complete unmixing matrix (*W*) of sources (*s*) needs minimally same outputs count (electrodes / measurements) as sources (motor units, integral muscle group activity).

$\hat{s}[k]=W\cdot x[k]$

If number of outputs is lower, we may decompose signal to significant components of (whole) muscle activity and these already can be used for next control feature-extraction.

In general it is an optimization problem:

$$min_W \sum_{i=1}^{N}\sum_{j=1}^{M} g(W_j x^{(i)}), W W^T = I$$

where *g* is nonlinear convex function, $g(x)=\log(\cosh(x))$, *W* is weight matrix and $x^{(i)}$ is *i*-th observation from given dataset.

There is a variety of ICA implementations tested for surface EMG signal processing. The most known are probably FastICA, Infomax and JADE (based on third and fourth order statistics), which does not perform best for surface EMG signal preprocessing for classification [68], but still provides good sources estimation results. Study [68] shown that implementations TDESP and second order blind identification (SOBI) combined with ANN performed with 90 and 97 % accuracy and were significantly better than FastICA, Infomax and JADE. SOBI and TDESP are based on second order statistics and takes advantage of the temporal structure in the acquired signals. The basis of the SOBI is a set of time lagged covariance matrices. For independent sources holds that these matrices are diagonal. SOBI can be also incorporated as preprocessing step for surface EMG decomposition.

ICA based methods and especially SOBI are useful tools to partially solve muscle crosstalk. Methods doesn't need prior information and yields better separation results than other multivariate techniques as is PCA.

It was shown [70, 121] that probability density function of surface EMG signals at lower contraction tends to be super-Gaussian, whereas at higher contraction forces nearing to 100% of MVC tends to a Gaussian distribution

To perform ICA the components should be statistically independent and must have nongausian distributions. Electrode count should be equal to number of sources, if ICA should perform optimally without utilizing some preprocessing method. Case where is number of sources higher than number of sensors is called overcomplete ICA. Overcomplete ICA needs some estimation processes. [69]

2.3.7 Recognition / Classification

For final classification task of surface EMG signals were involved probabilistic model algorithms like naive Bayes classifiers, support vector machine linear discriminant analysis. [52] Following hidden Markov models, decision trees (ID3, C4.5), random forest, but for control actually mostly utilized methods are fuzzy logic, neural networks (RBF, ART, majority takes multilayer perceptron), their hybrid combinations fuzzy-neuro, neuro-fuzzy [36, 37, 38] and also combinations of wavelet transform and neural networks as feature detectors, referred as wavelet networks in combination with classifying neural network [47, 87].

2.3.7.4 Neural networks, fuzzy logic

Neural networks are being used in most cases for recognition and classifying of extracted features as a final step of recognizing system, but experiments with direct applications on RAW surface EMG for movement resolution were also done. Most methods based on neural networks are developed to recognize between different discrete states (grasps).

Approach combining the neural network and fuzzy logic achieved very satisfactory results. Neuro-fuzzy approach incorporates resolution ability from fuzzy logic and learning – classification ability of neural network. Using fuzzy logic we obtaining ability of integrating prior knowledge to the system as mathematical model (as simple example: assigning decision to an output value). Using this approach were able investigators [37] achieve up to 97% of average correct movement and gesture recognition from time domain (like is RMS, slope sign change and AR model) and DWT feature-space. In this study different hand gestures like hand opening and closing, thumb and wrist flexion and extension from forehand muscles were recognized.

Another example is using a set of features as an input to the neural network. In the comparative study by Tsenov et al. [60] the different neural networks (multilayer perceptron, radial basis function and learning vector quantization) were examined. Authors were able to distinguish between different movement types (thumb, pointer and middle finger contractions and hand close) as a discrete states. Trained networks achieved classification accuracies between 70 and 98 percent.

NNs were also involved to task of denoising and preconditioning EMG signals.

2.4 Decomposition

This chapter covers the introduction to signal decomposition methods.

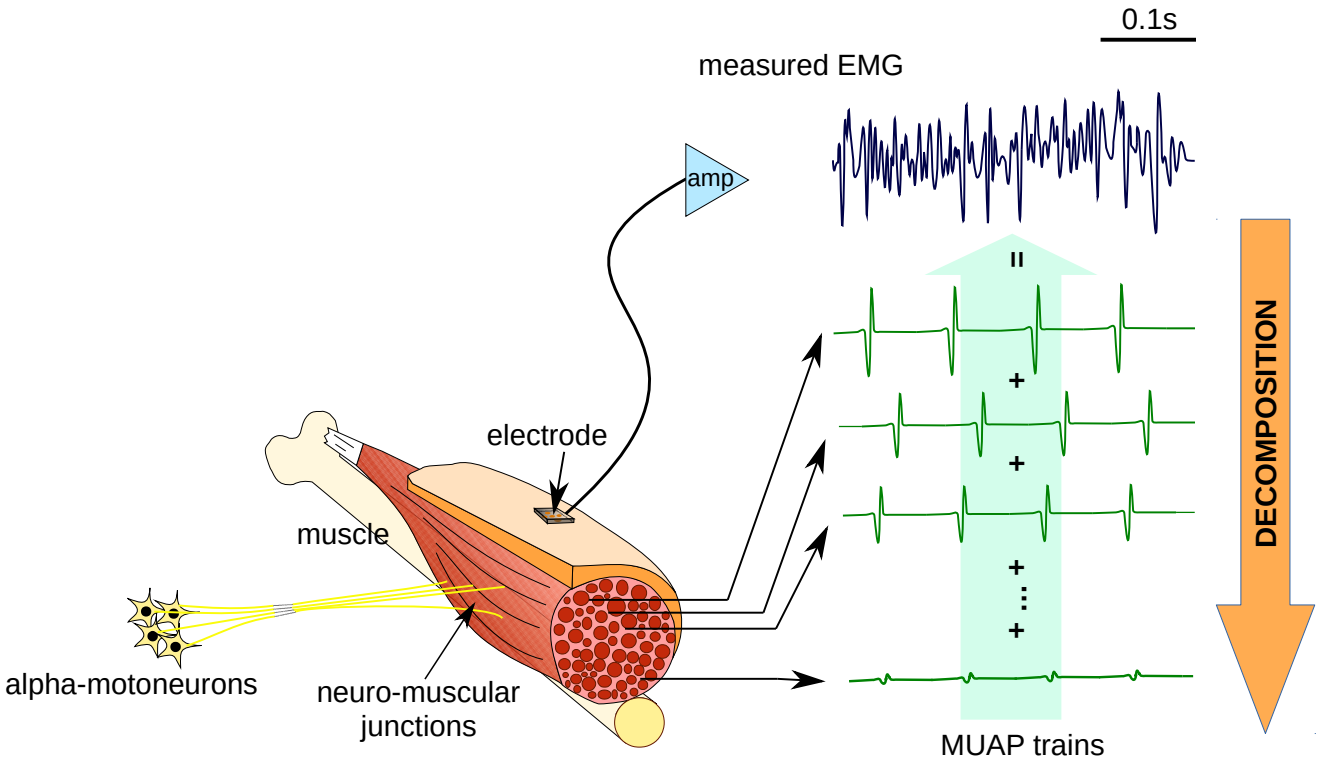

Decomposition is a process of sorting out the individual MUAP trains in EMG. Motor unit action potential corresponds to discharge of motoneuron in 1:1 way, thus proper decomposition describe precisely the neural drive sent to the muscle by the last neural layers of the neuromuscular system and provides information about behavior of single motoneurons and neural muscle control strategies. [1, 2, 91]

Decomposition to single motor unit action potentials as a method used for control may be utilized as an extension to detected feature set from EMG signal. Furthermore it gives us a better understanding of muscle control and physiology. In vast majority of works involving surface EMG for control is this step omitted. The word “decomposition” can be understood ambiguously in literature oriented on EMG. First, physiologically correct explanation is decomposition back to single action potentials from motor units. Up to date this approach is mostly used for physiological research and medical purposes – offline precise treatment. Second understanding is in essence feature extraction. In some works is decomposition of signal understood as preprocessing step (finding independent components, most variable components or trends) for better feature extraction sometimes also supported by simple statistics like mean average value, variance, zero crossing, etc. or more advanced techniques (direct neural network application). Task is extraction of unique signals for later distinction of

movements or states, their physiological origin correctness is for these purposes not so important. This is being achieved by learning classification algorithms by number of examples – transformed data from these methods are then virtual components corresponding to some process (rough distinct movement). Decomposition to single motor unit action potentials (in physiological understanding) is a valuable inter-step revealing more information about muscular behavior and helping better understand control processes in muscles. This may bring more precise control to human-machine interactive systems. In present the decomposition to MUAPs is mostly used for research and medical examinations.

The biggest challenge in signal decomposition task are superimposed MUAPs, especially in methods designed for low-channel count recording systems. It is appropriate to sum different approaches to decomposition of superimposed signals. Available works involve a large spectrum of various mathematical and analytical methods beginning with analysis in the time domain, using correlation, template matching iterative algorithms, higher-order statistics, blind source separation techniques, neural networks and frequency-time domain methods using wavelets, cepstral analysis and other transformations or combinations of all above. Some of approaches were concerned with achieving maximally correct decomposition and therefore were rather a decision support systems, because these algorithms needed an operator for supervision. Other approaches tried to be fully automatic, but many of them were intended only for offline data recognition due to their computational complexity or used method. Ideas and parts of these methods are often utilized in modern works, therefore were mentioned, but it is correct to take into account that some of them are from another computer era or for specific purposes.

Decomposition task may be divided into two subtasks. First of them – easier – is to extract single templates of MUAPs from signal. This may be achieved from low percentage MVC muscle activation signals, where is minimal occurrence percentage of superimposed MUAPs. Suitable methods of accomplishing this task consists of spike detector, maximum aposteriori classifier, correlation or time-frequency comparative method. Second part is decomposition of superimposed signals, which is not a trivial task regarding the characteristics of skin, which is acting as a filter, present noise and fact that new motor units are still being recruited, thus there is possibility of emerging new templates, which were not detected in nonsuperimposed signal. In signals measured during clenching over 40 percent of maximum voluntary contraction and above are nonsuperimposed MUAPs becoming very rare.

One of possible approaches to decomposition is raw brute-force method, i.e. trying various combinations and comparing them to actual detected pattern, but suboptimality of this method is obvious. For instance, if we have combination of 5 MUAPs, which may be present in superimposed pattern and we calculate with 100 sample length pattern with sampling 10kHz and known templates, then by brute-force method we have to try $\binom{5}{2}\cdot 100^2 + \binom{5}{3}\cdot 100^3 + \binom{5}{4}\cdot 100^4 + 100^5 = 12{,}011\cdot 10^9$ combinations, where binomicals are for

presence of signals, if we consider combination minimum of 2. And even if we use brute-force method, there is still possibility of wrong solution due to present noise and time-relative MUAPs (changing due to electrodes placement, sweat, physiological processes).

Following description of EMG processing methods is focused on decomposition in physiologic sense.

2.4.1 Time-domain methods

First attempts of automatic signal decomposition were supervised by expert operator and were only semi-automatic [3], but were able to achieve accurate decomposition up to 100 % MVC. Their importance shouldn't be ignored, since they were a good starting point for later development of automatic algorithms like is McGill's {ADEMG} (first automatic up to 30 % MVC) [6], De Luca's {PD[2]}, {PD3} [7] and {IPUS[3]} [8]. Used method for achieving decomposition was simple correlation – sliding known MUAPs templates over signal and detection of their presence. Automatic decomposition of superimposed signals was done using peel-off approach [57].

For decomposition into single MUAPs can be used simple spike detectors in combination with MAP receiver (also known as certainty classifier) for low levels of MVC (up to 5-20 percent[4]) are these methods very accurate. Same may be done by transposing MUAPs templates over measured signals – simple correlation and detecting potential presence of MUAPs. With increasing level of MVC more superimposed signal is obtained and therefore these methods needed superposition solver, which is in most cases implemented as an iterative algorithm. In some works are superimposed MUAPs simply ignored [104, 105, 106]. These algorithms are performing fast decomposition and working with acceptable accuracy for weaker muscle activations or for computing parameter like is MUAP conduction velocity.

2.4.1.1 Iterative superposition solvers

Iterative algorithms were first involved in superimposed MUAP solving task. In works [6, 8] of De Luca, LeFever, Newab et. al. and McGill {IPUS} {PD3} and their updated and revised versions[5] {IPUS-IGAT}[9], are examples of those created for decomposition of surface EMG signal only. They are an evolved versions of algorithms {ADEMG} and previous versions of {PD}, proposed in beginning of attempts to automatic decomposing signal into single APs. These algorithms are not suitable for real-time usage in human-machine interaction system – for instance [9] needs for decomposition of 1s of signal 3s on desktop computer (year 2010) processor (and coming thru whole signal more times). But

2 *PD stands for precise decomposition*
3 *IPUS stands for integrated procesing and understanding concept*
4 *this is an approximate value. Value depends on muscle type, type of used electrodes and preconditioning of measured signals.*
5 *Latest revision is called dEMG and is part of commercial system sold by Delsys, available at: https://www.delsys.com*

these algorithms were developed for purpose of precise and correct decomposition for deep research of MU behavior and physiologic investigation. Evolved commercial version (dEMG[6]) of {IPUS-IGAT} (iterative generate and test) [9] is actually one of most accurate approaches of precise decomposition. Yet unsolved problem and limitations of this algorithm are fast muscle activation changes (measured as fractions of MVC).

Generally two approaches are used in these algorithms: peel-off approach and model match approach (minimization of error function). Peel-off approach as term indicates is based on the progressive iterative subtraction of individual components from the signal.

For decomposing superimposed signals was proposed RLS (least squares algorithm) operating with least square estimates and also EM algorithm. EM algorithm was also successfully adapted on general superimposed signal decomposition problem [14]. The EM algorithm iteratively converges to local maximum[7] of maximum-likelihood estimate function. This method is also suitable for real-time usage and multi-input single-output system.

Last example of these algorithms is genetic algorithm – Florestal et al. [15] – combined with gradient optimization method. Algorithm iteratively generates random numbers, swapping columns and performing basic arithmetic operations, i.e. new populations and evaluates their fitness based on convergence criterion (measured by error function). This algorithm is very accurate and is capable of decomposing signals consisting of muscle activations over 90 percent of MVCs Unfortunately this method is not suitable for real-time recognition due to its computational cost and need for accessing all data. This algorithm was incorporated into EMGLAB [6] automated decomposition program, which was used in beginning of this work as testing tool of measurement setup.

2.4.2 Time-frequency methods and transformations

For purposes of signal decomposition into constituent MUAPs were used short time Fourier analysis, wavelet transforms, cepstral methods, independent component analysis and other variants. In its nature all methods were made to solve blind source separation task of a convoluted mixture.

In time-frequency representation the differences in energy locations of unique sources were observed [10]. Using spatial time frequency matrices (STFD) are calculated auto and cross-time frequency distributions from which is calculated the mixing matrix of sources. This method was used for multi-array electrodes and was suitable for signals up to 30 % of MVC, because for proper function was needed one non-overlapped pulse per source.

Wavelet transform is used in most cases as an analysis tool for stimulated EMG. Insight into EMG signal composition can be obtained when signal APs are convoluted with different

6 *Available at https://www.delsys.com*

7 *for reaching global maximum several starting points are needed*

MUAPs patterns (significant patterns are discoverable). Furthermore were wavelets used for denoising of signal as a preprocessing step [21, 22, 83] before decomposition.

2.4.2.2 Cepstrum methods

Cepstrum methods were also examined for MUAP shape estimation. [109] successfully applied their cepstrum of bispectrum reconstruction algorithm to wired and surface EMG signals. Method was tested on participants' muscles with and without loads during isometric contractions. Authors were also able to reveal an average appearance of the MUAP in the muscle from surface EMG and also estimate muscle crosstalk using this approach.

Recently [110] the homomorphic deconvolution using cepstral power transform was proposed for mean MUAP parameters estimation. The filtered spectrum obtained by homomorphic deconvolution (using cepstrum) is used to fit the mean parameters of the MUAP model function related to the shape and magnitude (amplitude, phase and length) using Levenberg-Marquardt nonlinear regression. Cepstrum based deconvolution removes the effect of stochastic impulse trains, that originates in surface EMG. Method utilizes 2s time windows and is proposed for fatigue estimation.

2.4.3 Blind source separation methods

BSS methods are built on a mathematical model of the MUAP mixing process.

2.4.3.1 Higher order statistics

Significant contributions on decomposition of signals revealed Holobar and Zazula et. al. [10, 11, 12, 13], whose proposed utilizing higher order statistics. Firstly, was proposed usage of ARMA[8] model for identification of measurement system transfer matrices.

In their work [11] they used third order cumulants for solving superimposed MUAPs. Third order cumulants (and higher) are blind to measurement of Gaussian noise, therefore signal to noise ratio is boosted due to nature of the method. Using Fourier transform on third order cumulants one obtain bispectrum (2D correlation[9] over two time delays), which is method used to search for nonlinear interactions, since it provides description to a continuous pseudo-random signal. This method is robust, but computationally demanding and thus is not suitable for real-time usage. Method was proposed for large-array electrodes. This investigation was proposed for use in medical field for analyzing muscle disorders.

---

8 ***ARMA*** *is abbreviation of* ***A****uto* ***R****egressive* ***M****ean* ***A****verage.* ***AR*** *part may be understood as predictor,* ***MA*** *part acts as a noise filter (estimator). With the correct application of ARMA model one can obtain correct zeros and poles of transfer system and therefore knows also impulse response, which is in this case single MUAP.*

9 ***Correlation*** *is a second order statistic, it's third order variant calculates with 2 time delays.*

2.4.4.2 Convolutive source separation

Their work results into gradient CKC (convolution kernel compensation) method [13]. CKC method is computationally simpler, and therefore can be after few modifications used in real-time system. Method uses model for multi input – multi output system, where is needed higher number of outputs (electrodes) than inputs (recognized MUAPs). Large electrode array (in [13] were used 65 and 48 electrode configurations) placed above single muscle can be seen in section 2.2.2, fig. 9(b), p. 13. In general convolutive mixture problems are hard to solve. Model for convolutive mixture is defined as:

$$x_i[k]=\sum_{j}^{d}\sum_{\tau}^{M_{ij}-1} h_{ij}[\tau]\,y_j[k-\tau]+n_i[k], \qquad i=1..m.$$

where m is number of measuring sensors, x_i original source, h_{ij} transfer path filter and n_i is measured noise.

CKC method increases input sample count by K measured previous samples $\boldsymbol{x}$.

$$\boldsymbol{x}[k]=\left\{x_1[k],x_1[k-1],\ldots,x_1[k-K+1],\ldots,x_m[k],\ldots,x_m[k-K+1]\right\}$$

This is more suitable for MUAP decomposition due to time-spatial properties of surface EMG signals. K is usually between 10 and 20, which results in much larger unmixing matrix (up to 1000x1000). Most of instaneous source separation methods like is ICA are ineffective for solving such a big mixing matrices. Holobar and Zazula's CKC method bypasses the need of estimation of convolution mixing matrices by estimating the cross-correlation vectors between i-th MUAP and extended sample vector:

$$\boldsymbol{c}_{s_i\bar{x}}=E\left(s_i[k]\boldsymbol{x}^{\boldsymbol{T}}[k]\right)$$

In second step the correlation matrix C_{xx} of this extended sample vector is calculated

$$C_{xx}=E\left(\boldsymbol{x}[k]\boldsymbol{x}^{\boldsymbol{T}}[k]\right)=\frac{1}{N}\sum_{i=0}^{N-1}\boldsymbol{x}[k]\boldsymbol{x}^{\boldsymbol{T}}[k] \quad \text{(E is expectation)}$$

and unknown mixing matrix (convolution kernel) is partly compensated by calculating an estimation of the discharge patterns of the i-th MUAP using the estimated cross-correlation vector and correlation matrix. [71]

$$\hat{s}_i[k]=\boldsymbol{c}_{s_i x^T}C_{xx}^{-1}\boldsymbol{x}^{\boldsymbol{T}}[k]$$

Processing of the signal using CKC method may take 6 times longer time than is the signal duration.

Another update of the method [82] which is presented as online is faster, provides 90 percent recognition accuracy, but finds significantly lower number of MUs than the batch CKC version. Correlation matrix is updated iteratively. Authors greatly optimized CKC method since they lowered the processing of 1s of signals to around 0.6s on personal computer.

Batch CKC method was later also modified by including of K-means clustering algorithm (KmCKC) [116]. In paper authors compared results with previous CKC implementations and Bayesian linear minimum mean square error estimation of MUAP pattern and shown that modified method is capable of identifying more MUAP shapes than its predecessor.

2.4.4.3 Instantaneous mixture separation methods

Model for instantaneous mixture separation is way simpler. Recalling from section 2.3.5:

$\boldsymbol{x}[k] = A \cdot \boldsymbol{s}[k] + \boldsymbol{n}[k]$ thus computation of the unmixing matrix is also simpler.

Great tool for blind instantaneous mixture source separation task in general is independent component analysis, which was mentioned in previous subchapter. Independent component analysis (FastICA implementation) was also utilized for direct signal decomposition during isometric contractions [24] up to 20% MVC. Main task of this method is to find proper unmixing matrix. Process of finding this matrix is iterative, but then unmixing is performed by use of linear calculations. Again multi input electrode configuration over one muscle is needed and must incorporate at least same output count as sources (electrodes or measurements), which grows with MVC level. We have to take into account that noise is also one of these sources. ICA is able to separate only a non-gaussian sources, because Gaussanity is a measure of independence. Study compared FastICA results with PCA and shown that PCA was not suitable for this task.

In attempt [20], was ICA used as preprocessing step. There was extracted lower number of MUAPs than was electrode count (system outputs) – signals were separated to individual components, where was then performed searching of spikes by utilizing above specified methods. Results were acceptable to 20 – 30 % of MVC (these levels are maximum for most of real-time capable implementations). Method can be utilized for unsupervised muscle crosstalk removal. Validity of this method depends also on the experimental situation. In general is this method more suitable for sparse signal [25, 26], sparsity may be achieved by transforming into time-frequency representation, thus is suitable with combination of STFT, discreet cosine or wavelet transforms. In general ICA is not suitable method for signal decomposition because signals will have different shapes on further electrodes and it is needed also to consider contraction changes. Convolutive mixture model fits better for this task.

Convolved mixtures in time domain can be converted to instantaneous mixtures in frequency domain using Fourier transform and then unmixed using ICA algorithm. Signals can be estimated by using inverse Fourier transform. But this approach brings new complications like problems of scaling and permutation. [117, 118]

As was mentioned in chapter (ICA), there are various implementations of algorithm and one of the best performing in preprocessing of signal in decomposition task is second order

blind identification (SOBI) algorithm. [68]

Very recently was developed a novel method using FastICA and peel-off approach for high density EMG [113]. In latter study [114] was algorithm evaluated by comparison with Holobar and Zazula's CKC method where was demonstrated high agreement. Both methods are designed for HD EMG. In most recent study [139] was developed automatic implementation of the algorithm.

2.4.5 Neural networks

An approach of Graupe and Liu [16, 111] involving neural networks as a direct decomposition step of signal into MUAPs. This was done by combination of 2 NN – Hopfield and Kohonen. Hopfield network was used for extraction of properties (MUAP described as gaussian mixture) with maximum distinguishability. Kohonen's network was propsed for recognition of MUAPs from these parameters. Work is rather theoretical since it does not present any results. Another more advanced realization of neural networks was NNerve [17] - 3 layer neural network. This method was used for invasive electrode recordings. With few modifications would be usable for surface EMG. Result of these approaches wasn't 100 percent correct decomposition, but enabled a possibility of repetitive correct analysis for medical purposes (muscle diseases). There were classified larger number of MUAPs shapes than were truly in combined signal in most cases during usage of method.

Most accurate results (of NNs) were achieved by unsupervised learning neural network ART2 NN [18]. In contrast with previous NN implementations ART2[10] NN was less sensitive to the selection of training samples (superimposed spikes mistaken for single MUAPs), from which suffered its predecessor – NNerve. Neural networks have to be firstly learned with training vectors (MUAP shapes), which is achieved by utilization of spike detector and methods described in 2.4.1 on lower MVC levels. But in contrast to previous NN implementations, this one beside the shape also learns typical MUAP firing patterns (frequency) and is capable of online learning during recognition (memory is reinforced when known shape is found, in other case is stored new shape). Although ART2 NN is capable of online learning it was in study [18] used offline and came through data 2 times. Second pass improved identification accuracy. ART2 NN was capable of decomposing up to 5 independent shapes and was tested for very low muscle activations (5% MVC). Method was targeted for diagnosis of neuromuscular disorders. Usage of streamlined form of ART2 called ART2-A would probably highly accelerated classification system and enabled online recognition faster.

10 **ART2** *is an abbreviation of* ***A****daptive* ***R****esonance* ***T****heory*

2.4.6 Conclusion

Up to date doesn't exist universal real-time absolutely correct method for decomposing of surface EMG signal. Developed surface EMG decomposition methods up to date usually identifies between 5 and 50 MU per contraction over the muscles, where may be active several hundreds during high contractions. [7, 8, 13, 82, 116] Most precise algorithms up to date are iterative time-domain IPUS-IGAT [8], gradient CKC [13] and KmCKC [116] which are operating offline. Gradient CKC is provided in commercial software DEMUSE[11]. Evolved version of IPUS-IGAT is provided in commercial package from Delsys[12]. Every method has its limitations and usually decomposes up to tens of individual MUAP individual shapes during contractions in which can be active hundreds of MU. Most of accurate precise decomposition methods are used for studying neuro-motoric diseases (like is for instance ALS[13]). Commercial software for these purposes is fully automated with manual signal editing options. Time-domain template matching iterative algorithms are able to solve this task with single channel measurements, whereas CKC and blind source separation methods require higher channel count recordings. CKC based methods are intended for HD EMG.

Online decomposition methods are summed up in chapter 3.3.

11 *Available at https://demuse.feri.um.si/*
12 *Available at https://www.delsys.com*
13 **ALS** *is abbreviation of* ***A****myotrophic* ***L****ateral* ***S****clerosis*

2.5 Control system requirements / targets

Measured surface EMG signal is affected by physiological factors:

- **muscle anatomy**: size of motor units, number of motor units and their distributions
- **muscle physical factors**: level of training, muscle or nerve disorders, fatigue onset
- **biological signal artifacts**: crosstalk between muscles, ECG interference

and also by measurement equipment setup:

- **electrode** – amplifier configuration (unipolar, bipolar, IB2, …)
- **electrode properties**
- **noise artifacts**: electronic device interference, mains power interference, electrode movement

Signal and motor unit strategies are affected by **speed of contraction**, **level of muscle activity**, **level of fatigue** and if contraction is **constant isometric** or **changing**. All of these factors should be considered while designing human-machine interaction system based on surface EMG. Furthermore such system should meet these requirements considering also applicability as assistive technology [81]:

1) **intuitive**

2) **robust**

3) **adaptive**

4) **minimal number of electrodes**

5) **easy training and calibration**

6) **feedback**: can be implemented for instance visual, presure or by vibrations

7) **low consumption HW**

8) **reasonable response time**: delay should be under 200ms [81], some works formulate under 300 ms [61]

3 Related works

Previous section described methods used for surface EMG processing and its decomposition. This section contains a brief review of works concerning utilization of surface EMG for real-time control and human-machine interaction. Mentioned is representatives of gesture recognition approach and works targeted on force estimation methods. Very recently emerged also few works, which propose decomposition as a step in surface EMG signal processing.

3.1 EMG signal for control

Most of works which proposing surface EMG signal for control of prosthesis or human-machine interaction trying to incorporate better classification techniques to recognize different grasps and patterns in surface EMG. These methods are mostly exploiting the presumption that for similar movement, similar MUs are activated, which would on average result in similarities in summed measured signal. Recognized grasps are discrete like commands, which can be utilized in active prosthesis (next section) or in human-computer interface.

Wheeler et al. [23] achieved very satisfactory result by involving moving average feature extraction for 4 channels of signals gathered from forearm with combination of hidden Markov models as recognition step. This method was used for classifying joystick-alike movement (4 classes: left, right, up, down) and digit typing control (using 3 fingers for typing on numeric keyboard – 9 classes). Study also mentions signal decomposition to MUAPs using modified version of dVCA for EMG (most differential variable component analysis, Bayesian approach), but technique is rather presented as blind source separation method to obtain clearer signals from fine movement control muscle groups and details about decomposition accuracy results using this technique are unclear. The method also had originally recognition delay of 1.5s, which authors optimized to 176ms at the expense of lower robustness, which is 83 % for joystick-like control and 88 % for digit typing using 3 fingers (calculated from presented confusion matrices). Authors used both dry and wet electrodes. Wet were used for digit typing due to weaker movements and corresponding weaker surface EMG signals.

Combination of wavelet transform and neural network was also applied on surface EMG signal. In this type of networks the radial basis functions (RBF) are replaced by wavelet functions. Neural network is then optimizing during learning phase not only weights, but also degress of freedom, which are represented as scales and positions of wavelets. Wavelet network computes features, which are input for second artificial neural network acting as classificator. Method operates on 1 differential input channel only and is able to distinguish between 5 movements. Method must be learned on individual subjects data to reach between 75 and 96 percent of accuracy (in study tested on 2 subjects only). Work from 2016 [87] uses also wavelet neural network (WNN) and achieves accuracy 95 % on 3 surface EMG input

channels. Study exposes information that recognition was most accurate for Morlet wavelet I and Gaussian wavelets. Similar results are reported also by other authors incorporating neural networks and many other classifiers for grasp recognition. In works where researchers tested day-to-day performance with trained model from previous session were observable accuracy decreases.

Zhang et al. [79] tested different feature sets as time-domain (1) MAV, RMS, ZC, WL, SSC, AR coefficients, frequency (2) MF, MDF, MP, WT coefficients, (3) sample entropy, nonextensive entropy and fractal analysis and combined (4) RMS, WL, SSC, WT coefficients. All of tested performed similarly (94-97) success rates but with very different processing times (worst for sample entropy and fractal analysis best for (1)).

Approach of Zhai et al. [128] does not provide such accuracy (78%) as methods mentioned before, but introduces self-recalibration ability on convolutive neural network. Self-recalibration ability is important for real-life every day usage due to day-to-day variability of surface EMG. Input of the network are PCA reduced sEMG spectrograms. The work used only measured testing datasets, which were analysed offline. Method was learned using only one grasp repetition. Similarly work of Liu [143] utilizes incremental adaptive SVM, which is also considering the overtime signal changes.

Summary of approaches and its performances is in table II (next page). Table lists theoretical studies from pioneering era of pattern recognition. Interesting is for instance Graupe's et al. Study [59], in which authors describe method written for 8080 CPU, where processing took about 2.5s with promise to speed up on 200ms with newer Motorola 68000 CPU. Follows very valuable comparative studies [60, 62, 68, 79, 131] comparing different features, feature sets, source separation methods and classifiers. And finally table contains also interesting concepts [23, 128, 136] or review [145] on HDEMG pattern recognition methods, which processing surface EMG by methods similar rather to image processing (ie applying 3x3 median filter, etc). All of them are a valuable inspiration for a researcher in signal processing.

Problem of most approaches based on learning algorithms is their day-to-day need of retraining and re-calibrating for each individual user. Most of the works listed in the table are targeting the rule of achieving recognition under 300ms, physiological muscle motion response is between 30-100ms. Many of works also doesn't describe the electrode build, size and inter-electrode distances, from which may reader get idea about the signal characteristics, acquired bandwidth and probable level of noise. Multiple works selected moving average feature as the best one from various tested, followed by AR coefficients and wavelet packed transform. Mostly utilized classifiers are neural networks (multi layer perceptron type), linear discriminant analysis and support vector machine. Many of concepts were also tested only offline in laboratory conditions with data set for learning and testing measured during same session and of course the performance in real-life conditions notably decreases.

Table III – Overview of methods utilizing machine learning methods for discrete grasps and movements recognition

Ref.	Methods	Accuracy [%]	Electrode no. [-]	Recognized movement classes [-]	sampling [Hz]	window [ms]	electrode type	features	bandwidth	feature reduction method	electrode distance [cm]	electrode size [cm]	experiment type
Graupe, 1982 [59]	Nonlinear discriminant functions	99	1-2	3-6	500 (300-2500)	160-240	?	AR coef, IAV	?	-	-	>2	online
Lee, 1984 [67]	Bayes classifier	91	2	3	6250	160	?	VAR, ZC	?	-	-	?	online
Ide, 1991 [63]	Fuzzy inference system (FIS)	80-90	1	5 (6th rest)	?	?	Ag/AgCl gel	FFT	up to 1000	-	-	?	online
Englehart2001 [61]	LDA	98	4	6	1000	256	Ag/AgCl gel	WPT (TD,STFT,WT)	10-500	PCA	2	?	offline
Itou2001 [136]	ANN	70	3	6	64	?	Ag/AgCl gel	Integrated EMG (rectified 2,6Hz)	-	-	Approx > 2	>2	online
Englehart, 2003 [65]	LDA	87-94	4	4	1000	256	?	MAV,ZC,SSC,WL	10-500		?	?	offline
Crawford, 2005 [66]	SVM	90	7 (unipolar)	7	2048	128	gel	MAV	-	-	-	?	online
Wheeler2006, [23]	HMM + dVCA	83/88	4	4/9	2000 (6000)	176	dry/gel	MAV	-	-	prox 2 wet/0.5 m	wet/electroc	online
Tsenov, 2006 [60]	ANN (MLP,RBF,LVQ)	93/84/88	2	4	4000	512 (64)	Ag/AgCl gel	STFT,MAV,VAR,WL,ZC	-	-	Approx > 2cm	approx >2cm	comparative
Arvetti, 2007 [47]	WNN	87	2 (unipolar)	5	500	100	gel	MAV,dMAV,ZC,SSC (AR coef, Wtc)	-	-	-	?	offline
Kherzi, 2007 [37]	adaptive neuro-fuzzy (ANFIS)	97	2	6	1000	200	gel (?)	MAV,SSC,AR,WT	20-500	PCA	?	?	online
Kakoty, 2009 [33]	Haar WT + SVM	86	2	6	5000	480	Ag/AgCl gel	Sum of WT coefs,	10-2000	-	?	?	offline
Karimi2011 [129]	ANN (optimized by Genetic algorithm)	98	16 (s) 6 (i)	10	1000?	?	needle/dry(?)	WT (DB44), STD	10-500		2		online
Kherzi2011 [130]	Neuro-fuzzy (ANFIS)	62	4	6	1000	200	?	MAV,SSC,AR,ZC of DWT	20-500	-	?	?	offline
Naik, 2011 [68]	ICA (SOBI, Infomax, JADE,...) + ANN	97	8	4	1024	-	dry wire	RMS, ICA (various)	-	-	1	0.1x1	comparative
Alkan, 2012 [131]	5 Discriminant analysis + SVM	96	2	4	1000	250 (pattern)	?	MAV	-	-	?	?	comparative
Phinyomark, 2012 [62]	LDA (comparative study)	45 – 89**	5	6	1000	256	gel	various	10-500		2	2.5	comparative
Delis, 2012 [132]	LDA / ANN	98/97*	8	6 (7th rest)	3000→1000	256	Ag/AgCl gel	AR coef (4, 6)	?	-	?	?	offline
Wang2013 [141]	SVM / LDA	98	2	8	1000 (12bit)	256	dry ?	10 sets (time, freq)	10-500	-	Approx 2	?	offline
Shin2014 [142]	Bayes/kNN/LDA/QDA/ANN(MLP)/Dec.	66-92	2	6 (7th rest)	1000	150 (50)	?	AR(4,6),MAV,WL,ZC,SSC,RMS	-	-	?	?	comparative
Xing, 2014 [133]	SVM	98	4	6 (7th rest)	1024	500 (250)	Ag/AgCl gel	WPT	2-750	multiple	Approx 2	>2	comparative
Zhang, 2014 [79]	Minimum distance classifier	97/95/94/96	4	9	1000	128 (32)	Ag/AgCl gel	4 groups	10-500	PCA=>LDA	>2	>5	comparative
Liu, 2015 [143]	incremental adaptive SVM	97	8	6 (7th rest)	3000		Ag/AgCl gel	MAV,ZC,SSC,WL,AR	10-400		1.9	1.25	comparative
Mane, 2015 [144]	ANN	93	1	3	1000		dry	mean of local max of WT(bior,coif,db,sym)	20-450	-	1	0.1x1	online
Duan2016 [87]	WNN	95	3	6	1500	200	Ag/AgCl gel	WT (various)	-	-	2	>2	online
Geng 2016, [145]	ANN(MLP),SVM,LDA,HMM,kNN,CNN,R	varies	8x16,7x24	8	100 (1000,2048)	200	HDEMG array	Varies (MAV,AR,MF...)	LP 75	-	0,75x1,05	tiny	comparative
Zhai, 2017 [128]	Self-recalibrating CNN	78	12 (offline db)	10	2000	200 (100)	-	Spectrogram	reject 50Hz	PCA	-	-	offline

* calculated from confusion matrices

** various features gave different results

NWFE – nonlinear discriminant analysis method = non-parametric weighted feature extraction

3.1.1 Advanced prosthetics

Designing system with an intuitive control is a challenge for researchers developing artificial limbs and prosthetic system. Intuitive control means reduced learning time and effort for an impaired user.

First pioneer attempts of artificial limb control using EMG were around the early 1950's, in USSR, then in Europe Canada and USA. [59] Despite that up to date most of current commercially available prostheses offers very limited movement controlled by on/off regulator (with set threshold) on detected filtered rectified signals from 2 surface EMG channels, which means less or equal to 2 degrees of freedom (DoF). This phenomena is naturally understandable since usage of simpler robust methods means less possibilities of system failure and complications. However, these solutions are superior to cosmetic prostheses. Example of this approach is Ottobock SensorHand™. Similar are solutions like i-Limb hand, Motion Control hand or BeBionic3, which was recently acquired by Ottobock. I-Limb is controlled by 4 different triggers from 2 channel EMG signals – hold, double impulse, triple impulse and co-contraction. These artificial limbs are providing low number of degrees of freedom and needs user to learn control of the devices. [33]

Prostheses like Southampton hybrid, MANUS or Fluidhand (offering 16 DOF) are using method to switch between different discrete grasps. Developed prosthetic system like AR III Hands System and Cyberhand are using individual finger control approach.

Most advanced projects are Smart Hand, UNB and DARPA's Revolutionizing Prosthetics program, which proposes system actuating up to 23 DOF in dependency on level of amputation or utilizing different bio signals otherwise. All of these allow user to make a grasps with all fingers.

Reconstruction of finger movement can be found also in variety of studies [137, 138]

3.2 Force estimation methods

Mean average, average rectified value, root mean square in combination with smoothing filter, integrated EMG and various low-pass filters are used to estimate force by most studies targeted on force estimation.

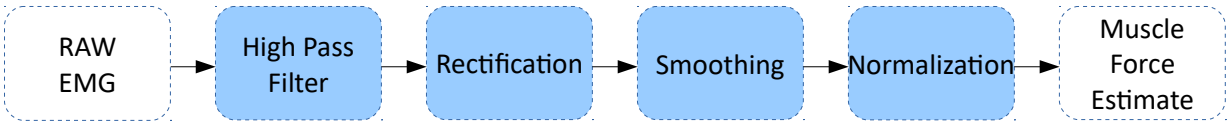

Figure 16: Typicial force estimation signal processing pipeline

Usual processing pipeline for muscle force estimation consists of rectification (or feature selection, that describes muscle force), low-pass filtering and normalization to measured real force using newton meter up to 100 percent of maximum voluntary contraction.

Recommended optimal low-pass filter settings of the rectified EMG signal for muscle force prediction is between 2 and 3 Hz. This values represent compromise between the dynamics of EMG, muscle force and time lag of the signals. [112]

Sanger [97] proposed Bayesian filtering method for estimating of the muscle contraction force. In study he tested method for muscle forces between 5 – 25 percent of MVC and compared results to classic approaches using low pass filters (0.1 – 5Hz). Method offers more rapid response and more stable results than linear filtering methods for this range. Author used 1000Hz sampling and 100 point time window and stated that optimal for this method would be 1000 point. Values for the method were found empirically.

In recent years was for this task also utilized continuous wavelet transform in combination with artificial neural network trained to derive mean-frequency (fatigue detection) relationship for later accurate muscle force estimation [101]. ANN was trained by normalized measured values with torque meter and corresponding normalized surface EMG mean frequency parameter (to maximum value) calculated by CWT. Researchers obtained correlation coefficients between estimated force and measure force 0.94 in average.

Zhang et al. [102] tested various features (MAV, IEMG, WL, VO, WA, logD) for predicting muscle force from surface EMG in combination with SVM, ANN and locally weighted regression LWR. Their study revealed that combination of MAV and ANN (back-propagation) performs best for this task. They reached similar correlation coefficient (0.94) as [101].

EMG based muscle force estimation using motor unit twitch model was presented by [73]. In study was incorporated offline decomposition method based on convolution kernel compensation method developed by Holobar and Zazula. They shown that this method for force estimation yields lower error and higher correlation coefficient with real measured force than amplitude based estimations (compared with Potvin method [85]).

3.3 Real-time decomposition intended for human-machine interaction

There are few attempts trying to utilize online surface EMG decomposition for control purposes up to date. Each of these is targeting different achievement – for instance detecting multiple gestures from just one EMG channel, creating online decomposition algorithm for later use in control applications or online muscle force estimation.

Into group of online algorithms can be also included Glaser's online CKC method [82], but since this work aims on low acquisition channel methods is this method only mentioned.

3.3.1 Detection gestures from a single EMG channel

Xiong et al. [80] uses a custom algorithm based on spike detection and sorting to decompose signal into several MUAPs. Algorithm does not consider superimposed signals. From decomposed MUAP trains were after decomposition extracted 4 features: integrated absolute value, maximum absolute value, median non-zero value and index of median non-zero value in 800ms time windows. Surface EMG signals were acquired using Ag/AgCl electrodes with 8mm radius, inter-electrode distance was 20mm. In this study authors' algorithm successfully recognized 5 gestures using LDA from a single surface EMG channel with differing accuracy for each gesture varying from 50 % to 98 % with mean 75 %. Authors doesn't mention the recognition delay, however since the method is utilizing an 800ms window with 200ms overlapping, it would be highly probable over 200ms. Authors successfully improved the classification of grasps from single channel 75 % vs 53 % using same feature set on RAW EMG without decomposition involved and proved that decomposition could refine accuracy of recognition, although resulting accuracy doesn't outperform non-decomposition pattern recognition methods in any way.

3.3.2 Online surface EMG decomposition

During development of the proposed system (section 4) emerged promising study [57], where authors were able to decompose and classify signal in 50ms windows with 25ms overlap. This process took only 5ms of CPU time on common desktop computer. They utilized a modified version of template matching method with bank of filters. Superimposed signal is solved using peel-off iterative method. The algorithm is able to decompose up to 99 percent MUAPs at low MVCs. Method requires previous knowledge of MU templates and fails for weak MUs. The algorithm was able to decompose up to 5 overlapping MUs on real EMG data and performance varied from 53 to 100 percent of accuracy. But due to needed prior knowledge of MUAP shapes and fact that MUAP shapes tend to change in time is not usable for real-time experiments. Algorithm is applicable on single channel recordings.

3.3.3 Online surface EMG decomposition for force estimation

Muscle force can be calculated from MUAP rate firing/s, activity index or by aplying muscle force twitch model [73, 74]. Authors of very recent study (Sun et al. [138]) bypassed this by direct calculation of the force by multiplication of windowed signal with inverse of learned sparse matrix and by thresholding the obtained coefficients. Study shown that surface EMG decomposition used for force estimation is less sensitive to fluctuations for higher percentage levels of MVC than classic amplitude processing approaches. In study authors needed only one channel of surface EMG and decomposed signal using recursive independent component analysis. Segments of single channel signal are reshaped to sample data matrix and unmixed by FastICA algorithm. Searching for peaks in learned basis is then performed and most representative shapes are selected to form a sparse matrix, which inverse form is then used for calculation of muscle force by multiplication with windowed signal and thresholding. Authors showed that they used algorithm to control prosthetic hand. The used Ag/AgCl electrodes were >5cm in bipolar configuration.

4. Methods and system description

4.1 Measurement setup

4.1.1 Amplifier

The first tests of decomposition measurement system setups were done on custom made 4 channel amplifier in combination with National Instruments USB acquisition device. Amplifier can be divided to 3 parts: preamplifier with low-pass filter, amplifier with high-pass filter at 150 Hz and a low-pass filter at 2kHz. These values were chosen to sharpen the individual motor unit action potentials. The muscle crosstalk cannot be removed by a simple filtration as was mentioned in chapter 2.2.3.2, but it still holds that signals from nearer MU are less blurred than from further ones, therefore this highpass filter settings focus the system on nearer units and making the signals sharpener for easier decomposition.

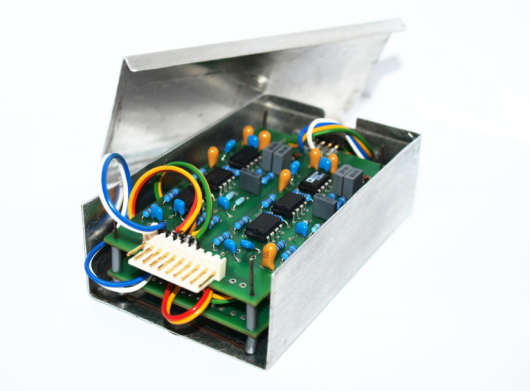

Figure 17: First version of 4 channel amplifier

For these purposes was chosen the AD620 biomedical grade amplifier with high CMRR (common mode reject ratio). Design of circuit was done with respect to minimizing of channel cross-talk. Simplified scheme of one channel can be seen on diagram in figure 18. Scheme begins with high-pass filter for filtering DC component from signal and design allows to connect it for differential amplification (this is important for actual electrode setup) or with common reference.

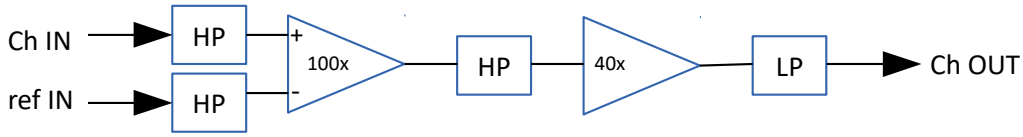

Figure 18: Simplified scheme of one amplifier's channel

Signals are being pre-conditioned by filtering with above described band-pass. Selected

value for high-pass filter is 150Hz. This step is needed with respect to physiology of signal generation. As was described in chapter 2, it is possible to detect signals from deeper and farther motor units on lower frequencies, but superimposed MUAPs from these units is practically impossible to decompose in realtime with low number of input channels. Therefore these low frequencies are being filtered and signal is being focused on nearer units. 150 Hz filtering moreover rejects movement artifacts, which typically emerging up to 20 Hz. Filter also attenuates omni present power line “50 Hz” and would remove possible ECG activity (up to 100Hz). Using this high-pass filter are signals absolutely rejected up to approximately 30 Hz. Signals between 30-150 Hz are present, but do not drown signals on higher frequencies. Furthermore it attenuates part of signal, which is not relevant for force estimation, which was shown by Potvin and Brown [85].

High pass filtration was designed in analog part of the device to prevent amplifiers from saturation with higher energies of lower frequencies and prevent possibility of effective signal loss in unwanted artifacts.

Low pass filter at 2 kHz is used as an antialiasing condition and also as high frequency artifacts noise-rejection filter. 2kHz value was chosen as a consequence of physiologic limits (skin low pass). Anything above this limit is with very high probability only high-frequency noise.

Amplifiers are set to high Amplification level (4000 times – most of the studies use 1000), because it is needed to amplify weak differential signals, that were obtained from small surface area and also notable part of EMG energy was filtered out (in opposite to classical surface myography, where are mostly desired signals in range 10-500Hz).

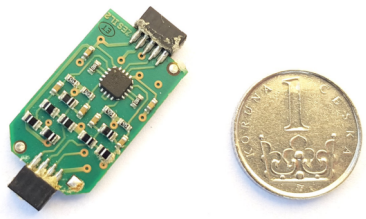

Figure 19: The third revision of developed 4 ch pre-amplifier

For later revisions of the system was designed tiny preamplifier (fig. 19), which can be snapped to body near to recording electrodes.

4.1.2 Electrodes (and tests)

4.1.2.1 Wire electrodes

In combination with above specified amplifier were used special custom made electrodes – pentodes (see fig. 20). Standardized gel surface ECG electrode were used as grounding. Similar electrodes for surface are proposed by De Luca [8] and Zaheer [5].

Following setup performs spatial filtering, which has positive results in suppressing of the muscle crosstalk effect.

As can be seen on diagram (fig. 20), these electrodes are used for gathering signals from small surface area, in other words are focused on small space (subtraction performed using differential amplification), measured signals are weak and thus mentioned large gain is needed. Before start of experiments the skin was only cleaned with soap.

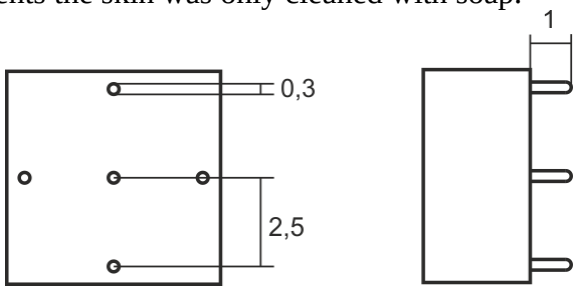

Figure 20: Scheme of used 5-pin electrode

In experiments were tested different sizes of gaps between pins of electrode. From smaller one was signal weaker, but contained sharper peaks (more higher frequencies signals). Taller ones contained higher percentage of blurred signals, this effect was present apparently due to gathering signal from larger area and also from further and deeper MUs (more MUs were imposed in signal). Optimal for decomposition in current configuration were pentodes with 2,5mm gaps between pins. For muscles with bigger motor units (biceps brachii, sartorius) were more suitable electrodes with gaps 8 mm.

4.1.2.1 Tests of the setup

The first tests of electrodes and amplifiers with filters were performed on thumb control muscles (abductor policis and flexor policis) and facial muscles. In these experiments were examined signal to noise ratio and maximal number of decomposable MUAPs. This was done using EMGLAB [6] at the beginning of the study [P1]. Using this setup was possible to decompose signals up to 70 percent of MVC and up to 20 MUAPs using offline method. In figure 21 can be seen very clean example of signal measured using 5-pin wire electrode in very low interference laboratory conditions.

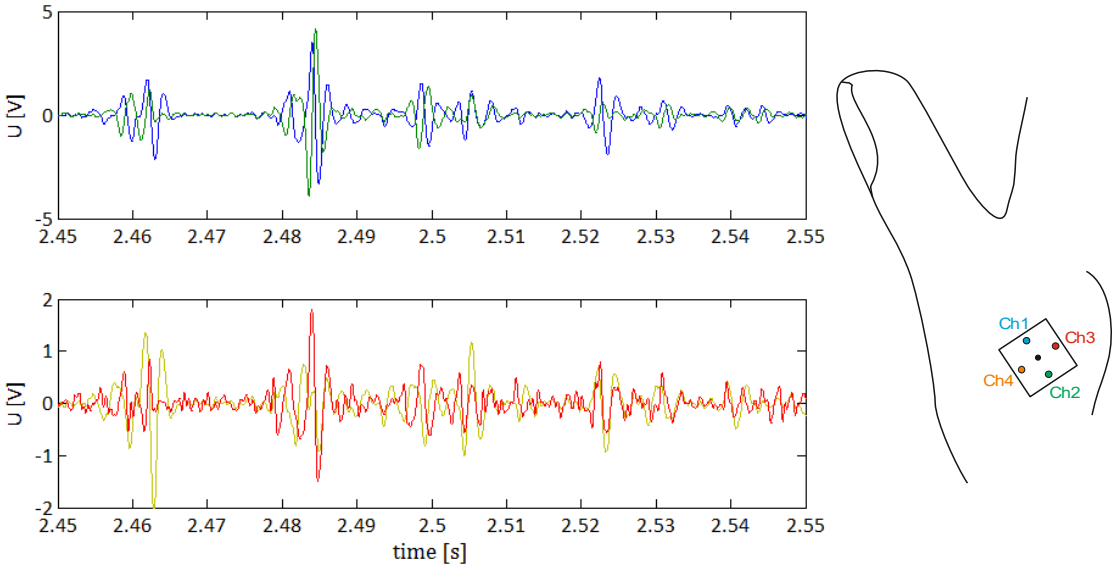

Figure 21: Placement of 5-pin electrode and its signal output, low contraction, MUAPs are observable by eye; in channels is also observable transition delay and reversed phase of signals (ch1-2 and ch3-4) due to electrode setup (reference is negative input of amplifier, whereas all channels are positive inputs)

Signal to noise ratio depends on level of muscle activation (signal strength) and also differs with muscle. For lower muscle activation signals (10%) were obtained signal to noise ratios from 12 to 15 dB in low interference laboratory conditions. Table shows results of tested setup. Input signal to algorithm was a single channel differential signal computed by normal double differential mask.

Table IV – results of decomposition test using EMGLAB

MVC [%]	decomp. MUAPs [-]	SNR [dB]
10	4 – 7	14
30	5 – 7	15,5
50	5 – 8	18
70	14 – 22	21
90	unsuccessful	26

Amplifier was powered using batteries, but in some circumstances there was a lot of noise coming thru USB port and digitization card itself. Some notebooks used with this setup transmitted interference signals around 400Hz-1kHz, which saturated amplifier, signal was then lost in noise. Also, there were problems in areas with fluorescent lights and sometimes undiscovered sources of interference… Probably most important was a proper grounding – otherwise there supervened problems with higher harmonics of 50Hz. Participants also mentioned uncomfort while wearing this type of electrodes. Consequence of these complications was impossibility of using this system in dynamic experiments or out of lab.

Online implementation of decomposition algorithm (described in section 4.2) was able to extract up to 4 templates. Signal distortion and problems with noise sources (with some laptops and on most locations) were impulses for redesign of hardware solution (section 4.1.3)

and also test different electrodes. With this setup emerged problems with usage of real-time decomposition due to high levels of amplified noise (especially out of lab).

4.1.2.2 Ag/AgCl electrodes setup

Described electrode setup in previous section works well for signal decomposition itself in laboratory conditions, but for real-life (and realtime) applications and dynamic experiments it is not suitable due to measured high noise levels (high impedance of electrode) and sensitivity to movement of the electrodes, which was proven to be an issue during tests with participants. Therefore in later steps of development of the system the classic ECG Ag/AgCl electrodes were used. These electrodes sticks well on the skin and provides much higher signal to noise ratios. Shape of the electrodes can be cut down to smaller form factor (fig. 22) to obtain wider bandwidth sharper MUAP signals from smaller skin surface.

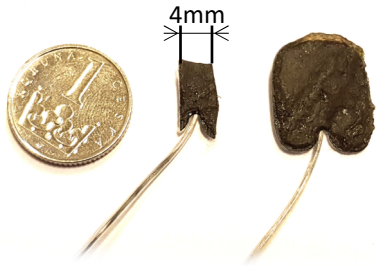

Figure 22: Cut down Ag/AgCl electrode

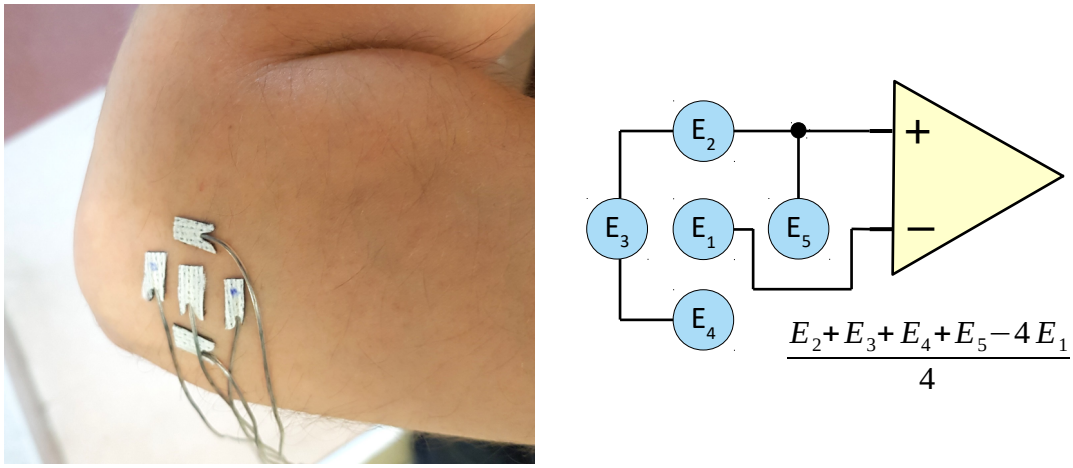

Figure 23: Laplacian differential electrode connection in branched configuration for low number of amplifiers setup

Figure 24 shows difference between 1:1 raw EMG acquired using standard Ag/AgCl electrodes in differential configuration and cut down Ag/AgCl electrodes in branched differential configuration over same muscle (f.d.i.). Graph shows visual evidence that signals from classic Ag/AgCl electrodes contains more superimposed signals and are more blurred, whereas branched configurations contains higher frequencies.

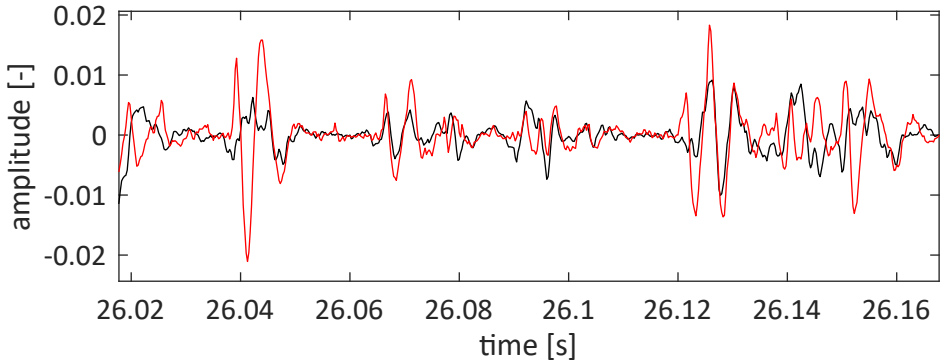

Figure 24: Comparison of signals in time domain acquired using standard Ag/AgCl electrodes (black) and cut down Ag/AgCl electrodes (red) in branched configuration

Difference in acquired bandwidth is observable in figure 25. Spectrum of branched electrode was multiplied by 2, since signals are weaker.

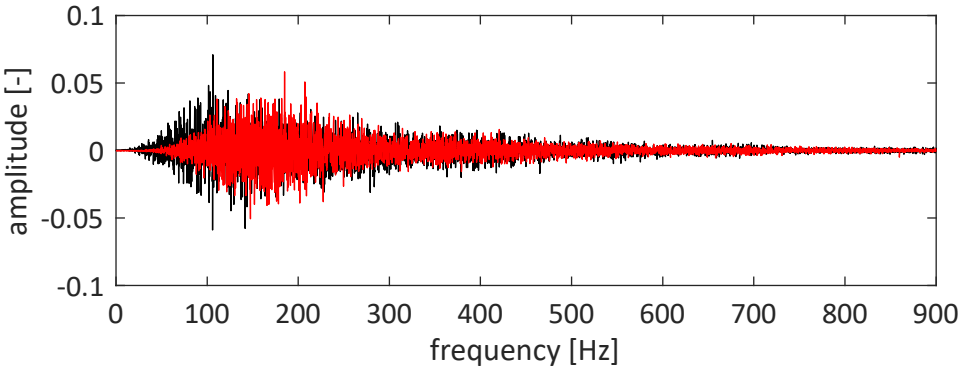

Figure 25: Comparison of spectra - standard Ag/AgCl (black), cut down Ag/AgCl (red)

4.1.3 Digital processing

During development were designed several revisions of measurement system for various purposes – precise measurement, high portability, stand-alone operation without computer and finally combination of all. In this subchapter are mentioned most notable setups.

In first setups and experiments the developed amplifier was connected to National Instruments digitization card (NI6015USB). For experimental purposes the digitization was set to 20kHz sampling rate (10 times higher rate than the skin low pass effect and the antialiasing filter limit value). For later analysis was then signal decimated to 5 kHz.

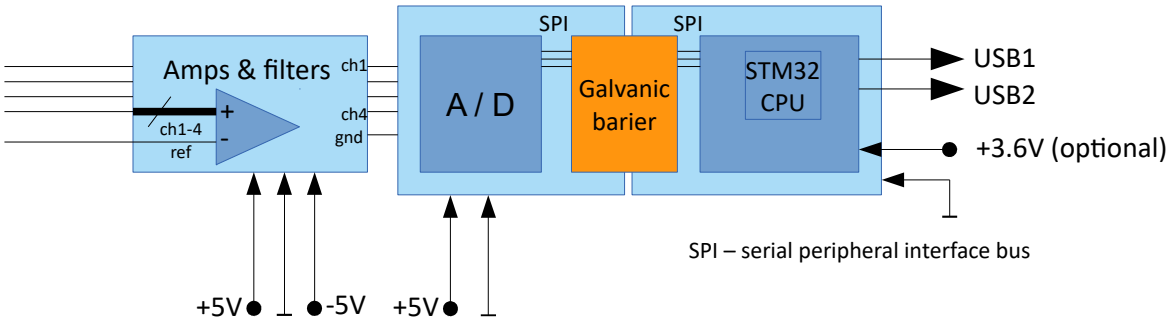

Figure 26: Scheme of hardware solution for pentode

The digital part of the device was designed, especially to achieve higher portability and get better noise characteristics during realtime tests with pentode. This solution (fig. 26 – scheme) consisted of precondition stage, amplifier part, digitization circuits, optical galvanic barrier and microprocessor, for which was implemented software in C language for ARM Cortex-M1 CPU – consisting of A/D setup part, A/D control, data collecting and finally, contains implemented protocol for USB data transmitting. Solution is scaleable up to 16 input analog channels, 10kHz and 16bit resolution per sample.

Later revision was modified to differential input design for all channels (Ag/AgCl electrodes), processor was updated to Cortex-M4 with floating processing unit and the force estimation algorithm was embedded into it. Also capability of driving an analog servos was added – 3 at once. This hardware revision was utilized in most of tests and human computer interaction studies.

Main reason of this effort was measurement hardware minimization (for direct snapping on body surface and to shorten cables with non-amplified signal) and also exchange of amplifier chips for their newer revisions, which promising better parameters – lower bias and higher common mode rejection ratio. Battery powered version of the system used on-board A/D of the STM32F4 chip, which delivered very similar performance with 12bit quantization, scalability up to 20 input channels and was notably smaller and more energy efficient than its predecessor. This version of amplification-digitization part also enabled possibility of outdoor testing and brought more dynamics into experiments (use for testing in VR environment, etc.).

Current solution of circuit design has option to be connected with joint reference for all amplification channels or to be connected differentially. This allows both described measurement electrodes setups.

Benefit of fully customized HW solution is completely known signal conditioning path, lower overall price of setup (if author's work not included) and also possibility of out-of-the-lab usage. Commercially available products offering same performance that are usable for same task are proposed for laboratory use (difficultly transferable) and during HW designing phase were multiple times more expensive. During development emerged solution by marketing name Myo[14]. Its early version's (spring 2015) API did not offer access to RAW EMG data and later revisions offered only 200Hz sampling rate. Myo was affordable, but didn't meet requirements for experimental setup.

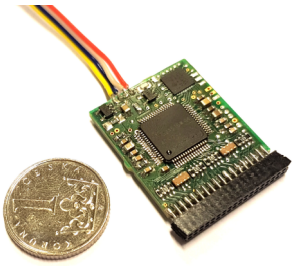

Figure 27: Latest solution based on ADS1299 chip and STM32F4 CPU

Most recent iteration of the custom hardware part is based on ADS1299 digitization chip. Solution enables acquiring data up to 8ch at 16kHz and 24bit per sample resolution. This solution enables greater variability in experimental setups, higher resolution and design is scaleable up to 24 channels (using 3 ADS chips on SPI bus), but hasn't been used in tests with participants described in chapter 5 since it was developed in later period of the project.

14 *Myo is wristband combining accelerometers and grasp recognition, available at: https://www.myo.com*

4.2 Real-time algorithm

This work tried to involve MUAP decomposition to recognize movements more precisely (for instance movement of fingers). Which may bring better estimation of muscle forces and recognition of smoother movements (low contractions) resolution. Proposed algorithms are partly embedded in external ARM CPU, decomposition is being processed in computer device driver.

On the diagram (in fig. 28) can be seen algorithm overview. System consists of 6 blocks. Their purpose is to obtain continuous muscle activity estimation and gather maximum possible control actions from measured surface EMG. Conditioning stage filters out noise and conditions the signal for easier later decomposition. Signal is then sent to block detecting approximate MVC using muscle activity estimator. For higher percentage levels of maximum voluntary contractions is signal analyzed only using muscle activity estimator, for weaker contractions is signal also analyzed using the decomposition block. Muscle activity estimator decides whether the decomposition block is involved. Outputs from decomposition block are then sent to force estimation model. Force estimates are mapped in middleware (section 5.2) mapping block on control actions or analog controls used in human-computer interface.

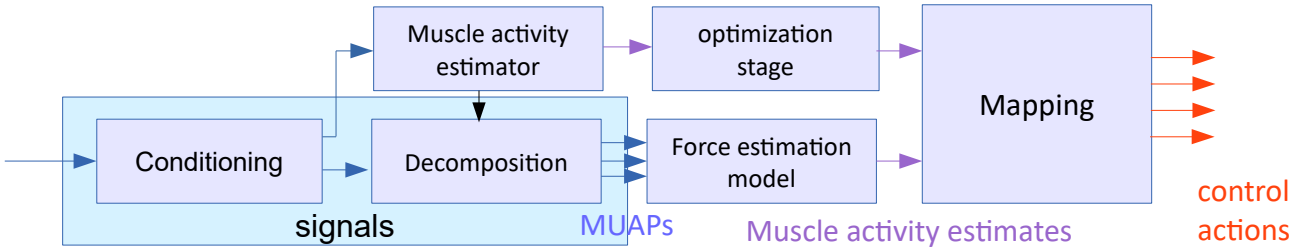

Figure 28: Diagram of real-time algorithm

4.2.1 Preconditioning stage

4.2.1.1 Conditioning

Digital conditioning of signal is indispensable part of system, especially when spike detector is involved. For better decomposition is appropriate to focus on nearer signal sources, which can be accomplished by use of simple IIR high-pass filter at 150 Hz and then low-pass at 2 kHz (some signal above 2kHz still comes thru analog HW part filter) – signal above 2 kHz hadn't much influence on MUAP shape, thus everything above this limit should be considered as noise due to physiologic facts explained in second chapter. This action will add order to already conditioned signals by analog circuity of the device.

4.2.1.2 Power-line noise reduction (50 and harmonics)

During experiments with participants higher harmonics of 50Hz were notable in measured signals. These higher harmonics are originating in most cases from mains power or are being emitted by fluorescent lights. To filter out higher harmonics of ubiquitous power line noise the simple comb notch filter can be used.

$$y[k]=x[k]+\alpha_f \cdot x[k-d_1]-\alpha_b \cdot y[k-d_2]$$

Where $y[k]$ is output sample, $x[k]$ is input sample, α_f is feed-forward form gain, α_b is feed-back form gain. Since notch behavior is desired the, filter has the feed forward form $\alpha_b=0$ and delay parameter for given sampling frequency f_s and attenuated frequency f_0 with its odd harmonics: $d_1=\frac{f_s}{f_0}$

Problem of this simple notch filter is low quality factor Q (Q = 1), which would lead to loss of wanted bandwidth of signal. The solution is to use high-Q comb filter [72].

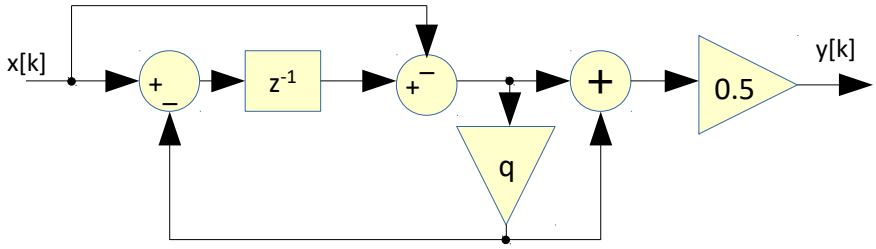

Figure 29: High-Q notch comb filter diagram

$$y[k]=q\,y[k-d]+(x[k]-x[k-d])\frac{(1+q)}{2}$$

Which quality factor Q depends on q: $Q\approx\frac{1.5}{1-q}$, $q=0$ results back in simple comb filter. Since Q factor is defined as $Q=\frac{f_0}{2f_{3db}}$ and $f_{3db}=(1-q)(1-0.36\,q)\frac{f_0}{4}$ for high-Q comb filter: $Q=\frac{2}{(1-q)(1-0.36\,q)}$. By selecting Q = 30 we get q = 0.9, which results in final formula for 5kHz signal:

$$y[k]=0.9\,y[k-100]+0.95\,(x[k]-x[k-100])$$

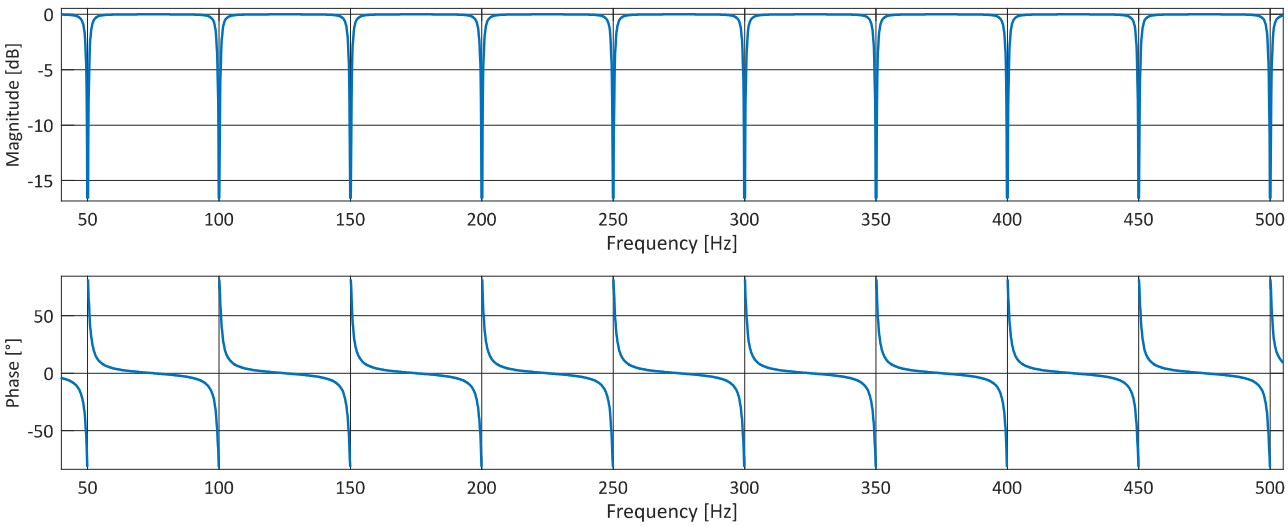

Figure 30: Part of frequency response of High-Q comb band stop filter for computed parameters

This step was necessary since following processing can be sensitive to higher harmonics of power-line interference. The Q parameter affects also adaptation time (which is raising with Q) and lower value of Q can cause false ripples in signal. Higher Q also means lower bandwidth (in stop range), which is unwanted due to potential wandering of power-line interference and its harmonics. Tests on synthetic surface EMG signals and measures using proposed setup shown, that Q should be optimally set higher than 30 ($q > 0.9$). This cause settling time over 1s (fig. 31).

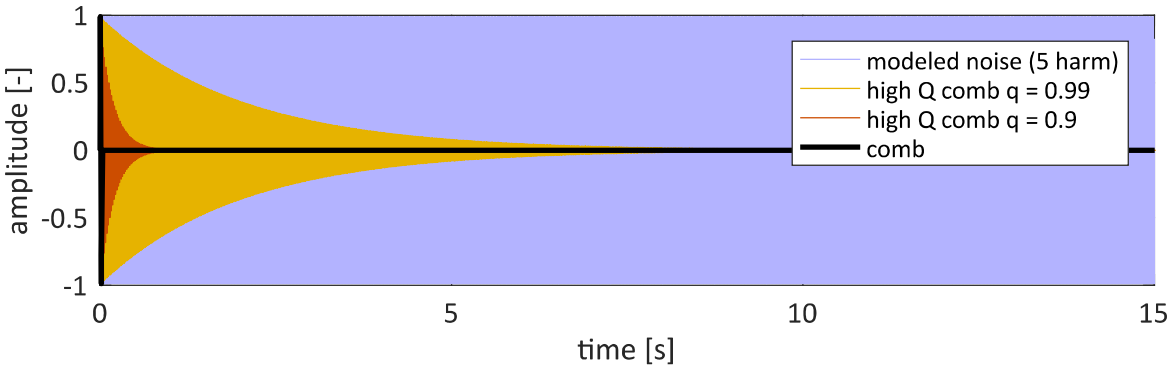

Figure 31: Filter settling times

In figure 32 are depicted results of filtered EMG signals with added noise (green) consisting of 50Hz and its first 5 harmonics after settling period. It is observable that results of this filter (yellow) are superior to basic comb filter (dashed black) and filtered noisy signals (green) are very similar to noise-free original simulated EMG (bold black).

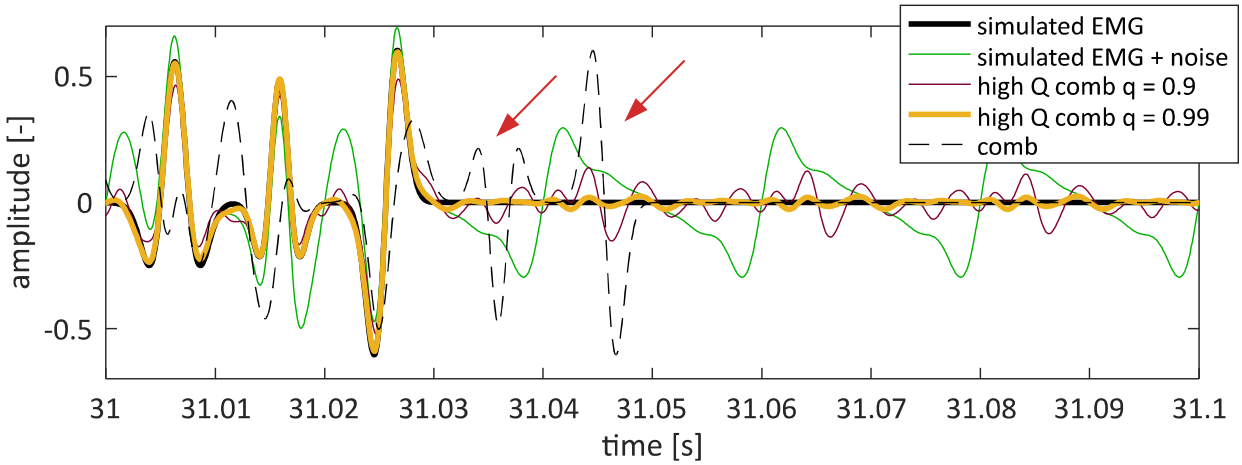

Figure 32: Graph shows simulated EMG signal with additive noise (green) filtered using high-Q comb filters and classic comb filter. High-Q comb filters (dark red and yellow lines) and classic comb filter. Red arrows show false ripples generated by classic comb filter. Black line represent clean signal.

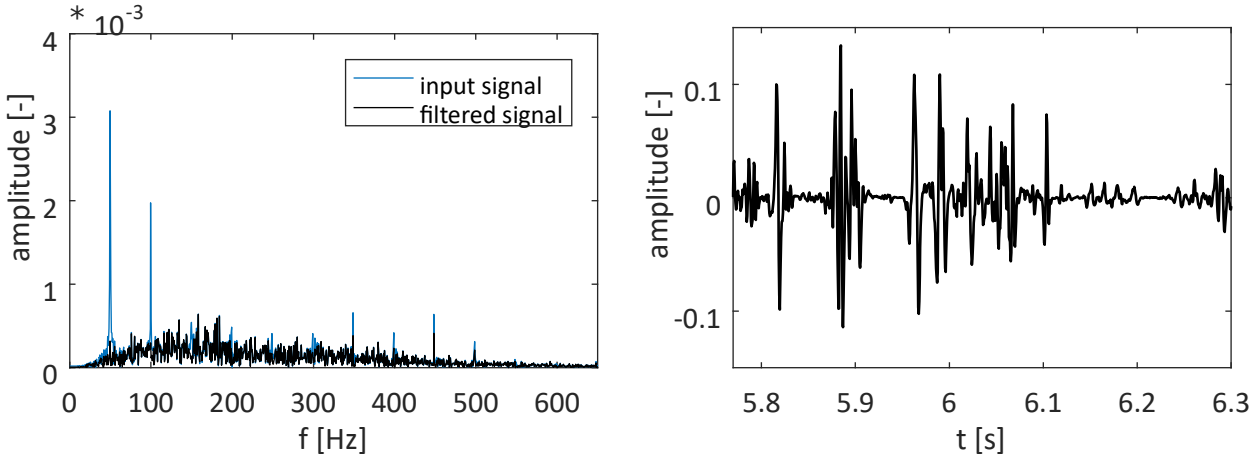

Figure 33: Real recorded raw surface EMG signal (blue) using Ag/AgCl electrode with IED=10mm, mostly baseline and then few seconds of muscle activation, filtered (black) using HighQ comb filter. Frequency spectrum on the left, filtered result in time domain on the right

4.2.1.3 Spike amplification and smoothing

If spike detector is involved (for lower MVCs) in later treatment of signal, then it is appropriate to amplify spikes with sought characteristics. In general, this may be done by simple differentiation – LPD filter (used for needle EMG recordings). Unwanted effect of this

filter is its preference to amplify noise rather than required component of signal. The solution is in use of WLPD filter [40], which is more noise resistant and amplifies spikes similar to motor unit action potentials when is properly set.

$$y[k]=\sum_{n=0}^{N-1}\sin\left(\frac{n\pi}{N}\right)\cdot\left(x[k+n]-x[k-n]\right)$$

Authors of the WLPD (weighted low-pass diff.) filtering method recommend its length set to N = 40 samples for 10kHz signal for usage in surface EMG analysis, which corresponds approximately to 9-18ms MUAPs spike duration with best response for spikes 12,8ms long. This duration range corresponds to surface EMG spike durations. From tested windowing functions was most suitable sinusoidal one. Length of the filter grows linearly with sampling rate. For proposed setup was more optimal an empirical setting. For purposes of following analysis was filter rewritten to normalized form:

$y[k]=w\cdot\sum_{n=0}^{N-1}\sin\left(\frac{n\pi}{N}\right)\cdot\left(x[k+n]-x[k-n]\right)$, where $w=\sum_{n=0}^{N-1}\sin\left(\frac{n\pi}{N}\right)^{-1}$ is normalizing constant.

Signal in figure 34 was measured in special laboratory conditions with minimal electronic interference using cut Ag/AgCl electrodes on abductor policis. One may observe the result after filtering (red). The desired spikes are amplified, noise is attenuated.

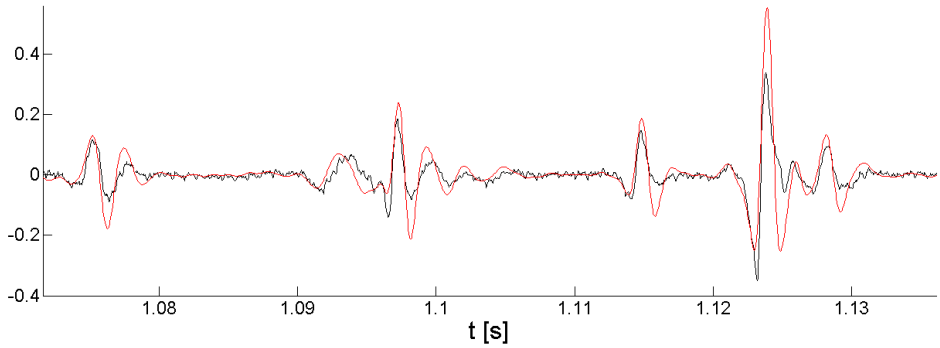

Figure 34: Example of conditioned 10 % MVC signal from abd. policis (black) and after applying WLPD filter and normalizing (to correspond original signal amplitude)

Tests on synthetic EMG data with added white noise showed that filter is reliable for signals with signal to noise ratio up to 15dB. For SNR above this value there are emerging false peaks. Resulting signals are depicted in figure 35.

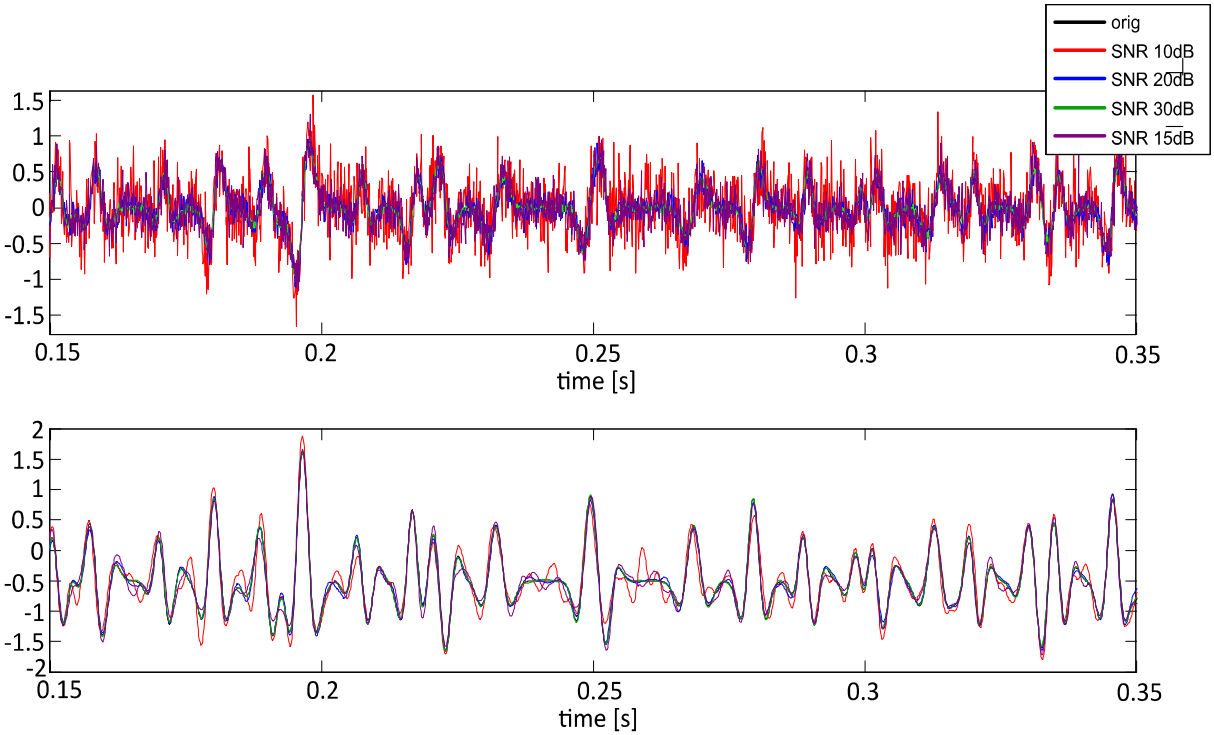

Figure 35: Example of synthetic simulated EMG with different signal to noise ratio, top: original signal, bottom: WLPD filtered signal, in signal with SNR 10dB (red) the false peaks emerged

Filter was sensitive to higher harmonics of power line interference, which supports importance of comb notch filter. Higher harmonics attenuated by notch comb filter after settling period.

4.2.3 Decomposition algorithm

Basic MUAP decomposition for non-superimposed EMG signals can be done with use of the correlation method or template matching during low muscle contraction if the MUAP shapes are known. Since they are not known, algorithm was designed to learn them automatically during low contractions. The method is targeted for assistive technology, therefore it is designed to work with minimum number of possible inputs – starting from one acquisition channel only. Algorithm consists of two phases. First is the calibration phase, which must be done after each electrode replacement, second is the real-time recognition phase.

Calibration phase (fig 36) uses an online iteration algorithm, i.e. gathered data are being analyzed multiple times, until is prepared satisfactory database of MUAPs. It may run simultaneously with muscle activity estimation algorithm. At beginning, the iteration algorithm is searching for single non-superimposed MUAPs and creates first estimate of MUAP database using shape recognition and clustering method. Searching (and segmentation) is done with use of spike detector. After a spike is detected, algorithm cuts (t-5ms, t+5ms) 10ms window for later processing. Non-superimposed spikes are considered those lasting shorter than 10ms. The dimension of data is reduced and clustered using online inverse weighted k-means algorithm. Number of clusters is then optimized using the gap statistic.

At the end of calibration stage the MUAP templates are built by averaging of detected samples. In next run are alone occurrences of MUAPs (outliers) examined with superposition solver module based on convolution filtering during online phase of the algorithm.

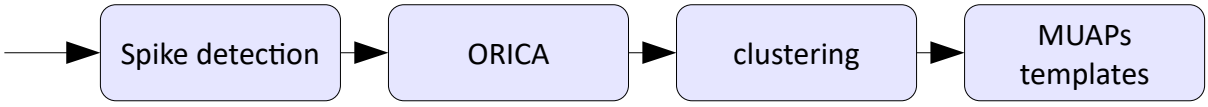

Figure 36: Calibration phase of real-time decomposition block

4.2.3.3 Spike detector

Input signal to spike detector should be smoothed to prevent detections of higher oscillations. WLPD not only amplifies desired peak shapes, but also smooths the signal.

Spikes are then in signal detected using:

$$s[k]=\begin{cases}|(x[k])| & if\ |(x[k-1]-x[k])|<0 \wedge |(x[k+1]-x[k])|<0 \wedge |(x[k])|>th \\ 0 & otherwise\end{cases}$$

Threshold is calculated from robust standard deviation statistic for unknown distribution:

$\sigma=\frac{median(|(\boldsymbol{x})|)}{0.6745}$, threshold of spike detector is then set empirically to: $th=2\cdot\sigma$

Second step selects sample index of maximum found peak to its maximum in 10ms sliding time window:

$$i[k]=\underset{n\in\langle k-N,k+N\rangle}{arg\,max}\ (s[n])$$

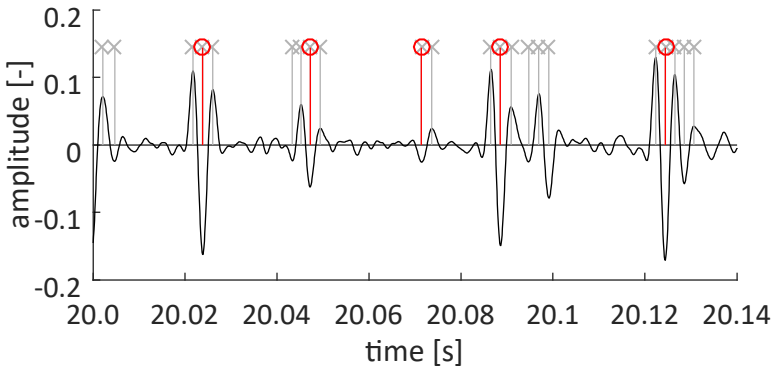

Figure 37: Visualized output of spike detector (1) detected spikes, (2) filtered maximum spike values in 10ms timespan

4.2.3.4 Shape clustering

Clustering and shape recognition is achieved using online recursive independent component analysis (ORICA), which is computationally reasonable and accurate ICA method, here utilized for lowering the feature space. It was shown, that ICA outperforms PCA and Wavelet approach in spike shape sorting task [99] especially in cases with lower signal to noise ratio.

Disadvantage of classic batch PCA and ICA methods is their need to access all input data in each iteration during optimization process. Second disadvantage is that these techniques require much more computational time and resources. Third disadvantage is that these methods cannot handle gradual changes of the underlying subspaces (ie: changing of MUAP shapes during time and electrode placement). Online implementation can deal with all of pitfalls mentioned.

Method processes one sample per a time instance and does not need to remember all the past samples. ORICA authors reformulated the objective function of the infomax ICA technique to be solvable by stochastic optimization algorithm.

Inputs to the algorithm are vectors of detected spikes, outputs are unmixing and whitening matrices used later for transformation of input vectors to reduced feature space. Main advantage of this method is its low computational difficulty and possibility to update matrices with new detected samples in realtime.

Online recursive source separation algorithm [75] tries to find the whitening matrix M_n and weight matrix W_n to unmix the input data to independent sources. Both matrices are initialized with random values and the iteratively updated by following update rules:

(1) $$M_{n+1}=\frac{1}{1-\boldsymbol{\lambda_n}}\left[I-\frac{\boldsymbol{v_n v_n^T}}{\frac{1-\boldsymbol{\lambda_n}}{\boldsymbol{\lambda_n}}+\boldsymbol{v_n^T v_n}}\right]\cdot M_n$$

where $\boldsymbol{v_n}=M_n\cdot\boldsymbol{x_n}$ are whitened data, $\boldsymbol{x_n}$ input observations and $\boldsymbol{\lambda_n}$ is forgetting factor.

(2) $$W_{n+1}=\frac{1}{1-\lambda_n}\left[I-\frac{\boldsymbol{y_n} f^T(\boldsymbol{y_n})}{\frac{1-\lambda_n}{\lambda_n}+f^T(\boldsymbol{y_n})\,\boldsymbol{y_n}}\right]\cdot W_n$$

where $f(y)=\begin{cases}-2\tanh(y) & \textit{for supergaussian source}\\ \tanh(y)-y & \textit{for subgaussian source}\end{cases}$, $\boldsymbol{y_n}=W_n\cdot\boldsymbol{x_n}$

$\lambda_n=\frac{\lambda_0}{n^y}$ is time-varying forgetting factor, a constant can be also used

For non-stationary data the adaptive forgetting factor can be used [76]:

$$\lambda_{n+1}=\lambda_n-\alpha\lambda_n^2+\beta\,G(z_{n+1})\lambda_n$$

where $z_n=\|R_n\|_F$ is Frobenius norm of leaky average $R_n=(1-\delta)R_{n-1}+\delta(I-y_n f_n^T)$ with weight parameter δ .

Updating the whitening and unmixing matrix for each sample is not optimal, therefore the block-update rule has been used:

$$W_{n+L}\approx\prod_{l=n}^{n+L-1}\frac{1}{1-\lambda_l}\cdot\left[I-\sum\frac{y_l f^T(y_l)}{\frac{1-\lambda_l}{\lambda_l}+f^T(y_l)\,y_l}\right]\cdot W_n$$

During unmixing matrix learning process user should perform low level percentage of MVC muscle activations with all the monitored muscle. Non-stationary criterion helps to faster converge of the algorithm, especially if movement of the electrodes occurs, but satisfactory results can be achieved also using simpler method with consant λ .

For purposes of this work was algorithm implemented in C++ with use of eigen library[15].

To identify which components are most significant the projection of data using unmixing matrix must be performed. Unmixing matrix is calculated as product of weight and whittening matrices:

$$U_{d\times d} = W_{d\times d} \cdot M_{d\times d}$$

Data matrix is then projected to independent coefficient space:

$S_{d\times n} = U_{d\times d} \cdot X_{d\times n}$, where *d* is dimension and *n* is number of samples

Feature is useful for linear separation if has a multi-modal distribution. This can be achieved by finding component least Gaussian-source components, which can be measured using Lilliefors test [94]:

$$L = max(|F(x) - G(x)|)$$

Where G(x) is empirical cumulative distribution function of one row vector from matrix $S_{d\times n}$ and F(x) is c. d. f. of normal distribution with same mean and variance.

Clustering is then done using online inverse weighted k-means (OIWK) method, which delivers much more accurate results and stability of the algorithm. Basic k-means approach is sensitive to poor initialization of the cluster prototypes and may end up in unwanted false result. Newer clustering approaches like are weighted k-means, inverse weighted k-means, k-harmonic means and their derivations solve the problem of reaching the local optima, since these methods are utilizing the whole data sets for each cluster prototype (center point). All of these has also online variants. [92] Following algorithm is able to learn in online mode for cases where one sample is available at the time. Furthermore, mean prototypes are affected not only by winning sample prototype like it is in k-means approach but also by the neighboring prototypes.

Algorithm for online inverse weighted k-means

Input: sample vectors $\{\boldsymbol{x}_1, \ldots, \boldsymbol{x}_N\}$

learning rate ζ … usually set to small positive number, can also gradually decrease

Initialize cluster prototype vectors $\{\boldsymbol{m}_1, \ldots, \boldsymbol{m}_k\}$ with random values

for 1 to M **do** M … iterations

1) For each sample vector $\boldsymbol{x}_i$ set $k^* = arg\min_{k=1}^{K}(\|\boldsymbol{x}_i - \boldsymbol{m}_k\|)$ (k* is index of prototype to which sample belongs)

15 *Available at: http://eigen.tuxfamily.org/index.php?title=Main_Page*

2) and update prototypes:

$$\boldsymbol{m}_{k*}^{(new)} = \boldsymbol{m}_{k*} - (\boldsymbol{x}_i - \boldsymbol{m}_{k*})\zeta\left[-(n+1)\left\|\boldsymbol{x}_i - \boldsymbol{m}_{k*}\right\|^{n-1} - n\|\boldsymbol{x}_i - \boldsymbol{m}_{k*}\|^{n-2}\sum_{j\neq k*}\|\boldsymbol{x}_i - \boldsymbol{m}_j\|\right]$$

$$\boldsymbol{m}_k^{(new)} = \boldsymbol{m}_k - (\boldsymbol{x}_i - \boldsymbol{m}_k)\zeta\frac{\|\boldsymbol{x}_i - \boldsymbol{m}_{k*}\|^n}{\|\boldsymbol{x}_i - \boldsymbol{m}_k\|}$$ n is chosen empirically, usually 1

end

return cluster prototypes $\boldsymbol{m}_1, \ldots, \boldsymbol{m}_k$

To estimate number of clusters the OIWK algorithm runs several times in parallel. Each instance runs with chosen different number of clusters. For each point is stored vector of cluster associations.

Using this method in combination with gap statistic it is possible to decide about the number of MUAP templates. The instance with lower number of clusters can be terminated in case that new cluster is found.

Real-time decomposition phase (fig. 38) uses learned database of MUAP templates for detecting them in signal, superposition solver has limited maximum number of iterations. Of course the consequence of limiting iterations is possibility of wrongly estimated decomposition, but for recognition and usage in human-machine interface is preferred fast and low computationally demanding processing.

Furthermore at lower levels of muscle MVC is signal easier to decompose, as was stated, the decomposition method is involved only for lower MVC signals therefore is superposition solver utilized infrequently. Superimposed spikes can be recognized by findings of unknown rare shapes, in many cases also lasting for longer time.

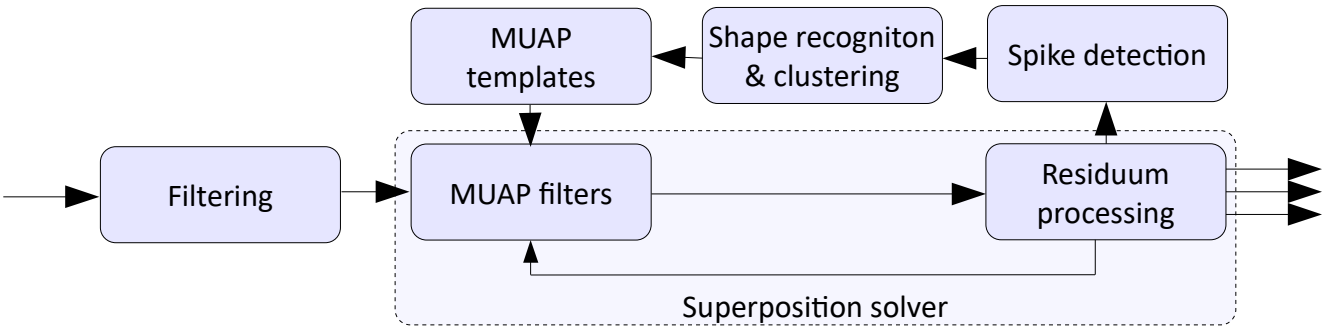

Figure 38: Real-time decomposition block

Earlier version of superposition solver was based on peel-off approach and later updated to presented solution by findings [57]. Superposition solver consists of MUAP filters defined by learned MUAP shapes from calibration phase of the algorithm and residuum processing block. Input to the algorithm is 30ms windowed signal. Successive windows are overlapping by 10 ms.

4.2.3.1 MUAP filters

This block convolves input signal *x(t)* with all MUAP templates (*h(t)*) and returns index *i* of MUAP template with maximum convoluted value and time of occurrence *t*. Convolution result is normalized by subtraction of MUAP shape energy E_i. If the normalized convolution result isn't greater than zero, no shape is detected and input signal is being processed by following blocks.

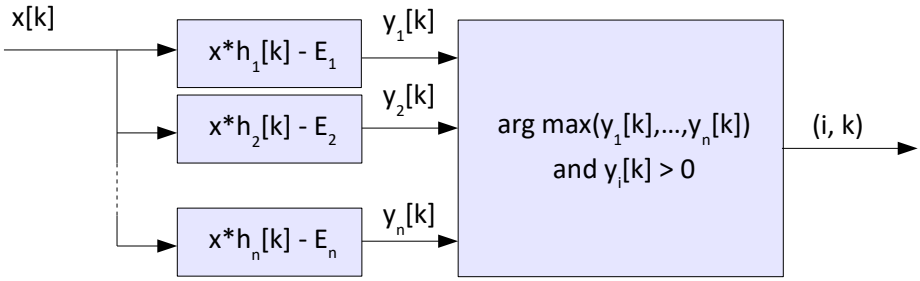

Figure 39: MUAP filtering block returns most probable MUAP shape (i) and its spike position (k) or returns null

Convolution is calculated as:

$$x * h_i[k] = \sum_{n=0}^{N-1} x[t-n] h_i[n]$$

Energy of the template is calculated during learning process from estimated MUAP shapes by formula:

$$E_i = 0.5 \cdot \sum_{k=0}^{L-1} (x[k])^2$$

Energy subtraction was introduced to prevent convolution detector from detecting false positives of unknown shapes. This kind of processing firstly identifies largest MUAP shape in superimposed spike, which is consistent with template matching approaches [8, 9, 41, 57]. Signal is then sent to residuum processing block.

4.2.3.2 Residuum processing (superposition solver)

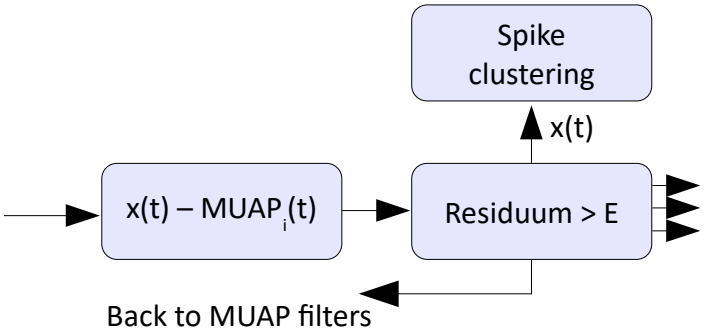

Figure 40: Residuum processing block

Residuum is computed as *i*-th detected MUAP substracted from signal. If energy of residual signal is greater than noise baseline, signal is processed once more thru MUAP detector otherwise detected MUAPs are returned. In case that no superimposed spikes were detected at all (signal does not have to be processed again) the spike is sent to clustering block. Similarly if MUAP filters block does not detect any MUAP shape and signal's energy

is higher than detection threshold of spike detector of online shape recognition and clustering block.

4.2.3.3 Evaluation of decomposition

Generally there are four possible ways to evaluate quality of the decomposition – by testing on synthesized signals, by comparing to results of generally accepted solution or by testing data on annotated signals by human expert and finally implementation of method from a paper, which is time consuming.

There are not any freely distributed fully automatic surface EMG decomposition algorithms, but Florestal's genetic algorithm MTLEMG [95]. MTLEMG is primarily intended for invasive EMG recordings, but was proposed also for surface EMG recordings measured with wire electrode (figure 20, p. 52). During early stages of work was algorithm tested on data generated from EMG simulator [96].

Another algorithm working with low number of input channels is dEMG, which is a paid part of commercial package by Delsys, inc. based on De Luca's and Nawab's algorithms [8, 9] and is not distributed freely. Second greatly performing decomposition algorithm – gradient CKC is decomposing multi-electrode array signals and is part of another paid package – DEMUSE.

It is also possible to analyze surface EMG signal by visual observation, however even visual analysis of EMG signal is not proof of correctly identified superimposed parts of signal. Due to this presumptions was decomposition algorithm evaluated by comparison with MTLEMG decomposition algorithm and on annotated surface EMG signals by an expert[16].

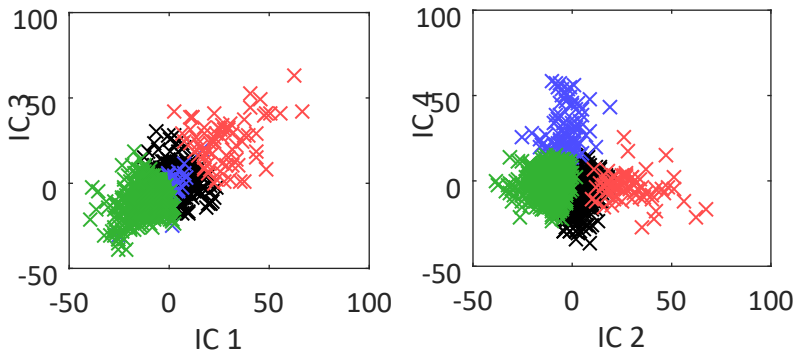

Figure 41: Projected data independent components calculated from set of detected MUAPs

Analyzed signal had annotated 4 MU firing trains by expert, MTLEMG identified 12

16 *Hogrel [100] Signals are available at: http://www.emglab.net/emglab/Signals/R011/index.html*

types of MUAP. Therefore even the results obtained by MTLEMG algorithm are questionable. Presented algorithm was able to detect all of the spikes annotated by an expert and after filtration of superimposed suspects formed 4 clusters, which is corresponding to annotated data.

Superimposed signal decomposition results after automatically formed database of MUAP gave weaker results of only 64 percent of the correctly recognized MUAP. Nevertheless, evaluation on signals measured by device setup was questionable – MTLEMG usually identified significantly less MUAP shapes than described method.

4.2.4 Force estimation model

All the previous signal processing blocks delivered us a new feature for later processing – statistics of single motor unit actions potentials and activated motor units. This statistics can be utilized in various ways. For estimating the muscle force or as an input to classifier, which for instance is able to recognize various gestures or movement patterns from just single channel EMG [80]. Since target of the work was to examine force estimates in user interface the model for muscle estimation is needed. This can be achieved by use of approximate twitch based model.

4.2.4.1 Twitch based force estimation model

Muscle force grows with number of activated motor units and frequencies of their repeated firings. Larger motor units generate higher twitch force and also stronger action potentials. Twitch force increases with frequency of pulses. This behavior can be modeled by twitch force based estimation model, which was proven to be most relevant for muscle force estimation [74].

Approximate muscle force can be expressed as convolution operation:

$$f[k] = x[k] * m[k]$$

where f denotes muscle force, x extracted pulses from EMG and m is the muscle model.

Transfer function of muscle model is approximated[17]:

$$M(s) = \frac{K\omega_n^2}{s^2 + 2\zeta\omega_n s + \omega_n^2}$$

where K is system gain, ω_n represents natural frequency, ζ is damping ratio and s is laplace variable. Natural frequency has been reported as 2Hz and damping ratio to be between 0.7-1.0 by Bawa et al. [119] Na et al. [125] later verified these values by implementation of this model together with Nawab‘s and De Luca’s [9] variant of decomposition algorithm[18] and

17 *More precise model and estimation of it can be found in [140]*

18 *DelSys – commercial system for decomposing of surface EMG, available: https://www.delsys.com*

estimated these parameters using Levenberg-Marquard method from 3 subjects. Resulting average values for these subject were laying on intervals $K \in \langle 0.08; 0.09 \rangle$, $\zeta \in \langle 0.94; 1.0 \rangle$, $\omega_n \in \langle 0.92; 1.14 \rangle$.

Resulting decomposition contains both of the parameters – temporal information and MUAP templates from which can be calculated their energy. Each pulse in discrete time *x[k]* can be modeled as dirac pulse of size of its energy. Input *x[k]* convolved with discrete form of the muscle model transfer function gives a muscle force estimate.

4.2.5 Amplitude based muscle activity estimation

Muscle activity estimation algorithm was originally based on mean absolute value of preprocessed surface EMG signal and was incorporated to prevent decomposition of higher level percentage of MVC muscle activities, which would generate wrongly classified spikes due to nature of the presented method and also as a standard of classical amplitude force estimation approach. Force estimation algorithm was planned to return estimates for highly superimposed signals generated during stronger muscle contractions due to high counts of superimposed spikes, which made the single channel decomposition task almost impossible.

During development was muscle force estimation algorithm also updated and further versions had fast and stable response on muscle activity. Algorithm is a way safer on processing power, thus was then incorporated into the embedded device and tested in various environments and also in applications without a computer.

4.2.5.1 Signal whitening and sources separation

Signal whitening improves the amplitude based muscle force estimate [64]. Successive samples of surface EMG signal are correlated. Each successive sample of acquired signal weights previous sample information, therefore direct amplitude processing would yield biased results. Correlation can be decreased by whitening the signal which results in improvement in signal to noise ratio for muscle activity over 10% of MVC using whitening filter. Whitening filter coefficients can be estimated using AR model.

Whitening filter has low gain at lower frequencies. Potvin et al. [85] showed that use of whitening filter can be bypassed by high pass filtering of signal with Butterworth filter at cutoff frequency above 140Hz. In study authors experimented with filtering frequencies from 140 to 410 Hz and different order of filters and found that signal filtered by high-pass filter over 140 Hz (6^{th} order) gives significantly more correlated estimates to measured force.

Input to the muscle activity estimation algorithm is conditioned signal using described WLPD and HighQ comb filters with regard to maximum selectivity to MUAPs. Therefore the muscle activity estimate is minimally affected by unwanted noise and irrelevant information.

Various algorithms (FastICA, SOBI, ORICA) were tested to prevent muscle cross-talk

and electrodes (Ag/AgCl) and to reduce electrode positioning errors. Problem of ICA algorithms for signal blind source separation is loss of amplitude information (and sign) in unmixed independent components, thus identified components were normalized before analyzing by estimation algorithm. Nevertheless results obtained using this technique were not satisfactory for later muscle activity estimation. In all scenarios the problem of crosstalk was solvable by proper electrode positioning or by use of the branched electrode (figure 23, p. 54)

4.2.5.2 Estimation

Designed amplitude muscle activity approach is superior to naive ones like is moving average or integral envelope. It brings fast response rate to fast muscle activity changes but provides smooth muscle activity level estimation. Of course this method does not provide physically accurate estimation of force without proper normalization, rather it is designed to provide comfortable response in human-machine interaction applications.

Algorithm consists of conditioning step, rectification by RMS, normalization and custom special smoothing filter.

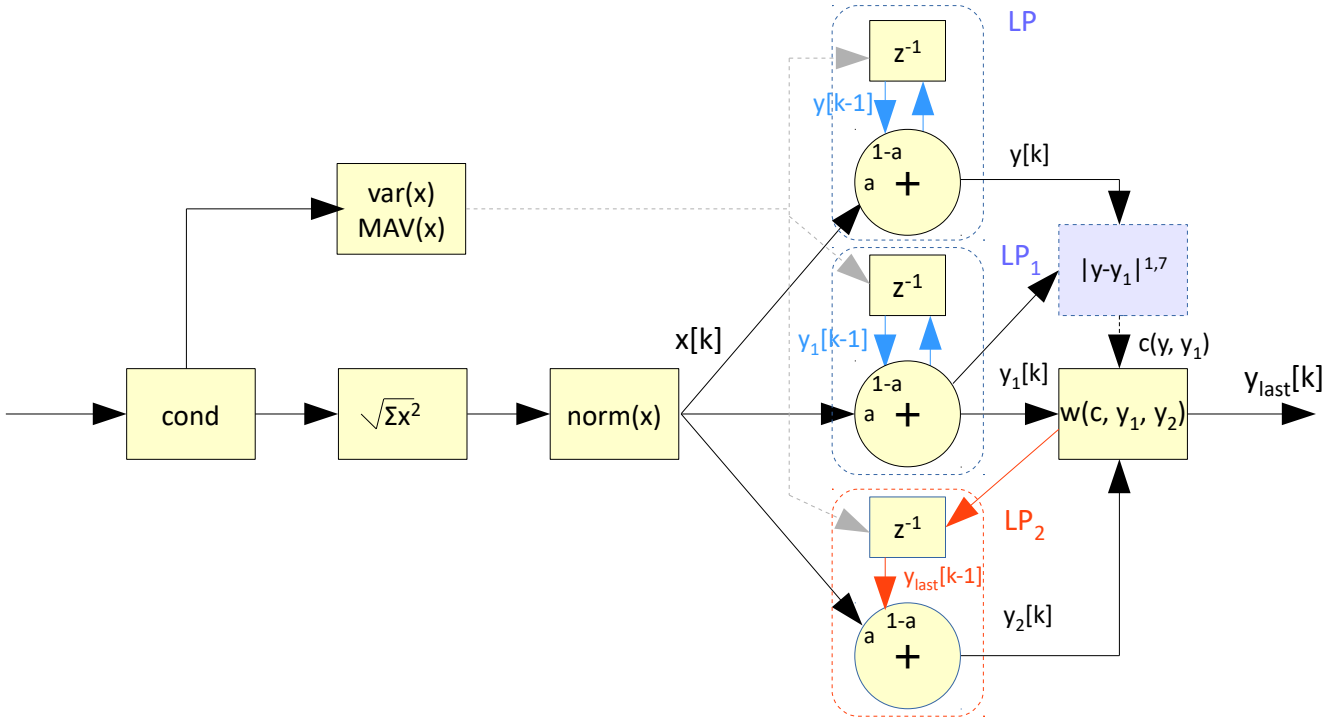

Figure 42: Diagram of muscle activity estimation algorithm

Signal is rectified using RMS value:

$MVC_{est}[k]=\sqrt{\sum_{i=k}^{k-39} x_i^2}$, where k is last sample of the window without overlapping

The rectification step decimates the signal from 5 kHz to 100 Hz. 100 Hz is smooth enough for human perception.

Signal is then being normalized. In this step it is possible to set sensitivity and maximum detected force (muscle activity).

$$norm_1(x[k]) = \frac{x[k] - th_{min}}{th_{max}}$$

th_{min} is the minimal sensitivity threshold

th_{max} sets the dynamic range of voluntary contraction (set on comfortable level)

To prevent negative values in rectified signal:

$$norm_2(x[k]) = max(th_{min}, min(th_{max}, x[k]))$$

$$norm(x[k]) = norm_2(norm_1(x[k]))$$

Smoothing

Smoothing is performed using a combination of 3 low pass filters. The first (fast response) is set on frequency of 7Hz (LP_1) to track fast movements. Slow filter (LP_2) is set on 0.06 Hz and last filter is used as decision criterion is set to 0.75Hz, if fast movement is present. Slow filter (LP_2 in fig. 42) has been modified – feedback value is provided from the output of whole filter system.

Filters LP_1 and LP_2 are defined by formula:

$$y_i[k] = a_i x[k] + (1 - a_i)\, y_i[k-1]$$

Weight a_i is defined: $$a_i = \left(1 + \left(\tan\left(\frac{\pi \cdot f_i}{fs}\right)\right)^{-1}\right)^{-1}$$

Third filter (the middle frequency) is used for computation of stability coefficient. This coefficient is used as weight – if difference between fast and middle frequency filter is higher, the fast filter is more affecting output estimate in other case (slower motion), slow filter is more affecting the output estimate value.

$$y_{last}[k] = |y_1[k] - y_2[k]| \cdot y_1[k] + (1 - |y_1[k] - y_2[k]|) \cdot y[k]$$

The improvement to the weighting function is adding a power function. Therefore the estimate of muscle activation is affected by faster filter during greater changes and signal is more stable and less vulnerable to noisy signal.

$$y_{last}[k]=|y_1[k]-y_2[k]|^{1.7}\cdot y_1[k]+(1-|y_1[k]-y_2[k]|^{1.7})\cdot y[k]$$

Also for fast response is needed to perform faster movement than with (estimate 1). The pow value was found empirically. Higher values would significantly raised delay of the filter. The response obtained by setting between interval <1; 1,7> was comfortable for all users. By modifying pow value can be set smoothness of the estimate.

Following test demonstrate constraints and performance of proposed smoothing method. Algorithm was designed with regard to physiological characteristics of the muscle [90], thus to obtain the delay between 30 and 100ms.

Unit step response in figure 43 show that smoothing block meets this condition for fast movements.

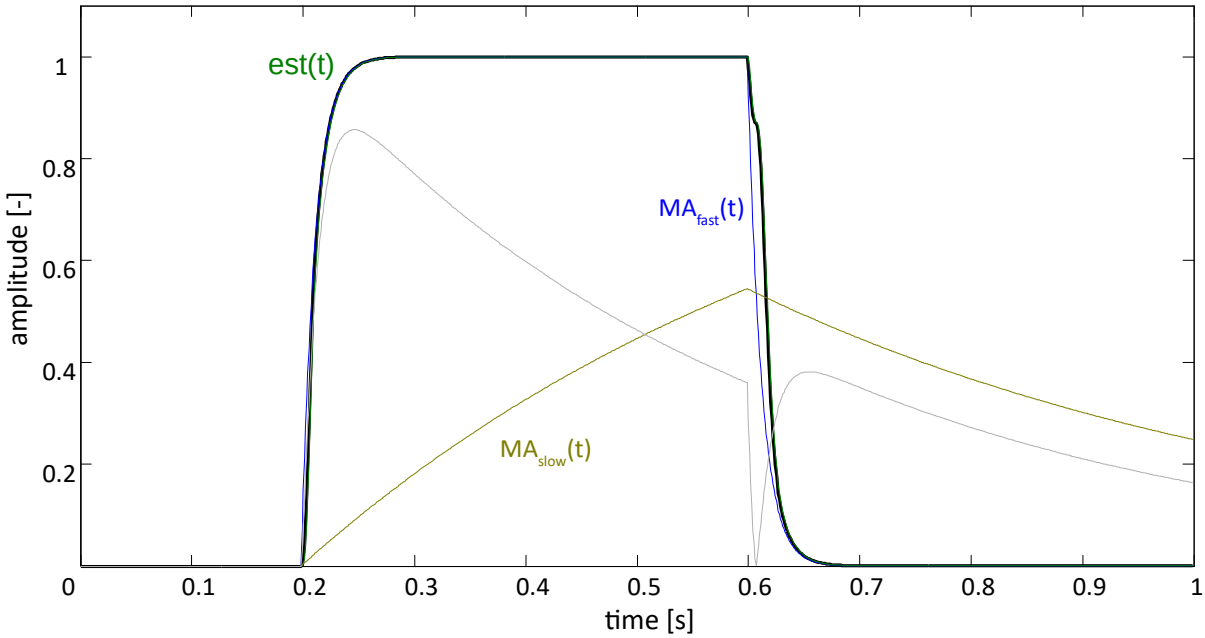

Figure 43: Real-time estimation algorithm step response comparison between classic moving average approach and proposed method: yellow – slow MA, blue – fast MA, green – proposed method

Behaviour of the filter at lower amplitude steps show that settling times are approximately same, delay is raising for lower differences between amplitudes of slow and fast filter.

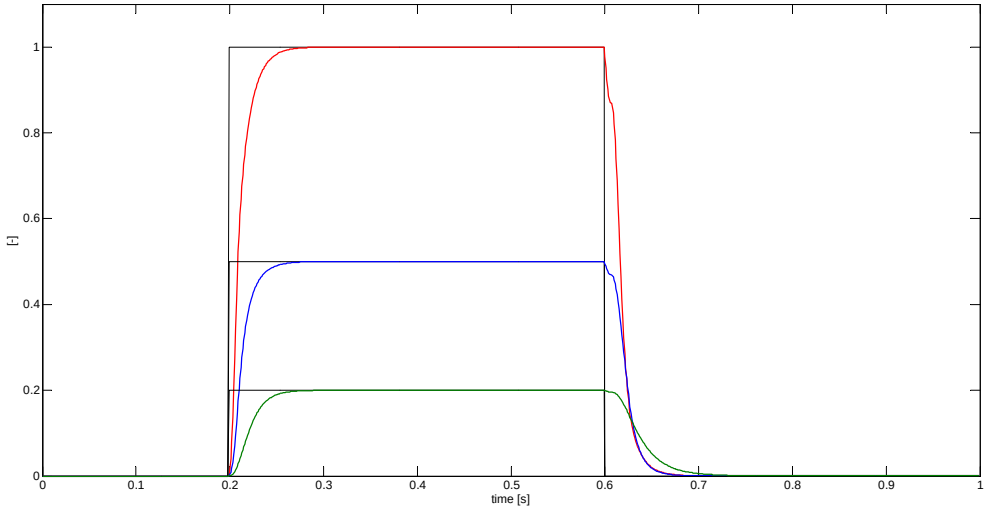

Figure 44: Settling times are constant for different amplitudes of unit steps

In figure 45 is depicted response to real measured and rectified EMG signal from extensor digitorum muscle compared to MA filter methods.

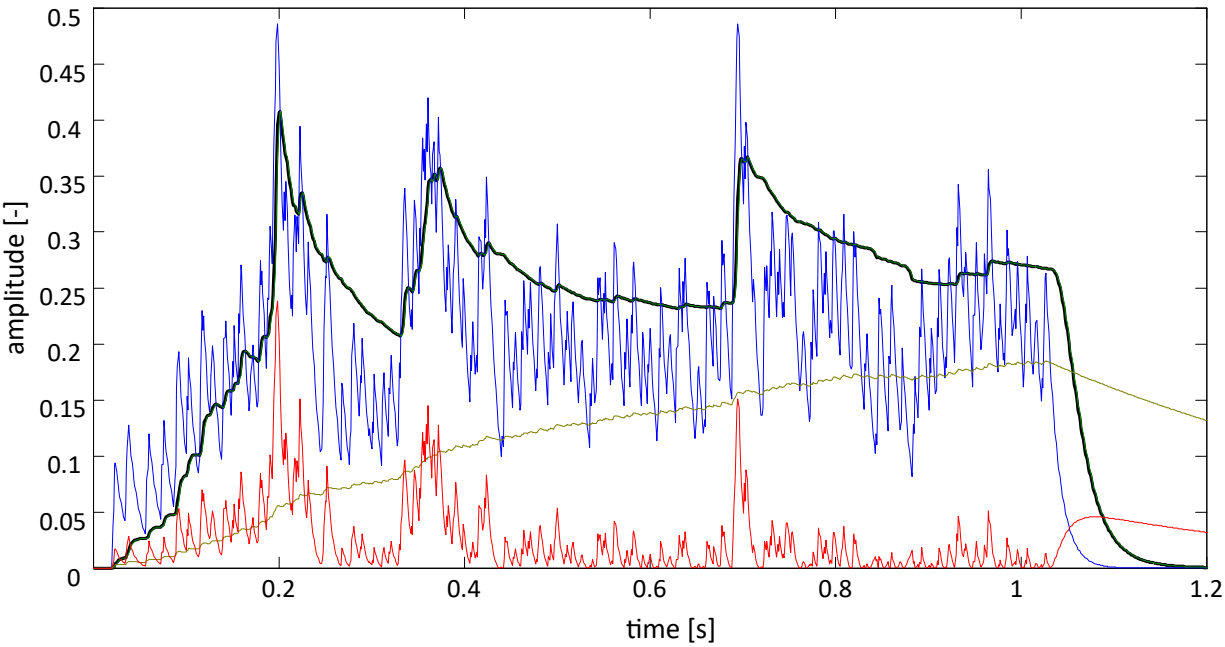

Figure 45: muscle activity estimation method compared to moving average approach on real signal during 3 fast consecutive finger movements: yellow – slow MA filter, blue – fast ma filter, black – proposed method

Figure 45 shows that proposed method has fast response as fast MA but is smooth and stable as slow MA. Therefore it has no observable delay for user and is stable enough.

Estimation algorithm works very well also for weak (low percentage of MVC) EMG signals, where motor units action potentials are observable by eye.

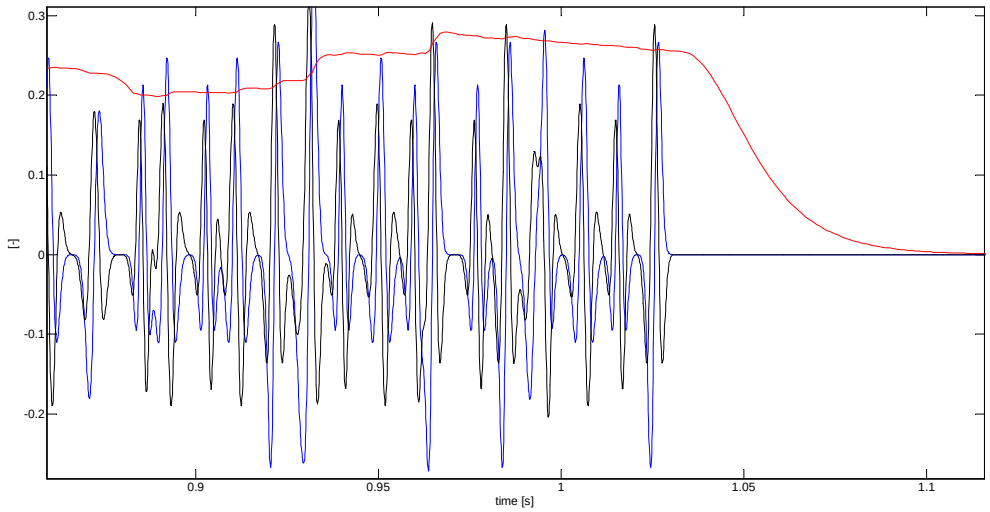

Figure 46: Synthetic EMG signal consisting just from firings of two motor units.

Delays at movement offsets are the removed by the variance detector, which resets smoothing filter to zero value if both variance and absolute mean of the signal are low. Result of adding the detector to algorithm is observable in figure 47 at the offset part of signal.

As was mentioned in chapter 3, there are various methods for force estimation from raw surface EMG. One of the most stable is Sanger's Bayesian filtration method [97], which was chosen for comparison and testing of proposed method on real recorded surface EMG signals due to its stability and fast settle times. Of course each method serves for different applications.

For standard recorded surface EMG and reasonable contraction forces Bayesian filtering method provides very accurate and stable predictions of contraction force (blue signal in fig. 47).

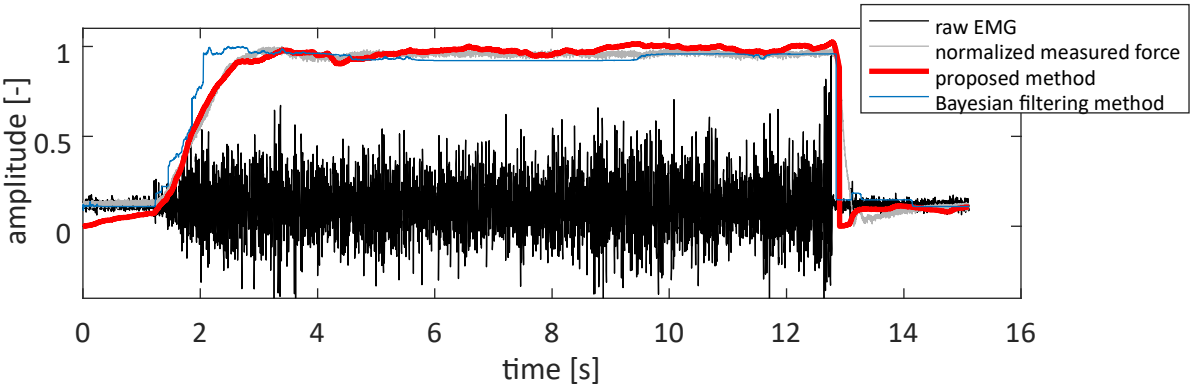

Figure 47: Proposed method (with setting to match the amplitud) and Bayesian filtering method compared on data from biceps muscle from study proposing Bayesian filtering method [97]

Good response and stability should be preferred over accurate contraction force estimation in human-computer interaction system controlled by EMG if feedback is present (for instance visual). Weaker muscle contractions are preferred in such a system to prevent fatigue and maximize comfort for user. For weaker (very low MVC normalized contractions) signals the Bayesian filtering method render oscillations which are unwanted for fluent control.

This can be corrected for instance by simple moving average filter or median filter, but that introduces we get higher delay and oscillations still persist. Notable fact is that Bayesian filtering method was developed for different signal characteristics and is giving best results for 10 to 20 % of MVC. Bayesian method was also included to developed online signal processing framework.

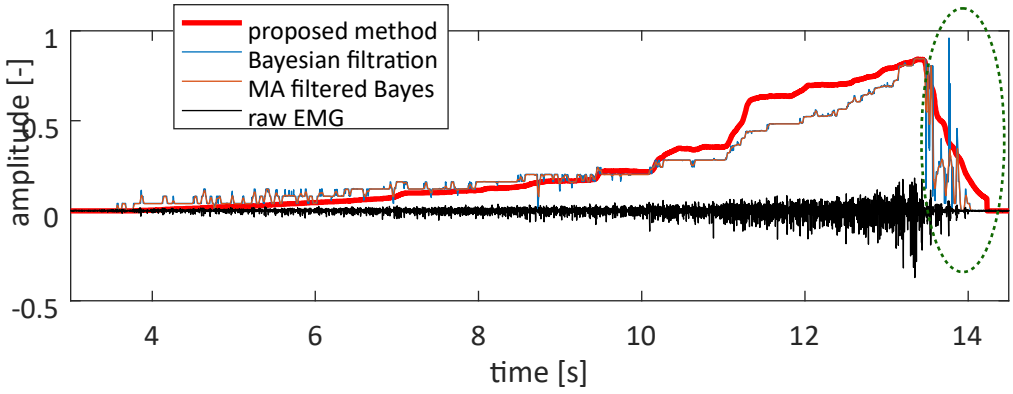

Figure 48: Slow ramp muscle activation (2-10s) and faster muscle activation (10-13.2s) then release (13.2-14s) Bayesian filtering method yields oscillations for lower muscle activity (4-9s) and during release (13.2-14s)

Sanger's Bayesian filtering muscle force estimator has by default 50 output quantization levels. Such low number results in "stairs" in the figures. Increasing this value will yield smoother signals, but oscillations will be still present. Increasing number of quantization outputs also significantly increases computational time for one sample, since method needs to compute exponential model, posterior and prior probabilities and perform convolution

operation of length equal to number of quantization outputs.

4.2.4.3 Calibration

Presented method offers fast and simple calibration for an individual user. The first step is measurement of noise baseline and selecting minimal muscle activity threshold, the second step is selection of maximal detected muscle activity as fraction of MVC for each detected muscle.

The calibration for each individual user is needed, since signal strength and characteristics for each individual person are different (in dependency on body fat, muscle training, etc.). The preferred force dynamic range determines comfortable use. There is also a possibility of difficult signal separation for some individuals in case of measurement above areas with high muscle group concentration. Branched type of electrodes should be used to get proper separation of the signals in each channel.

Method estimates similar muscle characteristic as force estimation methods mentioned in section 3.1, but since it is not normalized to corresponding muscle force but to comfortable range selected by user, it is rather reported as muscle activity estimator.

Algorithm can run stand-alone or in parallel with decomposition algorithm. If decomposition algorithm is involved, then muscle activity estimator serves as decision rule to decide whether signals contains lower or higher muscle contractions (as percentage of MVC). In this case should be calibrated to 100 percent of MVC.

4.2.6 Developed system overview

Implementation is done in C (for embedded system), C++ and C# for desktop computer part. Interface for applications in driver of actually developed device can be accessed through TCP/IP service or by library for C# as a plugin.

HW part of the system can work also without a PC, since it is powered by batteries and has embedded versions of precondition and estimation algorithm. Details on evaluation and developed applications are concluded in chapter 5.

System consists of:

- Design of electrodes and setup tests (details in section 4.1)
- Design of hardware part (multiple revisions, final revision in fig. 27, p. 57 with pre-amp fig.19, p. 51)
- Working code for measurement device with embedded version of muscle activity estimation algorithm, solved data transmitting protocol and computer driver (can act also as USB HID class device)
- Algorithm consisting of precondition, decomposing, and amplitude based muscle activity estimation methods evaluated on multiple users on individual finger control, limb and facial muscles (5.1)
- Middleware for text typing (5.2)
- Plugin for real time usage in applications (for instance in a game engine)

Diagram of solution for controlling applications is depicted in figure 49.

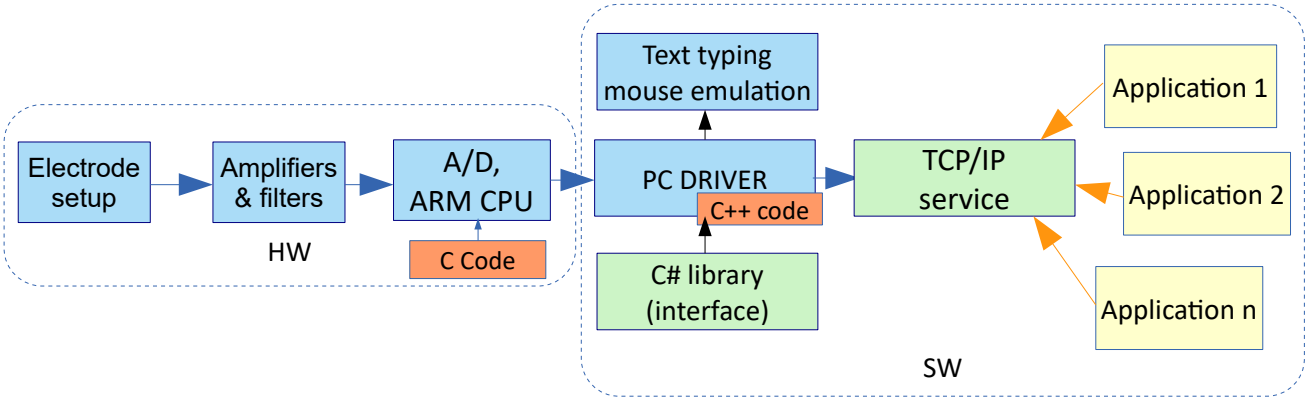

Figure 49: system overview

5 Evaluation of system

Proposed method was evaluated by qualitative approach based on tests with participants during development process. Participants also evaluated methods for text input and control of computer using developed applications (5.2). For most of the experiments and tests with participants was used the embedded variant with muscle estimation algorithm, since the decomposition part of the system was not reliable in all circumstances and needed much longer calibration period. Decomposition method did not provide better results than amplitude based algorithm and was way more demanding on computer resources. This variant enables the simple calibration and brought acceptable performance over all participants with minimal time to recalibration.

5.1 Test with participants

Muscle activity estimation method was evaluated by healthy and also disabled participants. Purpose of the published studies [P2, P3] was to investigate accuracy of the developed device and get knowledge to what extent the muscle clenching could be used as a virtual input device for 1-of-N selection since choosing one option out of N is a common atomic operation in user interfaces and also with virtual keyboards. Studies examined behavior of untrained users with different input methods based on their muscle activity from surface EMG. Examined parameters were also error rate and possible speed of selection. Learning curves were observable during experiments. During successive sessions were users much faster in the tasks.

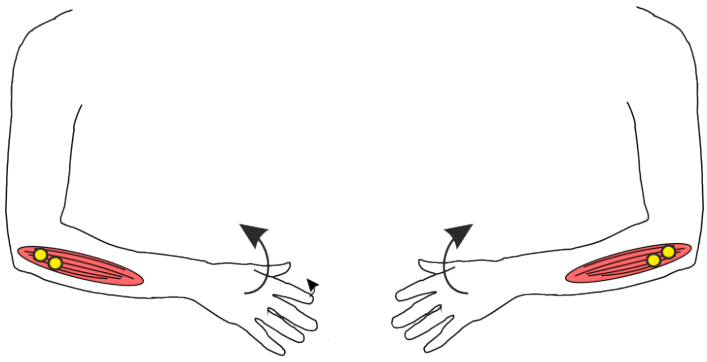

Figure 50: Electrode placement in experimental task

Experimental procedure

9 untrained people (2 F, 7 M, between 25 and 40 years of age) without any previous

experience with surface EMG human-machine interaction system and one disabled person took part in the study. Surface electrodes were applied to his or her skin in differential configuration and accordance to the method described in the previous section. Two electrodes per participant were used, one on either arm. The placement of the electrodes is shown in Figure 50. The electrodes were placed so that they were capable of monitoring the activity of extensor digitorum on both arms, specifically to detect and measure the muscle activity that inclined the palm from the desk. One hand (by the participant's choice) was considered the control hand while the other was the trigger hand. Our study was performed in relatively noise-free environment (the typical noise level readings were at 7 % of the chosen maximal contraction) and together with noise suppression filters the detection threshold could be set low. The device was very sensitive to weak contractions which did not even move the limb.

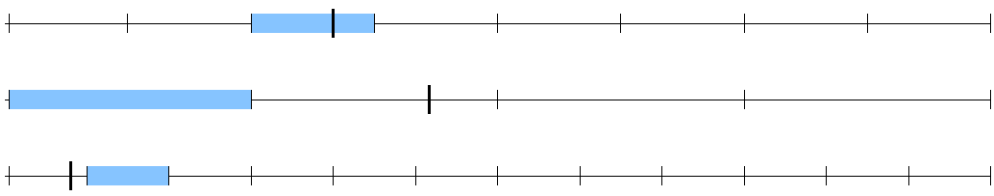

Figure 51: Examples of 1-D target acquisition task stimuli. User can control black cursor by his muscle activity and steers it on the blue highlighted target bin. Experimental application randomized current number of bins and target position.

The participants rested their hands on an office desk to minimize any muscular activity to maintain the position of the hands. A randomized sequence of stimuli was then presented to the user. Each stimulus (shown in Figure 51) was a 1-D target acquisition task. The goal in each task was to steer the vertical black line (cursor) to the target depicted as a color-filled interval. The position of the cursor was directly controlled by the force applied by the extensor digitorum of the control hand which roughly corresponded to the angle of inclination of its palm from the surface of the desk. The left end of the range corresponded to the relaxed muscle, the right end of the range corresponded to the maximum force of clenching which was still comfortable by the user as calibrated.

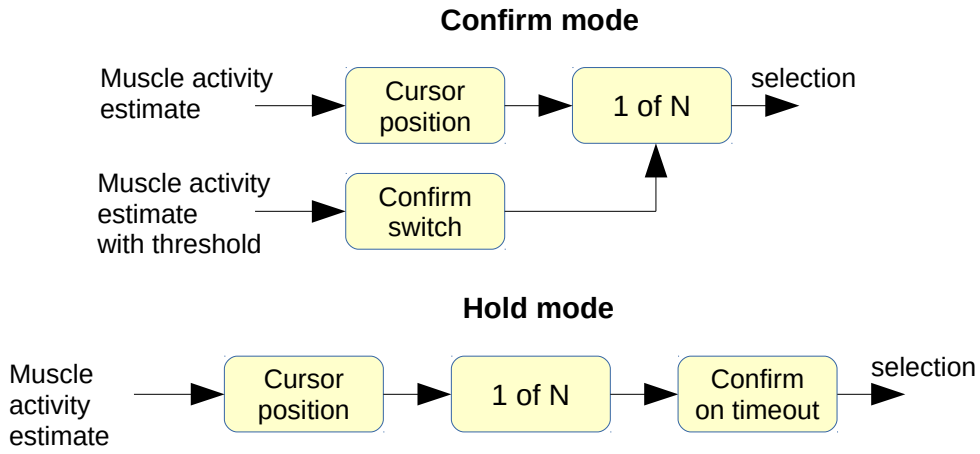

Figure 52: Two modes of input. Confirm mode: user has to confirm selection by activation of another muscle. Hold mode: selection is performed if bin is selected for longer time than is timeout.

There were examined two modes of input: The Confirm Mode and the Hold Mode (see Figure 52). In the Confirm Mode the user had to clench the extensor digitorum of the trigger hand in order to submit the current position of the cursor. In the Hold Mode the user was supposed to keep the cursor in the target bin for 0.75 s (timeout). (The trigger hand was not used.) If the user triggered the confirmation or let the cursor time out outside the target interval, the task was recorded as unsuccessful. The experimenter could prematurely end a task in case it proved too difficult for the user. The development of the cursor position (x) over time was logged for each task as well as the final outcome of the tasks. The tasks differed in the width of the target and in the input mode. The width of the target was 1/N, where N was 2, 4, 6, 8, or 12. Here is the overview of the tasks in each session:

– 4 training tasks, Confirm Mode (or Hold Mode)

– 4 training tasks, Hold Mode (or Confirm Mode)

– 32 tasks, Confirm Mode (or Hold Mode)

– 32 tasks, Hold Mode (or Confirm Mode)

These target acquisition tasks corresponded to menu selection tasks where n-th item out of N items is to be acquired. The users were asked to perform all unique combinations of N $\in\{2,4,6,8,12\}$ and n $\in\{1...N\}$. The sequence of the tasks was randomized for each participant.

The sequence of the modes (Confirm then Hold, or Hold then Confirm) was counterbalanced. There were three possible outcomes of each task: (i) the target was hit, (ii) the target was missed, (iii) the task was skipped (failure of the instrumentation or the user was not able to complete the task). Five randomly chosen users were also asked to carry out tasks with N = 16 and N = 24 for a subset of target positions. n $\in$ 2,4,6,...,16 for N = 16 and n $\in$ 3,8,13,18,23 for N = 24. The purpose of this extension was to collect the data to measure the acquisition time for larger N.

The two modes, Confirm and Hold, differed in the amount of errors as well as in the average time to complete the task. Samples of the output stream from the sensors are shown in figure 53. Both graphs are measured on untrained participants.

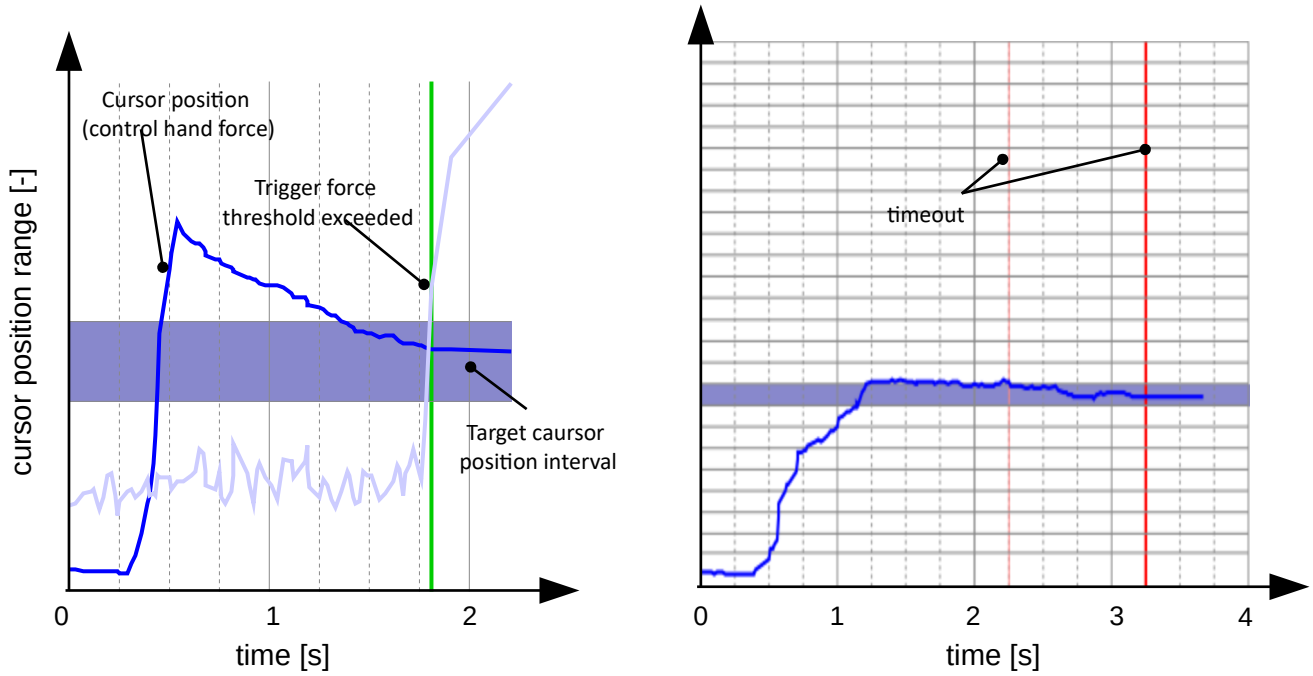

Figure 53: Muscle activity controlled cursor in time plots. Confirmation mode on the left, hold mode in the right graph. Left:user tried to quickly target the position, but missed, the he slowly moved the cursor in desired position. Right: user moved cursor in the borderline between two positions (from 24 total), after he move cursor slightly down to desired target and hold there for 0.7 second the selection was confirmed.

The confusion matrices for the completed tasks are shown for N = 12 in figure 54.

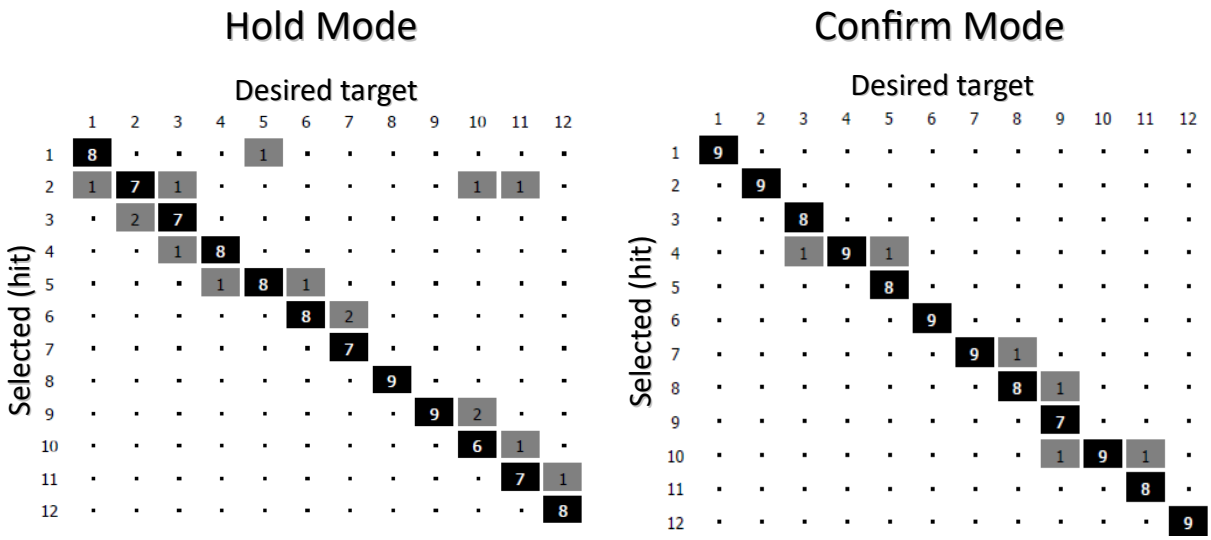

Figure 54: Confusion matrices for N=12. Confirm mode has higher accuracy. Participants reported that erroneous selections was mostly done due to lower concentration while performing movement by other muscle.

Figure 55(a) shows the average acquisition time as a function of N and suggest that decreasing the width of the targets made the tasks more difficult to complete. Analysis of acquisition times for N = 12 has indicated that the targets at either end took shorter time to hit. Figure 55(b) shows the average acquisition time. Most participants preferred the Confirm Mode over the Hold Mode. However, 2 people reported that they felt that the necessity to trigger confirmation by another muscle than the one they used to move the cursor was confusing them. During experiment emerged instances of the following problems: (1) Activating the muscle on the trigger hand made the users alter the force applied by the control hand which resulted in an unwanted movement of the cursor. (2) The users sometimes moved the trigger hand before they intended to issue a confirmation.

Two best performing participants were able to move the cursor immediately to the desired target position after few trials. Worst performing participant came after workout at gym and has most severe problems to aim on target position. Algorithm successfully followed his observably shaking hand movements.

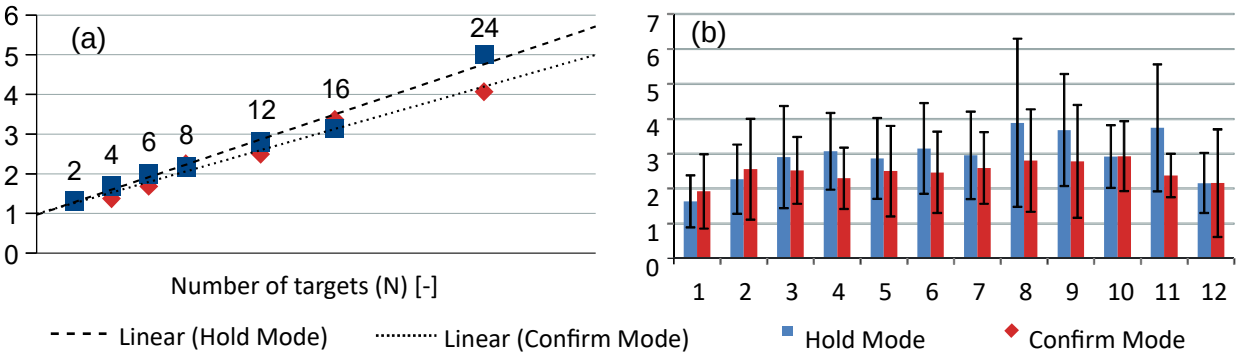

Figure 55: (a) time to select desired target in dependency on numer of bins (N) for untrained users (b) time to select the desired target from 12 positions for untrained users

A complementary study with one amputee participant who was accustomed to use an active prosthesis with two binary EMG channels (“on / off”) demonstrated that he was capable of using the same set of muscles for the continuous control and that his performance was better to average of the control group of participants with no disabilities. He did not have any experience with proposed method or continuous muscle activity estimation. During experiments he had 100 % percent correct results in target selecting task for higher resolution targets (N=12, N=24). Tests shown fast learning curve, participants were faster from task to task.

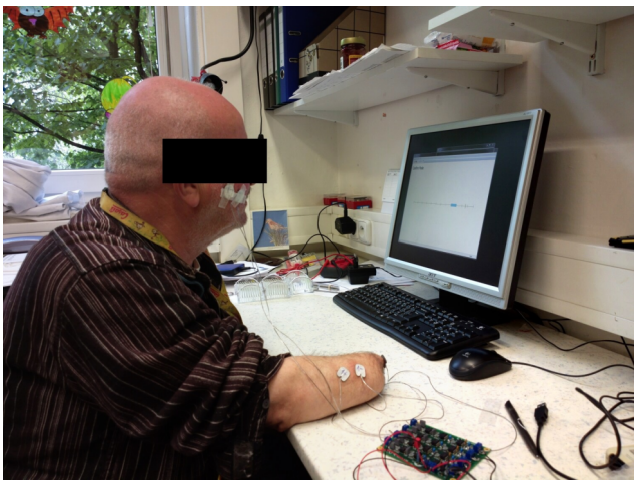

Figure 56: Disabled participant controls computer by using his EMG

All of these findings were later considered for designing of virtual keyboards utilizing this apporach to 1-of-N selection.

5.2 Applications

Proposed method was tested in various developed applications – predictive keyboards, general computer control interface, mouse control, EMG controlled manipulator for virtual reality and its embedded version also for controlling motor servos.

This chapter describes real use cases of developed system.

5.2.1 Controller

Device is capable of emulating various controller functions:

– **Trigger (button pressed down)**. A controller whose function is to enable the user to issue a trigger signal. May be physically realized as a simple button that can be pressed by a palm of the hand, or as a pressure sensor that is mounted on user's forehead. Triggers have a constant selection time. May be utilized for advancing the state of a system by one step or for triggering an action within a time window (scanning). Trigger is by default sent to application during exceeding the threshold of the trigger force. Some people voiced their preference the selection is triggered upon exceeding and then releasing the trigger force. Thus this option was also added to the system for our further setups.

– **On/off switch (button pressed / hold)**. May be realized for example as a button that reports the points in time when being pressed and released. May be utilized for advancing the state of a system by one or more steps, if held for longer period of time. It is configurable by selecting the on/off threshold or threshold with hysteresis.

– **Group of triggers**. The typical example is a keyboard where each key is an independent trigger (or on/off switch) but the functions assigned to the keys are complementing each other. An example may be the 4-way arrow keys and a confirmation key.

– **Analog input**. These devices quantify some action performed by the user, e.g. the amount of pressure applied to a pad or the position of a lever operated by hand. The quantity is reported to the middleware which maps it to some visual feature. The position of the level can be visualized as a position of a 1-D cursor pointer.

These emulated virtual controls operate the designed virtual keyboards.

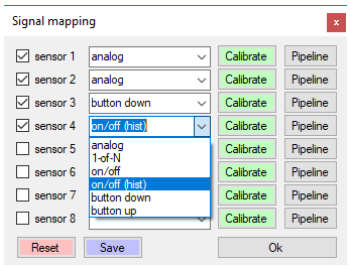

Figure 57: Signal mapping configuration dialog

5.2.2 Text input method

Text input entry can be carried out as a 1-D selection. This operation may be implemented by various interaction techniques, both “conventional” and assistive. One of the common assistive techniques used by people with severe motor impairments is a single-switch scanning [98, 124] where the user can see all the available options which are being highlighted one-by-one in an orderly sequence. The user chooses the item by activating the switch while the option is highlighted. The first option is usually presented for a longer time (typically between 1 and 1.5 s). Further options advance faster (between 0.5 and 1 s). Muscle clenching was reported in the literature as one way of operating a single-switch interface (i.e. only the presence rather than intensity of clenching was detected). The switch was activated when certain threshold of tension was detected [123]. The more options the user has to choose from, the longer the selection time is needed on the average. Using direct selection the user chooses one of the option out of N options presented, for example, a key on a keyboard, or a menu item using a pointing device. In this case, the number of inputs is equal to number of options. The intensity of clenching is not a binary (“on or off”) quality. It can be quantified by (and measured as) a single continuous value and this value can be mapped onto input.

After testing of performance of proposed muscle activation algorithm the users were asked to write random generated sentences using different input methods – with static and dynamic keyboard layouts, including also the predictive keyboards utilizing language corpus dictionaries results of this approach was published in [P2].

Input methods were developed for use as assistive technology and with respect to disabilities of target group. Respectively tries to utilize as low inputs as possible, since the target group are people after severe injuries or with motor disabilities.

5.2.2.1 Dynamic layouts

Predictive keyboard[19] layouts are being dynamically rearranged using statistical models. Letter selection regroups all letters on the keyboard according to probability of next possible letter. The most probable letters are placed on nearer positions with respect to letters and words typed earlier. Therefore for user is easier to reach the most probable letters, which may speed up text entry. Developed keyboards [P2] are also adaptive to number of available control signals.

In figure 58 are depicted variants which are able to utilize from 2 to 6 input signals. Keyboards are supporting 3 types of selection – direct selection, encoding and scanning. Direct selection addresses each group of letters directly by unique discrete signal. In encoding selection is letter selected in multiple steps (for instance row, column and the letter). Scanning require only one or two commands, this technique is similar to hold mode presented in section 5.1) – user can perform scanning selection by sending a command and if desired letter is

19 *Predictive keyboards with language corpus dictionaries were developed in cooperation with Ondřej Poláček and Adam Sporka*

selected after timeout is typed.

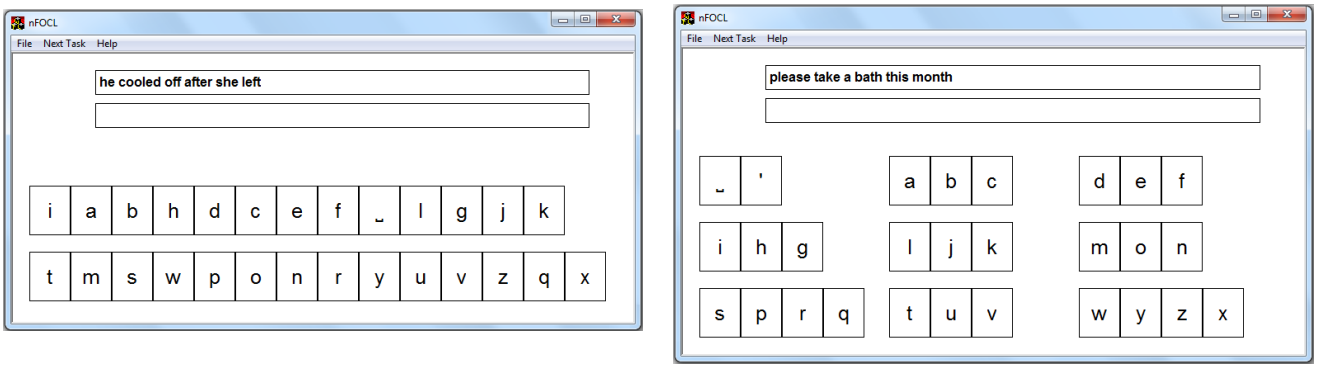

Figure 58: Predictive keyboard prototypes used for testing with participants

In figure 58 on the left the virtual keyboard needs at least 2 discrete signal inputs (3rd state if pressed together). With first input button is user able to select letter from first row, with second button from second row. Third button (or combination of both deletes letter) performs undo action. If third virtual button (input signal) is present, it can be utilized as confirmation of selection. Virtual keyboard on the right needs minimum of 2 input signals (simulated as buttons) but performs best with 3 inputs. If 3 unique discrete signals are present, keyboard works in encoding mode. Each button selects one of three possible columns, in second step rows, in third again sub-columns (desired letters). Therefore user is able to reach letters faster by performing three muscle activations for typing a letter.

Study was done with 3 participants without any previous experience with human-computer interaction using surface EMG signals. Participants had to copy randomly selected sentences using virtual keyboards. Users were able to type up to 4.5 words per minute (where word consisted in average from 5 letters). Each participant went through 5 sessions during 3 days. Average typing error rate was under 7 percent. Each participant was faster in typing and had less error rate in following sessions.

Disabled participant found dynamic layout to be confusing and preferred static layout described in following section.

5.2.2.2 Static layout

It would be very sub-optimal to have a static keyboard layout with only discrete virtual button inputs. For static keyboard layout was utilized proposed muscle activity estimation method which maps the muscle activity to 1-of-N selection task.

Proposed 1-of-N selection method using muscle estimation algorithm was far superior to common assistive techniques using single-switch scanning or only threshold-like activation methods. Of course proposed method needs user that is able to control his muscle with some level of precision (more precise control, more direct selections mappable over one muscle). Therefore the static layout keyboard was designed for analog/1-N selection entry in

dependency on muscle activation level.

Static layout was preferred over the dynamic by majority of participants and especially by disabled one, who perceived dynamic layout as a bit confusing. Therefore this method was incorporated to general purpose keyboard widget.

Composing and editing text is an activity which combines a number of tasks, including typing, cursor movement and block operations, specification of the text formatting, etc. When building an on-screen layout it is important to establish a profile of user's writing session. The user may sit down to a computer to type new text (write-up) or to edit an existing text (proofreading). During write-up the user would more often type new characters rather than navigating around the document and just replacing words here and there. In presented model the text editing operations were split into multiple categories:

– Typing, i.e. entering new text

– Cursor movement, i.e. navigation

– Formatting (layout specification)

– Application control

– Context switching (interface control)

It is obvious that for different tasks (writing up, proofreading, typesetting, etc.) the frequency of corresponding functions of the work processing environment (typing, navigation, setting the format, etc.) differ. Therefore it is of a great advantage that the middleware is capable of a response to these circumstances. This adaptation requires that the layout of the on-screen keyboard and toolbar is constructed automatically because the combinatorics of this task prevents from manual authoring. The necessary functionality of the middleware is shown in following section. The design of the word processing environment was an iterative process.

5.2.2.3 General purpose keyboard widget with context switching

The middleware for general computer control was developed with static layout since it was found by most of the users to be less confusing. It is a unified user interface supporting the entire use case of typing and editing text in word processing. Using this widget user is also able to format text, switch between applications, launch them and input also special characters. Keyboard widget has the adaptive capabilities to number of available control signals and can work with just only one available muscle activity estimation signal. The middleware was developed for Windows platform and is capable of sending keystrokes to operating system and control applications.

Virtual keyboards are being controlled using analog and discrete signals. At least 1 analog signal (muscle activity estimate) is needed. Letters are typed by performing two 1-of-N selections. First selects the row, second selects column. (fig. 59)

Middleware has adaptive capabilities. Next available discrete signal will be mapped to confirm action, following to undo action.

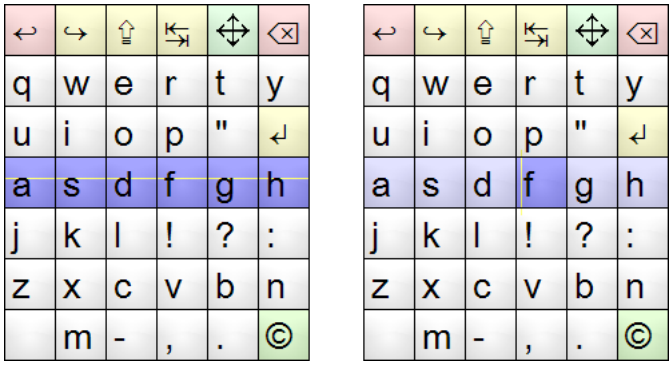

Figure 59: Two-dimensional selection: Selecting the row (left), selecting the column (right).The real position rendered as yellow line is provided to the user as visual feedback.

If there is not enough signals for mapping undo action (for instance one analog, one confirm or only one analog configurations) back action button is added to begin of each row (figure 60).

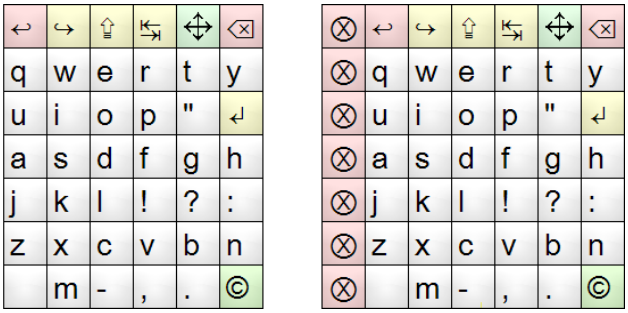

Figure 60: Adaptive design of virtual keyboards. If there is no signal left for undo operation, it is rendered as new virtual button (on the left of the right keyboard).

The participants who had an experience with the 1-of-N selections via scanning from previous studies with dynamic layouts mentioned that they found this technique more comfortable for this purpose. The extreme parts of the range, leftmost and rightmost, were easy to reach as they did not require much aiming. To achieve maximum resolution capability it is possible to optimize the gauge (figure 61) by shrinking the corresponding intervals and thus enlarging the intervals of the second to N −1-th options and thereby making them easier to reach.

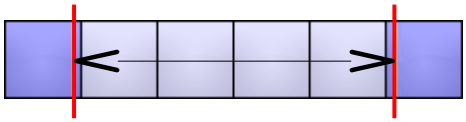

Figure 61: Optimized 1-of-N selection range to achieve more options at the effort of selection 1-of-(N-2) options. The muscle activity estimate value is mapped between end of first bin and beginning of the last. Reaching boundary selection is easier and does not need much of user's concentration. On this example the 1-of-6 selection shrinks to effort of 1-of-4 selection.

General purpose keyboard layout is depicted in figure 62. This layout (context) serves for performing most of the operations and typing tasks and also is representative example of largest keyboard matrix used (8x8 or with cancel action 9x8).

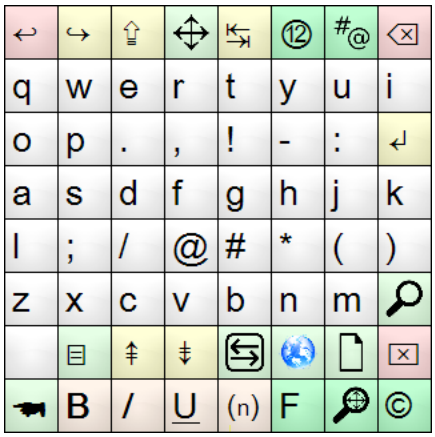

Figure 62: General purpose keyboard layout based on 8x8 matrix contains also function buttons for formatting text, selection and navigation, also shortcuts to switch between various contexts.

Because mapping of all the listed capabilities would need very huge keyboard layout, in which reaching the virtual control buttons would need much higher concentration of the user, the available typing keys and actions were distributed between set of virtual keyboards – contexts.

Figure 63 depicts scheme of available contexts. User is able to switch between contexts by selecting the green keys. For specific functions which are expected to be activated in rapid successions (browsing, navigation in text) were designed inline sub-contexts (fig. 63 i – l). These sub-context allows to highlight text, movement using arrows, page scrolling, switch applications and activate menu. In these context can user highlight the desired action and by trigger it with confirmation signal.

Contrary to default keyboard behavior – while holding the confirmation signal the action will repeat in short periods until the confirmation signal is released. Presence of second analog signal determines the speed of repetition in inline contexts.

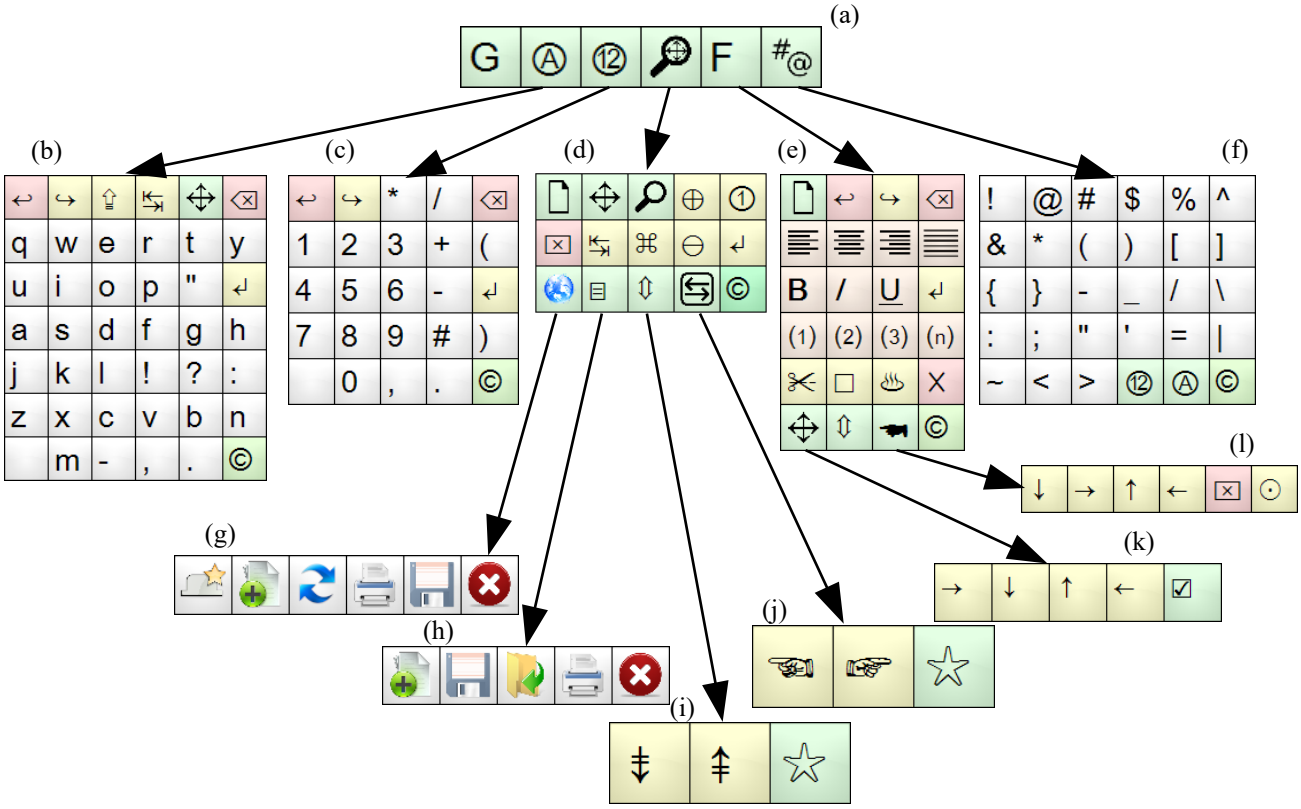

Figure 63: Scheme of available contexts consisting of character typing buttons (gray), function buttons (yellow), delete, undo and cancelation function buttons (red), text formatting shortcuts (orange) and context switching buttons (green)

(a) is a context switching panel
(b) is half-qwerty text typing context
(c) numeric context
(d) browsing and application control context – allows magnifying text, switching to rapid inline sub-contexts and open application menus
(e) text formatting and selection – consists of cut-copy-paste actions, formatting actions and selection actions
(f) special symbols context
(g-h) are specialized sub-contexts:
  (g) web browser control context
  (h) file operation context
(i-l) are inline sub-contexts for repeated operations
  (i) page scroll context
  (j) application switching context
  (k) arrow navigation context
  (l) text selection context

Developed keyboard widget is easily extensible. New contexts, actions, shortcuts and special letters can be added.

5.2.2.4 Mouse control

Muscle estimates has been also mapped to control mouse cursor.

To perform mouse control 1 analog and 2 discrete signals are needed. In this case first discrete signal switches the direction of mouse cursor movement direction (-x, -y, +x, +y), analog signal controls speed of movement in that direction. Second discrete signal emulates the mouse buttons – short activation for click, two short activations for double click, three for right click and holding has same behavior as clicking the mouse. 3th discrete signal would act as right click button. Feedback to the user is provided in form of visual changes of mouse cursor, which is being rotated in direction of selected movement. (fig. 64)

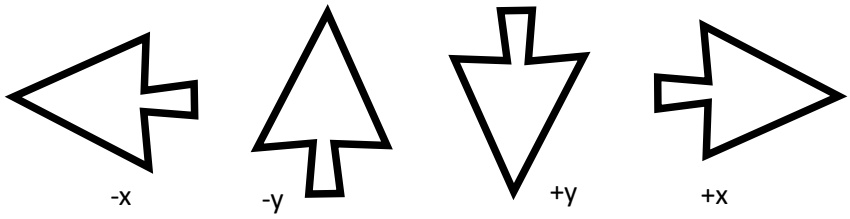

Figure 64: Direction of movement provided as a visual feedback to the user

Supported are also variants with 3 and 4 analog signals. In 4 analog signal variant each signal controls speed of mouse movement in corresponding directions (-x, -y, x, y). In 3 analog signal variant 2 signals controls angle of mouse cursor orientation and last controls movement in the direction of mouse cursor pointer.

Variant with 2 axes controlled by direct mapping of analog muscle activity estimates onto axes (x, y) was rejected due to high level of concentration needed and low comfort.

5.2.3 Motor control

The device is capable of driving an analog electric servo motor, since the embedded design of described system has implemented also multiple PWM modulation outputs and muscle force estimation algorithm is also embedded. Each connected motor is then rotated to corresponding angle in dependency on muscle activity estimation from each muscle connected to the device. Control signals had faster response to continuous movement (muscle activity) than used motors (0.4s / 180°).

The feedback would be optimal to achieve satisfactory and precise movements. This can be achieved by adding the vibrating element snapped to users body.

5.2.4 VR environment integration

In 2016 the device was successfully integrated with VR environment. Such system can be utilized for rehabilitation purposes, muscle fine movement training or added as another controller input to for interaction in virtual environment. During development was created a universal plugin and Unity game engine plugin.

Figure 65: from the left: designed room in virtual space mapped 1:1 to real room, artificial grabber controlled by user's surface EMG signals, real room, where user can move freely and perform the task

Engine plugin was utilized for development of virtual reality training application, where user has to pickup and place items. In experiment shown in figure 65 is user able to control virtual manipulator using his finger extensions (pointing, middle and small). Muscle estimate of each finger was mapped to different function of virtual manipulator. Middle finger opened claws, pointing finger rotated manipulator and small finger extended manipulator in forward direction. This application can be utilized for learning with such a human-computer interface and with proper calibration settings (high sensitivity) also for training of soft motor muscle movements. The 1:1 room model was designed and mapped onto the real room where user is able to move freely with head mounted headset. Screenshots form recorded footage are on the next page (fig. 66).

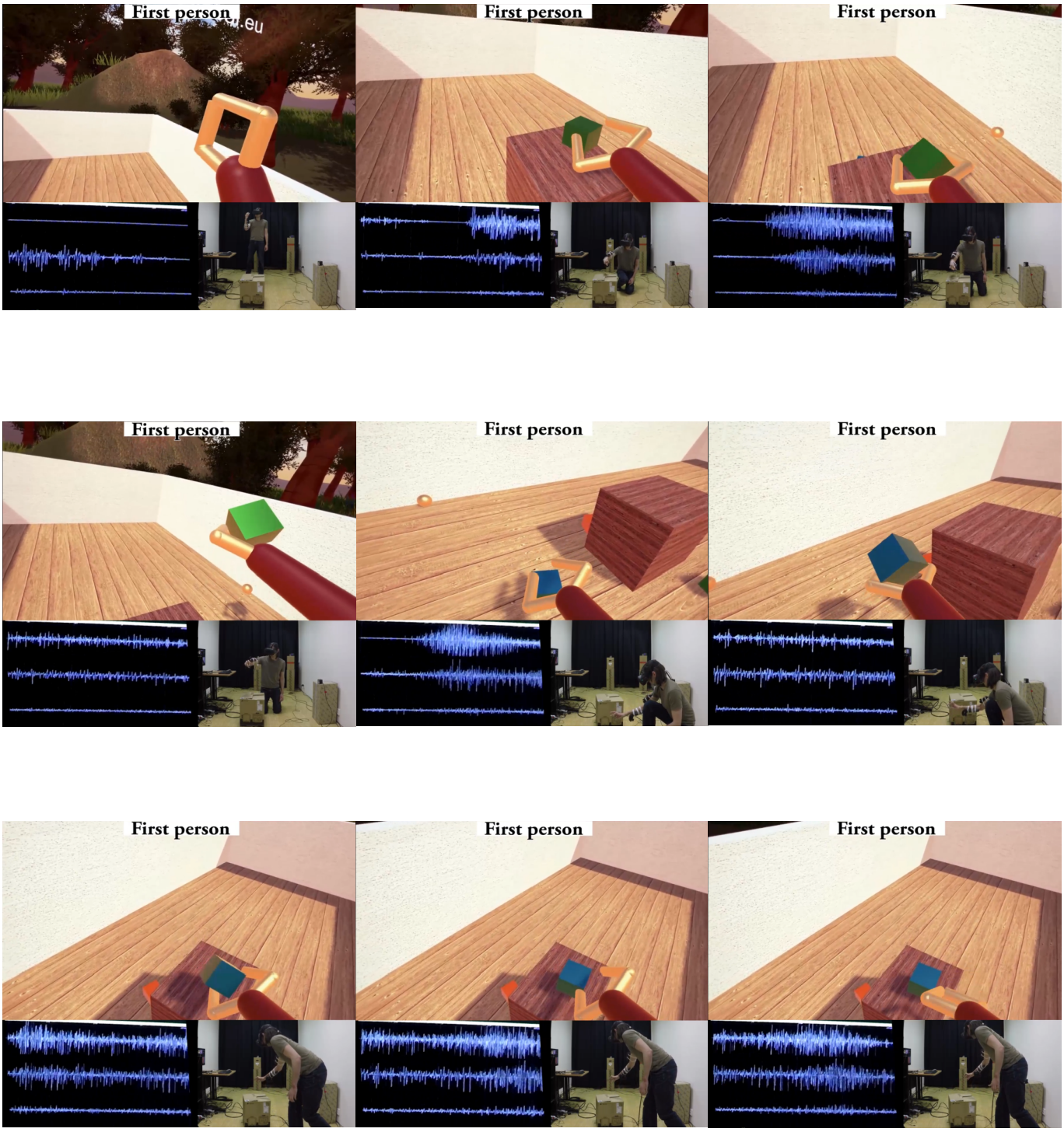

Figure 66: User is able to control manipulator using finger movements. He is able to open, rotate and prolong the manipulator by his surface EMG. In the upper part of each screenshot is first person view, left bottom part is actual EMG signal, right bottom part is footage from room, which is mapped 1:1 to virtual space.

6 Discussion

Decomposition

Up to date there are several works utilizable for realtime decomposition to single MUAPs. Glaser's et al. realtime CKC method [82] is designed for HD EMG setup and requires high number of channels. Multi-channel decomposition systems have been extensively investigated and have a great results. But for assistive technology can be usage of high density EMG systems disadvantageous since multiple elements and more complex system means multiple sources of possible noise and failures. (EMG channels, bad contacts on electrode, …) On the other side available online low and single channel decomposition methods does not yield much accurate results.

Online successfully implemented decomposition methods for single channel recordings usable for human-machine interaction are proposed by Xiong et al, [80] and very recently by Sun et al. [135].

If there would be precise realtime decomposition method working in all circumstances able to decompose all the MUAP spikes from the muscle, it would be possible to utilize cross-talk effect to identify muscle activity estimates of multiple muscles. Xiong et al. [80] uses spike clustering method without considering of superimposed signals. On resulting clustered spikes are calculated basic features (IAV, median and maximum, described in section 3.3.2) to recognize discrete states from just one acquisition channel with 75 percent success rate, which is not superior result to non-decomposition discrete grasp recognition approaches (overview of grasp recognition methods is in Table III on p. 45).

Work of Sun et. al [135] proposes novel online decomposition technique based on FastICA algorithm for estimating of the muscle force from one acquisition channel. Results of instantaneous BSS methods are still questionable and discussed by experts. Nevertheless, shown results does not seem to be stable enough for controlling of the user interface and presented correlation coefficient 81.3% ± 6.1% (with measured force) does not seem to be superior to some alternative amplitude based methods like is stable Sanger's Bayesian predictor [97] with correlation coefficient 87.2% ± 1.2 % or neural network based approach presented by [101] and [102] with similar correlation coefficient 94 %. Although, used method is impressive.

Best muscle force estimation results were shown by Istenic et al. [74] utilizing a twitch based estimation model on resulting decomposed MUAPs by gradient CKC algorithm. Algorithm processed 30s recording on Intel Pentium IV for 33.18s. Na et al. later presented similar finding with use of dEMG algorithm with noisier result and correlation coefficient 79 %. Neverthless for controlling of user interface is most important stability and response of the

method.

Online decomposition during dynamic muscle movements is still a challenging topic, another possible complication in decomposition task especially for low-channel number methods is tendency to synchronization of individual motor units, which emerges more evidently, when muscle is more fatigued.

One of the aims of this thesis was to consider use of online decomposition of to obtain more accurate and natural response of the system. Thesis outlined decomposition method without need of prior knowledge of MUAP templates, which are being automatically sorted using spike clustering method. Method was significantly slower and resource consuming than developed amplitude based muscle activity estimation method. Furthermore needed much longer calibration and did not yield better results than designed amplitude based muscle activity estimator. Decomposition method worked most optimally with dry wire 5-pin electrode, which has very selective properties (spatial filtering), but also has a high impedance and thus is more noise sensitive. 5-pin dry wire electrode was reported by participants to be uncomfortable.

Decomposition based methods works correctly in laboratory circumstances but are prone to fail elsewhere due to nature of surface EMG signals, present noise and complexity of the task. Online surface EMG decomposition methods are often studied during constant isometric contractions or lower forces and yields significantly worse results.

Device

Thesis presented developed device with embedded mentioned muscle activity level estimation algorithm. Analog part conditioning circuity of the device was designed with respect to compromise between obtaining best signal properties for muscle force estimation and signal decomposition while preserving as signal energy as possible.

Using WLPD filter in combination with HighQ comb filter was possible to obtain reasonable signal from digitized surface EMG signals. During experiments proposed HW solution performed from 10 to 25dB SNR for low-level percentage of MVC signals in with 5 pin wire electrodes. With Ag/AgCl electrodes was SNR better than 40dB, this value depended also on environment and varied across participants. Portable revision of the device was demonstrated live on several talks and conferences. Number of tests was performed in different environments with good results.

Presented electrode setup, preconditioning circuity and algorithms are designed with respect to suppression of noise, muscle crosstalk and provide high quality signals for decomposition, which proved to be beneficial also for amplitude based muscle activity level estimation algorithm.

Amplitude based method

Thesis presents muscle activity estimating method utilizable in human-machine interaction due to its stability, fast response and simple calibration. Method was extensively

tested by qualitative studies with participants. Amplitude based muscle activity estimation method was designed with respect to obtain best natural fast and stable response from an estimator to allow accurate control of specialized interface for controlling virtual keyboards. This was achieved and also is observable in figure 53 (p.85) presenting the recorded performances of the participants.

Altough MAV was reported to be most correlated feature with muscle force and activity, testing during qualitative studies revealed that RMS has much more natural response over selected dynamic range of muscle contraction by participants.

Recommended is using of weak muscle activations. This is intended for user comfort, since using full muscle force dynamic range could be exhaustive, and also to prevent fatigue, which would change parameters of signal.

Control of computer interface using muscle estimate

Many methods use data driven recognition approach for detection of discrete states (grasps). Machine learning methods needs learning process for each individual user. These methods are used in advanced active prosthetic systems to extend their degrees of freedom. Yet still are not too common. The sEMG characteristics significantly dependends on electrode position and changes during high muscle contraction forces due to rapid muscle fatigue. Therefore these algorithms mostly needs recalibration (learning process) and could be unreliable during long term and day-to-day use without relearning. Discrete grasps are being nowadays utilized also in commercial products (Myo wristband).

One of the thesis aims was to investigate if continuous muscle activity level estimates could be advantageous in controlling of user interface in human-computer interaction. This question was answered during qualitative tests of developed surface EMG controlled keyboard prototypes. Participants expressed that selecting characters from virtual keyboards is more intuitive and faster by continuous muscle estimates than discrete commands (repetitive movement to scan the keyboard characters). Requirements stated in chapter 2.5 have been met.

7 Conclusion

Thesis concerns the continuous surface EMG muscle activity estimation and its usage for control in assistive technologies. In this text were described physiological pre-requisities regarding the signal characteristics, presented research on methods utilized in human-machine interaction using surface EMG and methods for its decomposition, followed by description of the tested measurement setups for signal acquisition, real-time algorithms and design of whole movement interaction system. The possibility of real-time signal decomposition utilized for muscle activity estimation was presented and discussed.

During development of the real-time muscle force estimation methods various setups of electrodes were tested and several revisions of custom-made amplifier and embedded device were designed. Developed device was used for tests with participants and is capable of acquiring high resolution signals, signal processing and can operate stand-alone without computer needed in embedded applications, since it contains embedded version of presented muscle activity estimation algorithm. Development of the device included an implementation of computer driver with middleware for real-time text typing and general purpose TCP/IP based interface for later use in applications and control system. Actual hardware solution is independent on commercial hardware or special measurement computer setup and provides signals with high signal to noise ratio owing to galvanic barrier in its digitization part of and custom made measurement setup itself.

Simultaneously with developing of hardware part were prepared algorithms for decomposition of surface EMG. Decomposition approach yielded reasonable results for very low muscle activity EMG signals in laboratory conditions, noise-free environments and for stabilized user positions, but due to this limitations was not suitable for dynamic experiments (due to nature of used method). For this reason was developed also fast and stable muscle activity estimation algorithm, which was less sensitive to signal artifacts caused by movement or degraded electrode connection. Results shown that electrode setups and preconditioning methods, which are mostly used for decomposition setups can be advantageous for surface EMG amplitude processing techniques due to their ability to reduce the muscle cross-talk effect and filtering out the correlated part of the signal. Algorithm was examined in dynamic experiments – for instance control of artificial manipulator in virtual reality environment and by qualitative studies with participants.

Developed methods and device took part as a suitable human-computer interface for project TextAble – an alternative text input method for disabled people. Thesis also presents developed method for typing text using continuous muscle estimates in human-computer interaction system as an assistive technology. Method was designed with regard to universally intuitive usage, simple calibration and was successfully verified by continual testing during development with participants. Findings were utilized for design of text typing method.

Hypothesis considering possibility of controlling user interface using continuous muscle activity was successfully evaluated with positive result.

Abbreviations

CKC – convolution kernel compensation (method)

dVCA – differentially variable component analysis

DWT – discreet wavelet transform

ECG – electrocardiogram

EEG – electroencefalogram

EMD – empirical mode decomposition

EMG – electromyogram

HMM – hidden Markov models

ICA – independent component analysis

LPD – low-pass differential (filter)

MAV – mean absolute average

MU – motor unit

MUAP – motor unit action potential

MVC – maximum voluntary contraction

NN – neural network

PCA – principal component analysis

PD3 – precise decomposition III (algorithm)

ORICA – online recursive independent component analysis

RMS – root mean square

STFD – spatial time-frequency distribution

STFT – short time Fourier transform

SVM – support vector machine

WLPD – weighted low-pass differential filter

WT – wavelet transform

References

[1] De Luca C. J. – Physiology and mathematics of myoelectric signals. IEEE Transactions on Biomedical Engineering, vol. 26, no. 6, Jun. 1979

[2] De Luca C. J., LeFever R.S., McCue M. P., Xenakis A. P. – Behaviour of human motor units in different muscles during linearly varying contractions. Journal of Physiology vol. 329, p. 113-128, 1982

[3] De Luca C. J., Contessa P. – Hierarchical control of motor units in voluntary contractions, Journal of Neurophysiology vol. 107, p 178-195, 2012

[4] LeFever R. S., De Luca C. J. – A procedure for decomposing the myoelectric signal into its constituent action potentials – Part 1: technique, theory and implementation. IEEE Transactions on Biomedical Engineering, vol. 29, no. 3, Mar. 1982

[5] Zaheer F., Roy S. H., De Luca C. J. – Preferred sensor sites for surface EMG signal decomposition. Physiological Measurement, vol. 33, p. 195-206, Jan. 2012

[6] McGill K. C., Lateva Z. C., Marateb H. R. – EMGLAB: An Interactive EMG decomposition program. Journal of Neuroscience Methods, vol. 149, no. 2, p. 121- 133, Dec. 2005

[7] McGill K. C., Cummins K. L., Dorfman L. J. – Automatic decomposition of the clinical electromyogram. IEEE Transactions on Biomedical Engineering, vol. 32, no. 7, Jul. 1985

[7a] McGill K. C. – Optimal Resolution of Superimposed Action Potentials. IEEE Transactions on Biomedical Engineering, vol. 49, no. 7, p. 640-650, Jul. 2009

[8] De Luca C. J., Adam A., Wotiz R., Gilmore L. D., Nawab S. H. – Decomposition of Surface EMG Signals. Journal of Neurophysiology, vol. 96, p. 1646 – 1657, May 2006

[9] Nawab S. H., Chang S. S., De Luca C. J. – High-yield Decomposition of Surface EMG Signals. Clinical Neurophysiology, vol. 121, no. 10, p. 1602-1615, October 2010

[10] A. Holobar, D. Zazula – Surface EMG Decomposition Using Novel Approach for Blind Source Separation. Informatica Medica Slovenica, vol. 8, no. 1, p. 2-14, 2003

[11] Zazula A., Holobar D. – An Approach To Surface EMG Decomposition Based on Higher-order Cumulants. Computer Methods and Programs in Biomedicine, vol. 80, no. 1, p. S51-S60, Dec 2005

[12] Holobar A., Zazula D. – Correlation-based decomposition of surface electromyograms at low contraction forces. Med. Biol. Eng. Comput., vol. 42, no. 4, p. 487-495, 2004

[13] Holobar A., Zazula D. – Gradient Convolution Kernel Compensation Applied to Surface Electromyograms., LN in Computer Science 4666, p. 617–624, 2007

[14] Feder M., Weinstein E. – Parameter Estimation of Superimposed Signals Using the EM Algorithm. IEEE Transactions on Acoustics, speech and signal processing, vol. 36, no. 4, Apr. 1988

[15] Florestal J. R., Methieu P. A., Plamondon R. – A Genetic Algorithm for the Resolution of Superimposed Motor Unit Action Potentials. IEEE Transactions on Biomedical Engineering, vol. 54, no. 12, Dec. 2007

[16] Graupe D., Liu R. – A Neural Network Approach to Decomposing Surface EMG Signals. Proceedings of the 32nd Midwest Symposium on Circuits and Systems, 1989

[17] M.H. Hassoun, C. Wang, A.R.Spitzer – NNERVE: Neural Network Extraction of Repetitive Vectors for Electromyography - Part I: Algorithm. IEEE Transactions on Biomedical Engineering, vol. 41, no. 11, Nov. 1994

[18] Xu Z., Xiao S., Chi Z. – ART2 Neural Network for Surface EMG Decomposition. Neural Computing and Applications, vol. 10, no. 1, p. 29-38, Apr. 2001

[19] Chauvet E., Fokapu O., Hogrel J. Y., Gamet D., Duchene J. – Automatic Identification of Motor Unit Action Potential Trains From Electromyographic Signals Using Fuzzy Techniques. Med. Biol. Eng. Comput., vol. 41 , p. 646–653, 2003

[20] Garcia G. A., Nishitani R., Okuno R., Akazawa K. – Independent Component Analysis as Preprocessing Tool for Decomposition of Surface Electrode-array Electromyogram. 4Th International Symposium on Independent Component Analysis and Blind Signal Separation, Nara, Japan, April 2003

[21] Sobahi N. M. – Denoising of EMG Signals Based on Wavelet Transform. Asian Transactions on Engineering, vol. 1, no. 5, Nov. 2011

[22] Phinyomark A., Limsakul C., Phukpattaranont P. – Optimal Wavelet Functions in Wavelet Denoising for Multifunction Myoelectric Control. ECTI Transactions on Electrical Eng., Electronics and Communications, vol. 8, no.1, Feb. 2010

[23] Wheeler K. R., Chang M. H., Knuth K. H. – Gesture-Based Control and EMG Decomposition. IEEE Transactions on Systems, Man and Cybernetics – Part C: Applications and Reviews, vol. 36, no. 4, Jul. 2006

[24] Nakamura H., Yoshida M., Kotani M., Akazawa K., Moritani T. – The Application of Independent Component Analysis to the Multi-channel Surface Electromygraphic Signals for Separation of Motor Unit Action Potentials Trains: part I – Measuring Techniques. Journal of Electromyography and Kinesiology, vol. 14, no. 4, p. 423-432, Aug. 2004

[25] Naik G. R., Kumar D. K., Arjunan S. P., Palaniswami M., Begg R. – Limitations And Applications of ICA for Surface Electromyogram. Electromyogr. Clin. Neurophysiology, vol. 45, no. 5, p. 295-309, Sep. 2006

[26] Naik G. R. , Kumar D. K. – Source Separation and Identification Issues in Biosignals: A Solution Using Blind Source Separation. In book: Recent Advances in Biomedical Engineering, 10/2009, ISBN: 978-953-307-004-9

[27] Eftekhar A. , Toumazou C., Drakakis E. M. – Empirical Mode Decomposition: Real-time Implementation and Applications, vol. 73, no. 1, p. 43 – 58, October 2013

[28] Phinyomark A., Limsakul C., Phukpattaranont P. – Application of Wavelet Analysis in EMG Feature Extraction for Pattern Classification. Measurement Science Review, vol. 11, no. 2, 2011

[29] Kilby J. , Hosseini H. G. – Wavelet Analysis of Surface Electromyography Signals. Proceedings of the 26th Annual International Conference of the IEEE EMBS, San Francisco, USA, September 1.-5., 2004

[30] Mahdavi F. A. , Ahmad S. A. , Marhaban M. H., Akbarzadeh-T M.-R. – The Utility of Wavelet Transform in Surface Electromyography Feature Extraction – A Comparative Study of Different Mother Wavelets. World Academy of Science, Engineering and Technology 74, 2013

[31] Karlsson S., Yu J., Akay M. – Time-Frequency Analysis of Myoelectric Signals During Dynamic Contractions: A Comparative Study. IEEE Transactions on Biomedical Engineering, vol. 47, no. 2, Feb. 2009

[32] Canal M. R. – Comparison of Wavelet and short time Furier transform methods in analysis of EMG signals. Journal of medical systems, vol. 34, no. 1, p. 91-94, Feb. 2010

[33] Kakoty N. M., Hazarika S. M. – Classification of grasp types throught wavelet decomposition of EMG signals. 2nd international Conference on Biomedical Engineering and Informatics, 2009. BMEI'09., p. 1-5, 17-19 Oct. 2009

[34] Flanders M., Herrmann U. – Two Components of Muscle Activation: Scaling With the Speed of Arm Movement. Journal of Neurophysiology, vol 67., no. 4, p. 931-943, Apr. 1992

[35] Bosco G. – Principal Component Analysis of Electromyographic Signals: An Overview. The Open Rehabilitation Journal, vol. 3, p. 127-131, 2010

[36] Shalu G. K., K. S. Sivanandan, K. P. Mohandas – Fuzzy logic and probabilistic neural network for EMG classification – A comparative study. International Journal of Engineering Research & Technology, vol 1., no. 5, Jul. 2012

[37] Kherzi M., Jahed M. – Real-time Intelligent Pattern Recognition Algorithm for Surface EMG Signals. Biomedical Engineering Online [online], Dec. 2007

[38] Chu J., Moon I., Mun M. – A real-time pattern recognition for multifunction myoelectric hand control. IEEE Transactions on Mechatronics, vol. 12, p. 282-290, 2007

[39] Zeghbib A., Palis F., Ben-Ouezdou – EMG-based Finger Movement Classification Using transparent fuzzy system. EUSFLAT – LFA 2005

[40] Xu Z., Xiao S. – Digital Filter Design for Peak Detection of Surface EMG. Journal of Electromyography and Kinesiology, vol. 10, no. 4, p. 275–281, August 2000

[41] Rasheed S., Stashuk D. – Pattern Classification Techniques for EMG Signal Decomposition. In Book: Advanced Biosignal Processing, p. 267-289, 2009, ISBN: 978-3-540-89505-3

[42] Walker J. B., Scroggins B., Morse M. – Are Paralyzed People Really Paralyzed? Probably Not According to EMG Analysis. IEEE International conference on Engineering in Medicine and Biology Society, 1988

[43] Knuth K. H., Shah A. S., Truccolo W., Ding M., Bressler S. L., Schroeder C. E. – Differentially Variable Component Analysis (dVCA): Identifying Multiple Evoked Components Using Trial-to-Trial Variability. Journal of Neurophysiology, vol. 95, no. 5, p. 3257-3276, May 2006

[44] Henneman, E. – Relation Between Size of Neurons and Their Susceptibility to Discharge. Science 126, p. 1345–1347, 1957.

[45] Muscle Identification. [online] available at: http://droualb.faculty.mjc.edu/Lecture%20Notes/Unit%203/muscles%20with%20figures.htm, Retrieved 2017-10-08

[46] Piervirgili G., Petracca F., Merletti R. – A New Method to Assess Skin Treatments for Lowering the Impedance and Noise of Individual Gelled Ag–AgCl electrodes. Physiol. Meas., vol. 35, p. 2101–2118, 2014

[47] Arvetti M., Gini G., Folgheraiter M. – Classification of EMG Signals Through Wavelet Analysis and Neural Networks for Controlling an Active Hand Prosthesis. IEEE 10th International Conference on Rehabilitation Robotics, Noordwijk, Netherlands, 13-15 June 2007

[48] Nonna A. Dimitrova, George V. Dimitrov, Valery N. Chihman – Effect of Electrode Dimensions on Motor Unit Potentials. Medical Engineering & Physics, vol. 21, p. 479–48, 1999

[49] Fuglevand A. J., Winter D. A., Patla A. E. – Models of Recruitment and Rate Coding Organization in Motor-Unit Pools. J Neurophysiol., vol. 70, no. 6, p. 2470-88, Dec 1993

[50] Fuglevand A. J., Winter D. A., Stashuk D. – Detection of Motor Unit Action Potentials with Surface Electrodes: Influence of Electrode Size and Spacing. Biological Cybernetics, vol. 67, no. 2, p. 143–153, June 1992

[51] Merletti R., Rainoldi A., Farina D. – Surface Electromyography for Noninvasive Characterization of Muscle. Exercise and Sport Sciences Reviews, vol. 29, no. 1, January 2000

[52] Karlik B. – Machine Learning Algorithms for Characterization of EMG Signals. International Journal of Information and Electronics Engineering, vol. 4, no. 3, May 2014

[53] Roberto Merletti and Philip Parker Electromyography: Physiology, Engineering and Non-Invasive Applications. Wiley—IEEE Press, July 2004, 520 pages, ISBN: 0-471-67580-6

[54] van Vugt J. P. P., van Dijk J. G. – A Convenient Method to Reduce Crosstalk in Surface EMG. Clinical Neurophysiology, vol. 112, p. 583 – 592, 2001

[55] Mesin L., Smith S., Hugo S., Viljoen S., Hanekom T. – Effect of spatial filtering on crosstalk reduction in surface EMG recordings. Medical Engineering & Physics, vol. 31, p. 374 – 383, 2009

[56] Chowdhury R. H. , Reaz M. B. I. , Ali M. A. B. M., Bakar A. A. A., Chellappan K., Chang T. G. – Surface Electromyography Signal Processing and Classification Techniques. Sensors, vol. 13 no. 9, p. 12431-12466, 2013

[57] Siqueira A. L. D., Soares A. B. – A Novel Method for EMG Decomposition Based on Matched Filters. Research on Biomedical Engineering, vol. 31, no. 1, p. 44-55, 2015

[58] Winslow J., Dididze M., Thomas C. K. – Automatic Classification of Motor Unit Potentials in Surface EMG Recorded from Thenar Muscles Paralyzed by Spinal Cord Injury. Journal of Neuroscience Methods, vol. 185, no. 1, p. 165-177, 2009

[59] Daniel Graupe, Salahi J., Kohn K. H. – Multifunctional Prosthesis and Orthosis Control via Microcomputer Identification of Temporal Pattern Differences in Single-site Myoelectric Signals. Biomed. Engng., vol. 4, January 1982

[60] Tsenov G., Zeghbib A. H., Palis F., Shoylev N., Mladenov V. – Neural Networks for Online Classification of Hand and Finger Movements Using Surface EMG signals. 8th Seminar on Neural Network Applications in Electrical Engineering, 2006

[61] Englehart K. – A Wavelet-Based Continuous Classification Scheme for Multifunction Myoelectric

Control. IEEE TRANSACTIONS ON BIOMEDICAL ENGINEERING, vol. 48, no. 3, Mar 2001

[62] Phinyomark A.,Phukpattaranont P., Limsakul C. – Feature Reduction and Selection for EMG Signal Classification. Expert Systems with Applications, vol. 39, p. 7420-7431, 2012

[63] Ide H., Hosaka R., Ohtsuka M. – Fuzzy Control of Robot Hand Based on EMG. J. Robot. Mechatron., vol.3, no.5, p. 435-436, 1991

[64] Clancy E. A., Hogan N. – Single Site Electromyograph Amplitude Estimation. IEEE Trans. Biomed. Eng. vol. 41, p. 159–167, 1994

[65] Englehart K. – A Robust, Real-Time Control Scheme for Multifunction Myoelectric Control. IEEE Transactions on Bimodeical Engineering, vol. 50, no. 7, July 2003

[66] Crawford B., Miller K., Shenoy P., Rao R. – Real-Time Classification of Electromyographic Signals for Robotic Control. AAAI'05 Proceedings of the 20th national conference on Artificial intelligence, vol. 2, p. 523-528, Pittsburgh, Pennsylvania, July 09 - 13, 2005

[67] Sukhan L., Saridis G. – The control of a prosthetic arm by EMG pattern recognition. IEEE Transactions on Automatic Control, vol. 29, no. 4, Apr 1984

[68] Naik G. – A Comparison of ICA Algorithms in Surface EMG Signal Processing. International Journal of Biomedical Engineering and Technology, vol. 6, no. 4, p. 363 - 374, August 2011

[69] Naik G. R., Kumar D. K. – An Overview of Independent Component Analysis and Its Applications. Informatica, vol. 35, p. 63–81, 2011

[70] Naik G. R., Kumar D. K., Arjunan S. P. – Kurtosis and Negentropy Investigation of Myo Electric Signals During Different MVCs. ISSNIP Biosignals and Biorobotics Conference, Vitoria, Brazil, 6-8 Jan. 2011

[71] Holobar A., Zazula D. – Multichannel blind source separation using convolution kernel compensation. IEEE Transactions on Signal Processing, vol. 55, no. 9, p. 4487 – 4496, 2007

[72] Dobrev, D., Dobreva T., Tsvetanov, Mudrov N. – Simple High-Q Comb Filter for Mains Interference and Baseline Drift Suppression. Annual Journal of Electronics, 2009, ISSN 1313-1842.

[73] Istenic R., Holobar A., Merletti R., Zazula D. – EMG Based Muscle Force Estimation using Motor Unit Twitch Model and Convolution Kernel Compensation. In: Jarm T., Kramar P., Zupanic A. (eds) 11th Mediterranean Conference on Medical and Biomedical Engineering and Computing 2007. IFMBE Proceedings, vol 16. Springer, Berlin, Heidelberg , 2007

[74] Istenic R., Holobar A., Gazzoni R., Zazula D. – Motor Control Information Extracted from Surface EMG as Muscle Force Estimation. WSEAS Transactions on Biology and Biomedicine, vol. 5, no. 1, January 2008

[75] Hsu S.-H., Mullen T., Jung T.-P., Cauwenberghs G. – Online Recursive Independent Component Analysis for Real-time Source Separation of High-density EEG. in IEEE EMBS, 2014.

[76] Hsu S.-H., Pion-Tanachini L., Jung T.-P, G. Cauwenberghs – Tracking Non-Stationary EEG Sources Using Adaptive Online Recursive Independent Component Analysis. in IEEE EMBS, 2015.

[77] Liu J., Ying D., Zhou P. – Wiener Filtering of Surface EMG with A Priori SNR Estimation Toward Myoelectric Control for Neurological Injury Patients. Medical engineering & physics. Vol. 36

no. 12, p. 1711-1715, 2014

[78] Aschero G., Gizdulich P. – Denoising of Surface EMG with a Modified Wiener Filtering Approach. J Electromyogr Kinesiol., vol. 20, no. 2, p. 366-73, Apr 2010

[79] Zhang D., Zhao X., Han J., Zhao Y. – A Comparative Study on PCA and LDA Based EMG Pattern Recognition for Anthropomorphic Robotic Hand. 2014 IEEE International Conference on Robotics & Automation (ICRA), June 7, 2014

[80] Xiong A., Zhang D., Zhao X., Han J., Liu G. – Classification of Gesture based on sEMG Decomposition: A Preliminary Study. Proceedings of the 19th World Congress, The International Federation of Automatic Control Cape Town, South Africa, August 24-29, 2014

[81] Farina D., Jiang N.,Rehbaum H., Holobar A., Graimann B., Dietl H., Aszmann O. C. – The Extraction of Neural Information from the Surface EMG for the Control of Upper-Limb Prostheses: Emerging Avenues and Challenges. IEEE Transactions on Neural Systems and Rehabilitation Engineering, vol. 22, no. 4, July 2014

[82] Glaser V., Holobar A., Zazula D. – Real-Time Motor Unit Identification From High-Density Surface EMG. IEEE Transactions on Neural Systems and Rehabilitation Engineering, vol. 21, no. 6, November 2013

[83] Ren X, Hu X, Wang Z, Yan Z. – MUAP extraction and classification based on wavelet transform and ICA for EMG decomposition. Med Biol Eng Comput, vol. 44, no. 5, p. 371-382, 2006 Apr 20.

[84] R. Fontugne and P. Borgnat and P. Flandrin – Online Empirical Mode Decomposition. 2017 IEEE International Conference on Acoustics, Speech and Signal Processing, New Orleans, LA, USA, March 2017

[85] Potvin J. R., Brown S. H. M. – Less is More: Highpass Fltering, To Remove Up To 99% of the Surface EMG Signal Power, Improves EMG-based Biceps Brachii Muscle Force Estimates. J. Electromyography and Kinesiology, vol. 14, p. 389–399, 2004

[86] McGill K. C., Lateva Z. C., Xiao S. – A Model of the Muscle Action Potential for Describing the Leading Edge, Terminal Wave, and Slow Afterwave. IEEE Transactions on Biomedical Engineering, vol. 48, no. 12, December 2001

[87] Feng Duan, Lili Dai, Wennan Chang, Zengqiang Chen, Chi Zhu, Wei Li – sEMG-Based Identification of Hand Motion Commands Using Wavelet Neural Network Combined with Discrete Wavelet Transform. IEEE Transactions on Industrial Electronics, 2015

[88] Van Cutsem M., Duchateau J., Hainaut K. – Neural Adaptations Mediate Increase in Muscle Contraction Speed and Change in Motor Unit Behaviour After Dynamic Training. J. Physiol., vol. 513, p. 295–305, 1998

[89] Woods J. J., Bigland-Ritchie B. – Linear and Non-Linear Surface EMG – Force Relationships in Human Muscle. Am. J. Phys. Med. vol. 62, no. 6 , p. 287 – 299, Dec 1983

[90] Norman R. W., Komi P. V. – Electromechanical Delay in Skeletal Muscle Under Normal Movement Conditions. Acta Physiol. Scand., vol. 106, no. 3, p. 241 – 248, Jul 1979

[91] Farina D., Holobar A. – Characterization of Human Motor Units From Surface EMG

Decomposition. Proceedings of the IEEE, vol. 104, no. 2, February 2016

[92] Barbakh W., Fyf C. – Online Clustering Algorithms. International Journal of Neural Systems, vol. 18, no. 3, p. 185-194, 2008

[93] Zhang X., Zhou P. – Filtering of Surface EMG Using Ensemble Empirical Mode Decomposition. Med Eng Phys., vol. 35, no. 4, p. 537–542, April 2013

[94] H. W. Lilliefors – On the Kolmogorov-Smirnov Test for Normality with Mean and Variance Unknown. Journal of the American Statistical Association, vol. 62, no. 318, p. 399–402, 1967

[95] Florestal JR, Mathieu PA, Malanda A. Automated Decomposition of Intramuscular Electromyographic Signals. IEEE Trans Biomed Eng vol. 53, no. 5, p. 832-839, 2006. [The software is available at http://www.emglab.net]

[96] Hamilton-Wright A, Stashuk DW. Physiologically Based Simulation of Clinical EMG signals. IEEE Trans Biomed Eng, vol. 52, p. 171–183, 2005. [The software is available at http://www.emglab.net]

[97] Sanger T. D. – Bayesian Filtering of Myoelectric Signals, J. Neurophys, vol. 97, no. 2, p. 1839-1845, 2007

[98] MacKenzie I. S., Felzer T. – Sak: Scanning Ambiguous Keyboard for Efficient One-Key Text Entry. ACM Trans Comput Hum Interact, vol. 17, no. 11, 2010

[99] Lopes M. V., Aguiar E., Santana E. – ICA Feature Extraction for Spike Sorting of Single-Channel Records. 2013 ISSNIP Biosignals and Biorobotics Conference: Biosignals and Robotics for Better and Safer Living (BRC), Rio de Janerio, Brazil, 18-20 Feb. 2013

[100] Hogrel J-Y. [Online dataset R011, available at http://www.emglab.net]

[101] Bai F., Chew C.-M. – Muscle Force Estimation with Surface EMG During Dynamic Muscle Contractions: A Wavelet and ANN based Approach.3 5th Annual International Conference of the IEEE EMBS, Osaka, Japan, 3 - 7 July, 2013

[102] Zhang B., Zhang S. – The Estimation of Grasping Force Based On the Feature Extracted From EMG Signals. 2016 IEEE Advanced Information Management, Communicates, Electronic and Automation Control Conference (IMCEC), Xi'an, China, 3-5 Oct. 2016

[103] Naik G. R., Kumar D. K., Singh V. P., Palaniswami M. – Hand gestures for HCI using ICA of EMG. In Proceedings of the HCSNet Workshop on Use of Vision in Human-computer Interaction, VisHCI'06, Australian Computer Society, Inc., Darlinghurst, p. 67–72, Australia, 2006

[104] Doherty T. J., Stashuk D. W. – Decomposition-based quantitative electromyography: methods and initial normative data in five muscles. Muscle & Nerve 28, p. 204–211, 2003

[105] Kleine B. U., van Dijk J. P., Lapatki B. G., Zwarts M. J., Stegeman D. F. – Using Two-Dimensional Spatial Information in Decomposition of Surface EMG Signals. J. Electromyogr. Kinesiol. 17, p. 535–548, 2007

[106] E. M. Maathuis, Drenthen J., van Dijk J. P., Visser G. H., Blok J. H. – Motor Unit Tracking with High-Density Surface EMG. J Electromyogr Kinesiol 18, p. 920–930, 2008

[107] Kilner J. M., Baker S. N., Lemon R. N. – A Novel Algorithm to Remove Electrical Cross-talk

Between Surface EMG Recordings and Its Application to the Measurement of Short-term Synchronisation in Humans. J Physiol.; vol. 538, p. 919–930, Feb 2002

[108] Farina D., Févotte C., Doncarli C., Merletti R. – Blind Separation of Linear Instantaneous Mixtures of Nonstationary Surface Myoelectric Signals. IEEE Transactions on Biomedical Engineering, vol. 51, no. 9, Sep 2004

[109] Shahid S., Walker J., Lyons G. M., Byrne C. A., Nene A. V. – Application of Higher Order Statistics Techniques to EMG Signals to Characterize the Motor Unit Action Potentials. IEEE Transactions on Biomedical Engineering, vol. 52, no. 7, July 2005

[110] Biagetti G., Crippa P., Orcioni S., Turchetti C. – Homomorphic Deconvolution for MUAP Estimation from Surface EMG Signals. IEEE Journal of Biomedical and Health Informatics, vol. 21, no. 2, March 2017

[111] Liu R., Huang Q., Graupe D. – A neural network for noninvasive decomposition of surface EMG signals using Gaussian nodes. IEEE International Symposium on Circuits and Systems, IEEE 1990

[112] Staudenmann D., Roeleveld K., Stegeman D. F., van Dieën J. H. – Methodological aspects of SEMG recordings for force estimation – A tutorial and review. Journal of Electromyography and Kinesiology, vol. 20, no. 3, p. 375–387, 2010

[113] Chen M., Zhou P. – A Novel Framework Based on FastICA for High Density Surface EMG Decomposition. IEEE Trans Neural Syst Rehabil Eng., vol. 24, no. 1, p. 117-127, Jan 2016

[114] Chen M., Holobar A., Zhang X., Zhou P. – Progressive FastICA Peel-Off and Convolution Kernel Compensation Demonstrate High Agreement for High Density Surface EMG Decomposition. Neural Plasticity, vol. 2016

[115] Hargrove L. J., Englehart K., Hudgins B. – A comparison of surface and intramuscular myoelectric signal classification. IEEE Trans. Biomed. Eng., vol. 54, no. 5, p. 847-53, May 2007

[116] Ning Y., Zhu X., Zhu S., Zhang Y. – Surface EMG Decomposition Based on K-means Clustering and Convolution Kernel Compensation. IEEE J Biomed Health Inform., vol. 19, no. 2, p. 471–477, Mar 2015

[117] Torkkola K. – Blind Separation of Convolved Sources Based on Information Maximization. IEEE Workshop on Neural Networks for Signal Processing, Kyoto, Japan, p. 423-432, 1996

[118] Qiang Li, Ji-hai Yang, Xiang Chen, Zheng Liang, Yan-xuan Ren – The Decomposition of Surface EMG Signals Based on Blind Source Separation of Convolved Mixtures. IEEE Engineering in Medicine and Biology 27th Annual Conference, Shanghai, China, September 1-4, 2005

[119] Bawa P., Stein R. B. – Frequency Response of Human Soleus Muscle. J Neurophysiol, vol. 39, no. 4, p. 788 – 93, Jul 1976

[120] Ruiz-Olaya A. F., López-Delis A. – Surface EMG signal analysis based on the empirical mode decomposition for human-robot interaction. Symposium of Signals, Images and Artificial Vision – 2013, Bogota, Colombia, 11 – 13 September 2013

[121] Nazarpour K., Al-Timemy A. H., Bugmann G., Jackson A. – A note on the probability distribution function of the surface electromyogram signal. Brain Research Bulletin, vol. 90, p. 88 –

91, Jan 2013

[123] Felzer T., Strah B., Nordmann R. – Automatic and selfpaced scanning for alternative text entry. In: Proceedings of the IASTED international conference on Telehealth/Assistive Technologies, Telehealth/AT ’08. ACTA Press, Anaheim, p. 1–6, 2008

[124] Miró-Borrás J., Bernabeu-Soler P. – E-everything for all: Text entry for people with severe motor disabilities. In: Proceedings of the Collaborative Electronic Communications and eCommerce Technology and Research Iberoamerica, 6th CollECTeR, p. 1–7, 2008

[125] Na Y., Kim J. – Force Estimation using an Approximately Physiological Mechanism. 10th International Conference on Ubiquitous Robots and Ambient Intelligence (URAI) October 31 – November 2, 2013

[126] Quiroga R. Q., Nadasdy Z., Ben-Shaul Y. – Unsupervised spike detection and sorting with wavelets and superparamagnetic clustering. Neural computation, vol. 16, no. 8, pp. 1661–87, Aug. 2004

[127] K. Nazarpour, A. Sharafat, S. Firoozabadi – Application of higher order statistics to surface electromyogram signal classification. IEEE Transactions on Biomedical Engineering, vol. 54, p. 1762-1769, 2007

[128] Zhai X., Jelfs B., Chan R. H. M., Tin C. – Self-Recalibrating Surface EMG Pattern Recognition for Neuroprosthesis Control Based on Convolutional Neural Network. Frontiers in Neuroscience, 10.3389/fnins.2017.00379, 2017

[129] Karimi M., Pourghassem H., Shahgholian G., – A novel prosthetic hand control approach based on genetic algorithm and wavelet transform features. IEEE 7th Int. Colloquium on Signal Processing and its App., p. 287-29, 2011

[130] Khezri M., Jahed M. – A neuro–fuzzy inference system for sEMG-based identification of hand motion commands. IEEE Trans. Ind. Electron., vol. 58, no. 5, p. 1952-1960, May 2011

[131] Alkan A. Günay M. – Identification of EMG signals using discriminant analysis and SVM classifier. Expert Syst. with App., vol. 39, no. 1, p. 44-47, Jan. 2012.

[132] Delis A. L., Revilla L. M., Rodriguez D. D., Olaya A. R. – On the use of surface EMG for recognizing forearm movements: towards the control of an upper extremity exoskeleton. Andean Region Int. Conf., p. 181-184, 2012

[133] Xing K., Yang P., Huang J.,Wang Y, Zhu Q. – A real-time EMG pattern recognition method for virtualmyoelectric hand control. Neurocomputing, vol. 136, p. 345-355, 2014

[134] Mathiesen J. R., Bøg M. F., Erkocevic E., Niemeier M. J., Smidstrup A., Kamavuako E. N. – Prediction of grasping force based on features of surface and intramuscular EMG. 2010

[135] Sun W., Zhu J., Jiang Y., Yokoi H., Huang Q. – One-Channel Surface Electromyography Decomposition for Muscle Force Estimation. Front Neurorobot., vol. 12, 2018

[136] Itou T., Teraol M., Nagata J., Yoshida M. -- Mouse cursor control system using EMG. Proceedings of the 23rd Annual EMBS International Conference, October 25-28, Istanbul, Turkey, 2001

[137] Tenore F. V., Ramos A., Fahmy A., Acharya S., Etienne-Cummings R., Thakor N. V. Decoding of individuated finger movements using surface electromyography. IEEE Trans Biomed Eng., vol. 56, no. 5, 1427-34, May 2009

[138] Villarejo J. J., Costa R. M., Bastos T., Frizera A. – Identification of low level sEMG signals for individual finger prosthesis. 5th ISSNIP-IEEE Biosignals and Biorobotics Conference (2014): Biosignals and Robotics for Better and Safer Living (BRC), Salvador, Brazil, 26-28 May 2014

[139] Chen M., Zhang X., Chen X., Zhou P. – Automatic Implementation of Progressive FastICA Peel-Off for High Density Surface EMG Decomposition. IEEE Transactions on Neural Systems and Rehabilitation Engineering vol. 26, no. 1, October 2017

[140] Hayashibe M., Guiraud D., Poignet P. – In Vivo Identification of Skeletal Muscle Dynamics with Nonlinear Kalman Filter: Comparison between EKF and SPKF. ISRN Rehabilitation, vol. 2013

[141] Wang N., Chen Y., Zhang X. – The recognition of multi-finger prehensile postures using LDA. Biomedical Signal Processing and Control, vol. 8, no. 6, p 706-712, November 2013

[142] Shin S., Langari R., Tafrershi R. – A Performance Comparison of EMG Classification Methods for Hand and Finger Motion. Conference: ASME 2014 Dynamic Systems and Control Conference, DSCC 2014

[143] Liu J. – Adaptive myoelectric pattern recognition toward improved multifunctional prosthesis control. Medical Engineering & Physics, vol. 37, no. 4, p. 424-430 April 2015

[144] Mane S. M., Kambli R. A., Kazi F. S., Singh N. M. – Hand Motion Recognition from Single Channel Surface EMG Using Wavelet & Artificial Neural Network. Procedia Computer Science, vol. 49, p. 58-65, 2015

[145] Geng W., Du Y., Jin W., Wei W., Hu Y., Li J. – Gesture recognition by instantaneous surface EMG images. Sci Rep. vol. 15, no. 6, November 2016

[146] Kang W. J., Shiu J. R., Cheng C. K., Lai J. S.,Tsao H. W., Kuo T. S. – The Application of Cepstral Coefficients and Maximum Likelihood Method in EMG Pattern Recognition. IEEE Trans Biomed Eng., vol. 42, no.8, p. 777-785., Aug 1995

Author’s publications

[P1] Pošusta A., Otáhal J. – Recording and conditioning of surface EMG signal for decomposition. Bulletin of Applied Mechanics, vol. 8, no. 30, p. 28-31, 2012

contribution: 90 %

[P2] Pošusta A., Poláček O., Sporka A. J., Flek T., Otáhal J. – Text Entry Methods Controlled by Myoelectric Signals. Bulletin of Applied Mechanics, vol. 9, no. 34, p. 23-30, 2013

contribution: 33 %

[P3] Pošusta A., Sporka A. J., Poláček O., Rudolf Š, Otáhal J. – Control of word processing environment using myoelectric signals. Journal on Multimodal User Interfaces, vol. 9, no. 4, October 2015

contribution: 50 %